By Architects. For Architects.
By Engineers. For Engineers.

Architecture
Civil and Structural Engineering
Mechanics of Materials
Building and Construction
Urban Planning and Development
Transportation Issues in Construction
Geotechnical Engineering and Engineering Geology
Designing, Operation and Service
of Construction Site Engines

CONTENTS

Architecture

Civil Engineering

Architecture

ENHANCING STUDENTS' CAMPUS WALKABILITY AS A SUSTAINABILITY INDICATOR

Ahlam Eshruq Labin

Architecture Engineering Department, Al al-Bayt University, Mafraq, Jordan

E-mail: ahlam.labin@aabu.edu.jo

Abstract
Introduction: Walking has recently become an essential and sustainable way of mobility for university students in their daily lives. The walkability of students is affected by the characteristics and context of the campus's built environment. **Purpose of the study:** The purpose of the study is to determine the time benchmarks needed to classify the students' campus walkability and study the factors that affect students' campus walkability, which include four groups: campus infrastructure, campus layout, context and services, and students' behavior. **Methods:** A questionnaire was distributed to students at the Faculty of Engineering at the AABU University in Mafraq, Jordan. SPSS software was used to analyze the data and obtain results. **The results** of the study show that students' walkability can be divided into the following categories: convenient walkability, tolerable walkability, and weary walkability. Meanwhile, the factors are grouped into those that increase, decrease, or have no effect on students' campus walkability. The significance of the research lies in the investigation of walkability as one of the primary modes of mobility on the university campus. It is considered an essential component of sustainability and is used as a design consideration for determining accessibility to the various services that students need within the university.

Keywords: sustainability; walkability; walking behavior; campus walkability.

Introduction

Walkability is an essential component of urban development. It also offers unexpected health, environmental, financial, and community benefits. The term "walkability" refers to a method that assesses how pedestrian-friendly a location is.

Several studies have examined issues related to students' campus walkability (Peachey and Baller, 2015). To begin, a literature review was conducted to investigate the concept of walkability, which is defined as the relevance of the built environment to human behavior, whether for living, shopping, visiting, enjoying, or spending time (Abley, 2005).

One of the goals is to determine the factors that affect students' walkability. The study classifies these factors into four groups, including campus infrastructure, campus layout, context and services, and students' behavior. In general, most universities include a variety of facilities and spaces that enable students to learn and walk. These facilities can be classified in various ways; some studies divide them into academic and non-academic services. Another option is based on students' priorities and frequency of use per week.

The AABU University in Mafraq, Jordan, was selected as a case study. It includes 13 faculties and a variety of facilities. Based on Akomolafe and Adesua (2016), the campus services were classified into two groups: academic services and non-academic services (Fig. 1).

Another aspect is to review the measuring tools that the researchers used to assess walkability and establish the most appropriate model that can serve the study objective of measuring the students' campus walkability. For example, Frank et al. (2010) proposed a walkability index, and Dörrzapf et al. (2019) described other tools such as audit-based methods, sensors for walkability assessment, geodata analysis, and Walk Score.

The ability to walk decreases over time, resulting in different levels of walkability. These include convenient walkability, when students can walk comfortably; tolerable walkability, when students walk feeling tired; and weary walkability, when students cannot walk any longer.

The main goals of this study are to:

1. Determine the time benchmarks needed to classify students' campus walkability into weary walkability, tolerable walkability, and convenient walkability.

2. Study the factors that affect students' campus walkability.

The literature review examines several aspects of walkability: firstly, studies that determine the factors affecting walkability, such as Grasser et al. (2016) and Koschinsky and Talen (2015); secondly, studies that determine the walkability measurement

```
                          ┌─────────────────────────┐
                          │     Campus Services      │
                          │                          │
                          └────────────┬─────────────┘
              ┌────────────────────────┴────────────────────────┐
    ┌──────────────────────┐                      ┌──────────────────────┐
    │  Academic Services    │                      │ Non-Academic Services │
    │                       │                      │                       │
    └───────────┬───────────┘                      └───────────┬───────────┘
   ┌────────────────────────┐        ┌──────────────────────────────────┐
   │ Public Teaching Buildings,│      │ Canteen and Restaurant, Retail store,│
   │ Library, Administrative building,│ │ Square and green spaces, Bus station,│
   │ Students activity center │        │ Stadium, Coffee shop, Bank       │
   └────────────────────────┘        └──────────────────────────────────┘
```
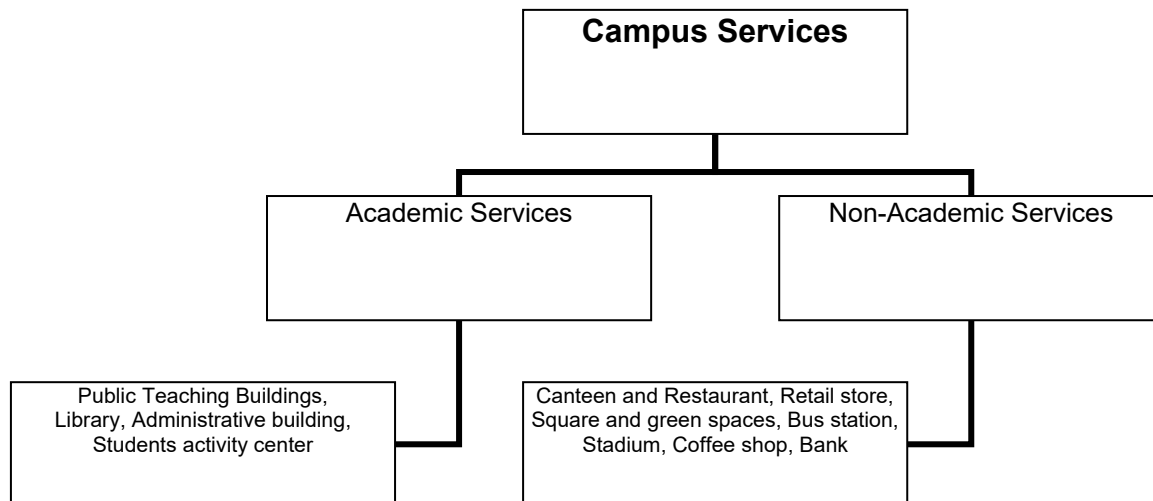
Fig. 1. Campus services

tools, such as Zhang et al. (2020), Saghapour et al. (2017), and King et al. (2020); and finally, studies on campus walkability, such as Sisson et al. (2008) and Peachey and Baller (2015).

Literature Review

This section will discuss the concept of walkability, walkability measurement tools, campus walkability, and campus services.

1. Walkability: definitions and tools

Walking has recently become an essential and sustainable way of mobility for university students in their daily lives. Sustainability aims to create a healthy environment by promoting an active lifestyle and increasing accessibility and freedom of choice by making more facilities accessible (Eshruq Labin et al., 2022).

Walkability is defined as the relevance of the built environment to human behavior, whether for living, shopping, visiting, enjoying, or spending time (Abley, 2005; Frank and Engelke, 2005). It is an important aspect of personal cognition and social coexistence. Besides, walkability is an important consideration in designing public spaces (Ewing and Handy, 2009).

Several studies have found a correlation between public health and a city's walkability. Furthermore, walkability enhances leisure and mobility (Brownson et al., 2009; Dörrzapf et al., 2019; Grasser et al., 2016; Sarkar et al., 2018). Neighborhood walkability is defined as the ability to support physical activity while considering residential density and city block size, as well as access to various destinations, street connectivity, sidewalk access, aesthetics, and other community features. Meanwhile, more detailed elements could also be studied, such as pedestrian safety and comfort, walking preferences, and friendliness for walking in a walkable environment (Zhang et al., 2020).

According to Clarence Perry, the unit of measurement for walking distance is 400 meters,

or a five-minute walk, which is the walkability from a school to a residential area. However, it is not suitable for some countries that have hot or cold climate. For example, in Malaysia, the preferred distance to walk before choosing to drive is 200 meters (Azmi and Karim, 2012). Walkability refers to a pedestrian's ability to walk short distances of less than 100 meters for a certain reason, such as going to work or school (Dörrzapf et al., 2019).

Walkability encompasses measurable functional and physical requirements as well as subjective walkability features, including the importance of personal preferences and individual perceptions of the environment (Dörrzapf et al., 2019). To study the relationships between walkability and physical environmental aspects, Lee and Moudon (2006) divided the elements that affect walkability into 13 VIP (variables with strong theoretical support) and 19 non-VIP (built environment variables) variables. The linkages with the physical elements of an environment are based on walking purposes. Forsyth et al. (2008) listed over 200 factors that influence walkability, including street pattern, pedestrian-oriented design elements, and attractions.

Walkability can be quantified in various ways, including the opportunities to walk in a particular environment and walking behavior. Thus, the results of the experience are affected by what people perceive while walking, which means there is a strong relationship between walking behavior and perceptual qualities (Ewing and Handy, 2009; Dörrzapf et al., 2019). Knapskog et al. (2019) categorized the factors that affect walkability into three groups: infrastructure and traffic, urbanity, and surroundings and activities.

Walking experience is a tool that is used to assess walking behavior. Safety, convenience, and pleasure are aspects of a good walking experience that enhance the walkability of an area. Moreover,

familiarity with an area increases comfort while walking (Azmi and Karim, 2012).

Walking behavior refers to a pedestrian's performance in terms of walking duration and route selection. Walking behavior takes several forms due to a variety of factors that influence pedestrian behavior (Azmi and Karim, 2012). Another aspect that influences walkability is the walking distance, which affects walkers' comfort and willingness to walk. The walking distance can be measured from the origin to the destination in miles or meters, or in minutes (Mohamaddan, 2010).

Azmi and Karim (2012) investigated two characteristics of the walking experience, namely safety and convenience. They are based on the World Bank's Global Walkability Index (GWI), which is a metric that measures the walkability of a neighborhood. Security, motorist behavior, and crossing exposure are all part of the safety component, while visual appeal, pedestrian amenities and coverage, and connectivity are all part of the convenience component. The researchers used walking distance, time taken to walk, walking formation, strategic position, accessibility, and walking experience to assess walking behavior.

Frank et al. (2010) proposed a walkability index that considers density, land use mix, and retail floor area ratio. Glazier et al. (2012) also proposed a walkability index for Canadian settings, emphasizing residential housing density, population density, roadway connectivity, and retail outlet density. Moreover, the impact of several criteria on walkability, such as street connectivity, destination accessibility, aesthetics, pedestrian facilities, residential density, safety, and land use mix, was investigated (McCormack and Shiell, 2011; Grasser et al., 2016).

A pedestrian-friendly index combines four sub-indices: land use density index, population density index, commercial density index, and intersection density index (Peiravian et al., 2014). Whereas, a walking access index (WAI) studies the effect of travel distance and walking time on walkability (Saghapour et al., 2017).

Several methods exist for assessing walkability, such as audit-based methods, sensors for walkability assessment, and geodata analysis. Audit-based methods are used to assess walkability and urban space using a rating system for various parameters, such as walking distance, proportions of green space, and traffic volume (Brownson et al., 2009; Krenn et al., 2015). An audit-based method is based on movement-specific models, which study the effects of social, individual, and physical settings, as well as aspects of functionality, safety (personal safety and traffic safety), aesthetics, and business or service (Dörrzapf et al., 2019; Long et al., 2018; Pikora et al., 2003).

Sensors for walkability assessing are used to analyze walkability and how people use public spaces. They include permanently installed, mobile, and biosensors. Pedestrians' behavior in urban spaces can be observed through a mobile or permanently installed camera and permanently installed sensors. Smartphone sensors can be used to collect data either directly from users via surveys or questionnaires, such as the eDiary app, which is used to acquire subjective assessments of walkability, or indirectly by tracking the environment.

Generally, this method is not ideal for measuring walkability since data protection makes it difficult to access the information. Biosensors, for example, provide objective measurements of skin conductance and skin temperature (Dörrzapf et al., 2019; Resch et al., 2020; Zhou and Long, 2017).

Geodata analysis is an objective evaluation of pedestrian movements and interactions. It is used to assess urban walkability by analyzing traditional and urban geodata related to walkability, enabling data to be spatially and temporally referenced. Urban functions, land use categories, street network, road widths, traffic volumes, green index, and population are all included in the geodata study. Dörrzapf et al. (2019) used a comprehensive approach to assess walkability by combining existing qualitative and GIS-based techniques with biosensor technologies to capture the impact of the physical environment on pedestrians' perceptions and emotions.

GIS-based approaches for measuring walkability, such as network analysis, distance-based, gravity-based, potential-, topology-, or infrastructure-based methodologies, are widely used to analyze the spatial accessibility of a single facility or several facilities (Vale, 2015). The Integrated Spatial Equity Evaluation (ISEE) examines the spatial equality of diverse community facilities (Taleai and Yameqani, 2018).

Walkability assessment utilizes field audits, qualitative analysis, and quantitative empirical research to examine the relationship between walking and health, the environment, the economy, and social aspects (Reyer et al., 2014).

Zhang et al. (2020) used a subjective evaluation method of walkability based on questionnaires, an objective evaluation method based on field audits, and an integrated method combining subjective and objective approaches. They also proposed a walkability index method that incorporating various environmental features such as land use mix, residential density, and street connectivity to assess pedestrian walkability.

Walk Score has recently gained international recognition as an essential quantitative measurement technique for a variety of reasons, including evaluating the time and distance required to walk to destinations. It also considers the number and type of facilities,

as well as their layout pattern. To adjust the value, Walk Score takes into account population density, street length, and intersection density. Using a standardized scale of 0–100, with higher values indicating a more walkable environment, Walk Score divides that scale into five intervals: 0–24 car-dependent, 50–69 somewhat walkable, 70–89 very walkable, and 90–100 walker's paradise (Zhang et al., 2020).

Walk Score is used by many researchers to evaluate various aspects of walkability, the living environment, urban design features and qualities, physical activity, affordability, and walking behavior. Walk Score is an international walkability measurement metric based on block length, street connectivity, and facility layout (Wu and Shen, 2017; Zhang et al., 2020). However, Walk Score has not been used as an acceptable way to evaluate a pedestrian's walkability in the campus environment. The most important study that used Walk Score to measure the students' campus walkability is by Zhang et al. (2020), which is the main reference for this research.

2. Campus walkability and campus facilities

Generally, universities have several facilities and spaces that are likely to encourage students to learn and be walkable, such as classrooms, libraries, hostels, shuttle buses, cafeterias, clinics, cultural facilities, prayer rooms, security guard posts, laboratories, games and sports facilities, farms and gardens, restrooms, information and communication technologies (ICT), transportation and security, and counseling centers. These can be categorized into two groups: academic services and non-academic services (Akomolafe and Adesua, 2016).

Ramli and Mohd Zain (2018) examined the effect of campus facilities on students' achievements. They explored three factors that can impact students' achievements: system management (e-learning, management information system), learning environment (classrooms, teaching aids, and library), and infrastructure (hostels, sports facilities, parking and transportation).

Easy way-finding is one of the factors that affects walkability. Students' way-finding behavior on campus is influenced by several factors grouped into individual factors and built environment legibility factors. The built environment legibility factors include such elements as architectural features, visual communication features (graphical), audible communication (verbal) features, and tactile features (Eshruq Labin, 2020).

Campus walkability studies serve a variety of goals, including assessing walkability on a single campus, comparing two or more campuses, and comparing on-campus and off-campus built environments. Two methodologies, subjective and objective, were employed to evaluate campus walkability in two directions. The first direction focuses on the university campus built environment. The walkability and bikeability of the University of North Texas campus streets were assessed by Li et al. (2016). King et al. (2020) used a different method to assess campus walkability by combining participants' perceptions of walkability, environmental factors, and other physical activity-related features on campus.

The second direction involves the subjective evaluation of walkability in relation to campus walkability, students' physical activity, built environment features, social aspects, and travel modes. Scholars have primarily used audit tools, such as pedestrian environment data scan and cycling environmental scan (Zhang et al., 2020).

Various environmental factors, such as residential density, land use mix, aesthetics, safety, and existing infrastructure such as sidewalks and walking routes, were investigated to determine how they affect walkability, walking behavior, and walking activity intensity (Iakimovich et al., 2022; Peachey and Baller, 2015). Peachey and Baller (2015) revealed in their study that the campus built environment elements have an impact on students' physical activity. They found that a campus with land use mix diversity, aesthetics, and a lack of cul-de-sacs can enhance students' physical activity. Furthermore, some research examines how walkability affects students' physical activity in terms of proximity to facilities and perceived safety (Peachey and Baller, 2015).

Students who reside on a campus with wide streets and restricted access to destinations had lower walking intensity than those who live on a campus with main academic areas, many destinations, and few parking lots (Sisson et al., 2008). Furthermore, studies have focused on the effects of a destination's geographical location on walkability and the level of access to various destinations in order to investigate the link between campus walkability and commuting modes. Students prefer to walk or bike to campus in areas with strong walkability and a dense service infrastructure (Vale, 2015).

Walking speed, walking directions, walking experiences, group formation, and density are five elements that demonstrate walking behavior. However, only three parameters were utilized to examine walking behavior on the campus of UNIKA St. Thomas University: walking distance, walking time, and walking speed. The average walking speed is 1.40 meters per second, and it is determined by numerous factors such as age, gender, height, and weight. Walking distance is the distance that can be covered on foot within a certain amount of time. It is commonly used in planning as a benchmark for a comfortable walking distance of 400 meters, which takes about five minutes. Walking time is influenced by many factors, such as gender, age, health and leisure (Silitonga, 2020).

Zhang et al. (2020) developed a campus walkability evaluation tool that enhances the Walk

Score approach by taking into account the variety, frequency, and distance that students travel to and from public facilities.

Methodology

1. Study setting

This study took place on the large urban campus of AABU, located 65 kilometers northeast of Jordan's capital, Amman. The campus spans over 7,539,000 square meters in Mafraq. AABU University comprises several faculties, including the Faculty of Engineering, the Princess Salma Faculty of Nursing, the Faculty of Information Technology, the School of Business, the Faculty of Sharia, the Faculty of Law, the Faculty of Arts and Humanities, the Faculty of Science, the Faculty of Educational Sciences, the Faculty of Political Sciences and International Studies (Bayt Al-Hikmah), the Faculty of Earth and Environmental Sciences, and the Institute of Astronomy and Space Sciences (Fig. 2).

In addition to the faculties' buildings, there are many service buildings inside the campus, such as a bank, a mosque, and an elementary school for the children of university employees (Al Abrar School).

2. Participants

AABU University comprises nearly 19,455 students pursuing doctorate, master's, and bachelor's degrees, with 11,308 of them being female and 8,147 male (for the academic year 2021/2022). Among them, 1,297 students are registered at the Faculty of Engineering, 406 at the Architecture Engineering Department, 404 at the Civil Engineering Department, 319 at the Renewable Energy Engineering Department, and 150 at the Surveying Engineering Department (Al al-Bayt University Annual Report 2020/2021, 2021).

The survey assesses students' campus walkability from the Faculty of Engineering to various campus services. A total of 372 participants from the Faculty of Engineering responded to the questionnaire, with 219 being female and 153 being male. Among the participants, 11 % are in their first year, 30 % in the second year, 27 % in the third year, 31 % in the fourth year, and 1 % in the fifth year. Additionally, 41.8 % of the participants are from the Architecture Engineering Department, 27.6 % from the Civil Engineering Department, 15.3 % from the

1	Main gate	7	Student activity center
2	Faculty of Engineering	8	University Presidency building
3	Elementary school	9	Mosque
4	Quraish building	10	Students' housing
5	Registration department	11	Bank
6	Al-Hashemite library	12	Hashem building

Fig. 2. Campus master plan

7

Renewable Energy Engineering Department, and 15.3 % from the Surveying Engineering Department.

3. Data collection

This study is mainly based on a literature review to collect secondary data. Subsequently, questionnaires were distributed to the students of the Faculty of Engineering at AABU University. The questionnaire is structured into four parts:

1. Demographic data, including gender, department, and study year.

2. Frequency of using campus services by students.

3. Time needed to reach various student destinations from the Faculty of Engineering and time required to determine the benchmarks for classifying walkability.

4. Factors affecting students' campus walkability.

To determine the time benchmarks for classifying students' campus walkability, a specific conceptual methodology is used, following the sequence below:

1. Determining the actual time that students need to access various university services from the Faculty of Engineering.

2. Determining the walkability type experienced by students during the walking trip to access various university services from the Faculty of Engineering.

3. Determining the time benchmarks required for each type of walkability by students. Walkability is categorized into three groups: weary walkability, tolerable walkability, and convenient walkability.

4. Estimating the walkability type required to reach each service based on the actual time determined in step No. 1, using the time benchmarks determined in step No. 3.

5. Comparing the walkability type in step No. 2 with the walkability type in step No. 4 to study the consistency of the results.

The students' campus walkability factors were clustered into four groups, including:

1. The campus infrastructure includes traffic aspects such as street features, street intersections, street furniture, vehicle density, pollution, noise, car parks, and the availability of public transit.

2. The campus layout includes aspects that form the campus master plan, such as the proximity of buildings, interconnection of spaces, open spaces, building orientation, building scale, building permeability, pedestrian pathway networks, green areas, and student density since the distribution of functions affects student density.

3. Context and services include the style and quality of the service, such as the type of function (library, restaurant, etc.), building design, building facades, diversity of services, place vitality, destinations, and regular maintenance.

4. Students' behavior includes safety, way-finding, walking alone, students' walking or staying, and walking with friends.

Results

Zhang et al. (2020) divided the average frequency of using various facilities per week into three categories: high frequency (more than five times a week), medium frequency (more than one time a week), and low frequency (less than one time a week). After comparing the non-academic services, the results show that the bus station falls under the high frequency category due to its functional necessity. A comparison was then made between the cafeterias, revealing that the engineering cafeteria is of medium frequency use due to its proximity, while the business cafeteria and other cafeterias are of low frequency use. This proves that as the distance increases, the desire to walk decreases. Meanwhile, other facilities fall under the low frequency category (Table 1).

When comparing services based on the time it takes to reach them, the engineering cafeteria is the closest, only 5 minutes away, which is of medium frequency. The time required to reach the business cafeteria is 6–10 minutes, and it is of low frequency. Other cafeterias and coffee shops are 16–20 minutes away and of low frequency. The bus station is 6–10 minutes away and of high frequency. The bank, student activity center, registration building, and library are 16–20 minutes away and of low frequency. The Okath shop is 26–30 minutes away and of low frequency, and the stadium is more than 30 minutes away and of low frequency as well.

The walking distance was measured from the origin (Faculty of Engineering) to destinations in meters (when walking on foot) and minutes. The time required to reach various services from the Faculty of Engineering was determined by the students (Table 2). For instance, 98.9 % of the students need 5 minutes to access the engineering cafeteria, 73.1 % of the students need 6–10 minutes to access the business cafeteria, and 69.9 % of the students need the same amount of time to reach the bus station. Additionally, 46.2 % of the students need 6–10 minutes to reach the public halls.

Besides, 67.7 % of the students need 16–20 minutes to reach the AlRefadeh Wa AlSeqayeh cafeteria; 51.6 % of the students need 16–20 minutes to reach the Hashem cafeteria; and 57.0 % of the students need 16–20 minutes to reach the Iqbal cafeteria. Additionally, 16–20 minutes are needed to reach the Quraish coffee shop, nursing coffee shop, IT coffee shop, Hashemite coffee shop, Hashemite library, student activity center, bank, and registration building.

The percentages were 67.7, 51.6, 57.0, 46.2, 59.1, 55.9, 63.4, 59.1, 51.6, 53.8 and 48.4 %, respectively.

In addition, 49.5 % of the students need 26–30 minutes to reach the Okath shop, and 48.4 % of the students need more than 30 minutes to get to the stadium.

Table 1. **Frequency of facilities use**

Campus services			Frequency of use per week, %		
			Less than once a week	1–4 times a week	More than 5 times a week
Non-academic services	Cafeterias	Engineering cafeteria	8.6	55.9	35.5
		Business cafeteria	46.2	45.2	8.6
		AlRefadeh wa AlSeqayeh cafeteria	90.3	7.5	2.2
		Hashem cafeteria	93.5	6.5	0
		Iqbal cafeteria	77.4	20.4	2.2
	Coffee shops	Quraish coffee shop	51.6	41.9	1.1
		Nursing coffee shop	87.1	12.9	0
		IT coffee shop	91.4	8.6	0
		Hashemite coffee shop	91.4	8.6	0
	Okath shop		73.1	25.8	1.1
	Bus station		17.2	29.0	53.8
	Stadium		92.5	6.5	1
	Bank		68.8	30.1	1.1
Academic services	Student activity center		90.3	9.7	0
	Registration building		64.5	34.4	1.1
	Public halls		52.7	38.7	8.6
	Hashemite library		57.0	41.9	1.1

Due to the inverse relationship between time and walkability, walkability decreases as time increases. Therefore, walkability was divided into three groups: convenient walkability, when students can walk comfortably without feeling tired; tolerable walkability, when students can walk despite feeling tired; and weary walkability, when students can no longer walk due to tiredness (Fig. 3).

The students determined the time benchmarks for convenient, tolerable, and weary walkability. The minimum value given by the students for convenient walkability is 2, which corresponds to 6 to 10 minutes.

The maximum value is 6, indicating 26–30 minutes, while the mean is 3.5, indicating that the students walk for 15 minutes without feeling tired (Tables 3, 4).

The minimum value given by the students for tolerable walkability is 3, which means 11–15 minutes, while the maximum value is 9, which means 41–45 minutes. The mean is 6.04, indicating that the students feel tired after walking for 15 to 30 minutes (Tables 3, 4).

The minimum value given by the students for weary walkability is 5, which means 21–25 minutes, while the maximum value is 11, which means more

Table 2. **Time needed to reach the services**

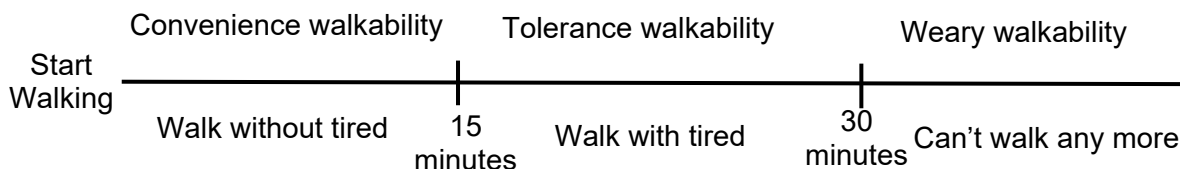| Campus services	Time needed to reach the services (in minutes)						
	5	6–10	11–15	16–20	21–25	26–30	30<
Engineering cafeteria	98.9	1.1	–	–	–	–	–
Business cafeteria	21.5	73.1	5.4	–	–	–	–
AlRefadeh wa AlSeqayeh cafeteria	–	–	28.0	67.7	4.3	–	–
Hashem cafeteria	–	–	28.0	51.6	20.4	–	–
Iqbal cafeteria	–	–	29.0	57.0	14.0	–	–
Quraish coffee shop	–	–	31.2	46.2	22.6	–	–
Nursing coffee shop	–	–	24.7	59.1	16.1	–	–
IT coffee shop	–	–	36.6	55.9	7.5	–	–
Hashemite coffee shop	–	–	19.4	63.4	17.2	–	–
Okath shop	–	–	–	–	21.5	49.5	29.0
Bus station	24.7	69.9	5.4	–	–	–	–
Stadium	–	–	–	–	22.6	29.0	48.4
Bank	–	–	23.7	53.8	22.6	–	–
Student activity center	–	–	33.3	51.6	15.1	–	–
Registration building	–	–	36.6	48.4	15.1	–	–
Public halls	–	46.2	41.9	11.8	–	–	–
Hashemite library	–	–	25.8	59.1	15.1	–	–

Fig. 3. Students' walkability types

Table 3. **Time needed to reach the services to classify walkability**

Type of walkability	Time (minutes)									
	0–5	6–10	11–15	16–20	21–25	26–30	31–35	36–40	41–45	46–50
Convenient walkability	–	12.9 %	31.2 %	48.4 %	6.5 %	1.1 %	–	–	–	–
Tolerable walkability	–	–	3.2 %	8.6 %	16.1 %	38.7 %	20.4 %	11.8 %	1.1 %	–
Weary walkability	–	–	–	–	1.1 %	5.4 %	4.3 %	3.2 %	11.8 %	41.9 %

Table 4. **Maximum and minimum walkability values**

Type of walkability	Minimum distance	Maximum distance	Mean
Convenient walkability	2.00	6.00	3.5161
Tolerable walkability	3.00	9.00	6.0430
Weary walkability	5.00	11.00	9.7419

than 51 minutes. The mean is 9.7, indicating that the students cannot walk any more after 30–45 minutes (Tables 3, 4).

The students considered walkability convenient while walking from the Faculty of Engineering to the engineering cafeteria, business cafeteria, bus station, and public halls. They also considered walkability tolerable for the AlRefadeh wa AlSeqayeh

Table 5. **Determining the walkability type to reach the campus services**

Campus services	Type of walkability		
	Convenient	Tolerable	Weary
Engineering cafeteria	98.9	1.1	0
Business cafeteria	97.8	2.2	0
AlRefadeh wa AlSeqayeh cafeteria	20.4	76.3	3.3
Hashem cafeteria	10.8	64.5	24.7
Iqbal cafeteria	24.7	67.7	7.6
Quraish coffee shop	45.2	52.7	2.1
Nursing coffee shop	28.0	67.7	4.3
IT coffee shop	20.4	75.3	4.3
Hashemite coffee shop	22.6	72.0	5.4
Okath shop	3.2	55.9	40.9
Hashemite library	23.7	69.9	6.5
Bus station	90.3	8.6	1.1
Stadium	4.3	47.3	48.4
Student activity center	20.4	71.0	8.6
Bank	17.2	68.8	14.0
Registration building	30.1	67.7	2.2
Public halls	53.8	39.8	6.4

cafeteria, Hashem cafeteria, Iqbal cafeteria, Quraish coffee shop, nursing coffee shop, IT coffee shop, Hashemite coffee shop, Okath shop, Hashemite library, student activity center, bank, and registration building. Walkability to reach the stadium was considered weary (Table 5).

The next step was to examine the congruence between the walkability type based on the students' experience (when walking between the Faculty of Engineering and other services) and the walkability type based on the time needed to reach the services. The results show that they are congruent (Table 6).

The factors that affect students' campus walkability can be grouped into four categories. The first group contains the factors related to the campus infrastructure. The results show that 48.4 % of the students believe that street features, such as the width of the street, increase walkability. Besides, street furniture such as benches, lighting, and waste paper baskets increases walkability. In addition, 45.2 % of the students concluded that the street intersection did not affect the level of walkability. Meanwhile, 63.4 % of the students believe that the density of vehicles on campus decreases walkability (Table 7).

It also should be noted that 67.7 % of the students believe that pollution and noise decrease walkability, while 34.4 % of the students concluded that the design and architectural style used for the buildings on campus did not affect students' walkability. Additionally, 48.4 % of the students believe that the availability of public transportation within the campus decreases their desire to walk (Table 7).

As for the second group of factors related to the campus layout, 41.9 % of the students believe that the density of students has no effect, while 52.7 %

Table 6. **Walkability congruency**

Campus services	Type of walkability			Congruency
	Walkability based on the students' experience	Average time needed to reach the services	Walkability based on the time needed to reach the services	
Engineering cafeteria	Convenient	5	Convenient	Congruent
Business cafeteria	Convenient	6–10	Convenient	Congruent
AlRefadeh wa AlSeqayeh cafeteria	Tolerable	16–20	Tolerable	Congruent
Hashem cafeteria	Tolerable	16–20	Tolerable	Congruent
Iqbal cafeteria	Tolerable	16–20	Tolerable	Congruent
Quraish coffee shop	Tolerable	16–20	Tolerable	Congruent
Nursing coffee shop	Tolerable	16–20	Tolerable	Congruent
IT coffee shop	Tolerable	16–20	Tolerable	Congruent
Hashemite coffee shop	Tolerable	16–20	Tolerable	Congruent
Okath shop	Tolerable	26–30	Tolerable	Congruent
Hashemite library	Tolerable	16–20	Tolerable	Congruent
Bus station	Convenient	6–10	Convenient	Congruent
Stadium	Weary	More than 30	Weary	Congruent
Student activity center	Tolerable	16–20	Tolerable	Congruent
Bank	Tolerable	16–20	Tolerable	Congruent
Registration building	Tolerable	16–20	Tolerable	Congruent
Public halls	Convenient	11–15	Convenient	Congruent

emphasize that the proximity of buildings on the campus increases walkability. Additionally, 57 % of the students considered the spatial connection to increase walkability. The campus covers 7,539,000 square meters, which is considered a large area. It should be noted that 66.7 % of the students stated that this reduces walkability. Meanwhile, 45.2 % of the students believe that the building orientation and building scale have no effect. Building permeability facilitates students' movement through the campus and helps them find shortcuts, ultimately increasing walkability. It should be noted that 47.3 % of the students acknowledged this. Additionally, 71.0 % emphasized that the accessibility of pedestrian pathways connecting various campus services contributes to walkability, while car parks have no effect on it. Furthermore, 69.9 % highlighted that the availability of open spaces and green areas increases students' desire to walk (Table 7).

Most context and service group factors increase walkability. It should be noted that 52.7 % of the students believe that the proximity of their destinations increases walkability. The closer the destination, the greater the desire to walk. Additionally, the type of activity, such as dining, visiting the library, doing sports, and studying, also increases walkability. Two factors have no effect on walkability, including when students are walking along the pedestrian paths or sitting at the squares, as well as the building facades. It should be noted that 52.7 % of the students emphasized that service diversity increases walkability; as a result, the greater the number

of facilities, the greater the diversity of services. In addition, 78.5 % of the students highlighted the role of place vitality in increasing walkability, and 57 % said that the regular maintenance of public services and utilities increases walkability (Table 7).

The last group is the students' behavior factors. It should be noted that 81.7 % of the students emphasized that feeling safe increases walkability and ease of way-finding. Additionally, 38.7 % of the students believe that walking alone has no effect on walkability, while 74.2 % stated that walking with friends increases the desire to walk. The hot or cold weather factor is one of the most important factors affecting students' walkability; 77.4 % of the students believe that it decreases walkability (Table 7).

Table 8 summarizes the factors that increase students' walkability on campus, the factors that decrease it, and the factors that have no effect on it.

Discussion

Zhang et al. (2020) used a subjective evaluation approach based on questionnaires to assess campus walkability. King et al. (2020) based their study on the views of campus participants regarding walkability. A questionnaire survey was used in the study to measure participants' perceptions of the campus walkability.

Dörrzapf et al. (2019) and Zhang et al. (2020) showed that there is an inverse relationship between time and walkability, indicating that walkability decreases as time increases. Silitonga (2020) used walking distance, walking time, and walking speed to analyze walking behavior on the campus. He found

that the average walking speed is 1.40 meters per second, which is affected by age, gender, height, and weight.

The study used the time benchmarks acquired from the questionnaire survey to categorize walkability into three types: convenient walkability, when students can walk comfortably without feeling tired, up to 15 minutes; tolerable walkability, when students can walk despite feeling tired, from 15 to 30 minutes; and weary walkability, when students can no longer walk due to tiredness, after 30 minutes of walking. Most campus services are within tolerable walkability.

Various studies proposed various factors affecting walkability, such as density, land use mix, retail floor area, residential housing density, population density, roadway connectivity, and retail outlet density (Glazier et al., 2012). Other factors include street connectivity, destination accessibility, aesthetics, pedestrian facilities, residential density, and safety (Grasser et al., 2016; McCormack and Shiell, 2011; Zhang et al., 2020). The researchers categorized 29 factors into four groups: campus infrastructure factors, campus layout factors, context and services

factors, and students' behavior factors, and each group has its own attributes.

Street features are one of the factors increasing walkability. Forsyth et al. (2008) indicated that the roadway pattern as well as the features of the built environment affect walkability.

Another aspect that influences walkability is the walking distance, which is affected by the proximity of facilities (Mohamaddan, 2010; Peachey and Baller, 2015). Researchers studied the effect of travel distance and walking time on walkability (Saghapour et al., 2017). The factors that influence walking time include gender, age, health, and leisure (Saghapour et al., 2017; Silitonga, 2020). It was found that building proximity, spatial connectivity, building permeability, and pedestrian pathway network decrease the distance between facilities and increase students' campus walkability.

Destination accessibility was proposed as a walkability index (McCormack and Shiell, 2011), and Grasser et al. (2016) used GIS-based approaches to measure walkability and analyze the spatial accessibility of a single facility or multiple facilities

Table 7. **Factors' impact**

Factors	Attributes	Increase walkability	No effect	Decrease walkability
Campus infrastructure	Street features	48.4	30.1	21.5
	Street furniture	68.8	24.7	6.5
	Street intersections	8.6	45.2	46.2
	Vehicle density	0	36.6	63.4
	Pollution and noise	0	32.3	67.7
	Car parks	37.6	45.2	17.2
	Public transit	16.1	35.5	48.4
Campus layout	Student density	24.7	41.9	33.3
	Building proximity	52.7	25.8	21.5
	Space connectivity	57.0	29.0	14.0
	Large university area	11.8	21.5	66.7
	Building orientation	30.1	45.2	24.7
	Building scale	28.0	52.7	19.4
	Building permeability	47.3	34.4	18.3
	Pedestrian pathway network	71.0	19.4	9.7
	Open spaces and green areas	69.9	19.4	10.8
Context and services	Destinations	52.7	40.9	6.5
	Activity type (dining, visiting the library, etc.)	59.1	34.4	6.5
	Building design	31.2	34.4	33.3
	Building facades	32.3	54.8	12.9
	Service diversity	52.7	37.6	9.7
	Place vitality	78.5	15.1	15.1
	Maintenance	57.0	21.5	21.5
Students' behavior	Safety	81.7	15.1	3.2
	Way-finding	69.9	25.8	4.3
	Walking alone	34.4	38.7	26.9
	Students walking or staying	41.9	44.1	14.0
	Walking with friends	74.2	25.8	0
	Hot or cold weather	0	22.6	77.4

Table 8. **Walkability factors' effect**

Factors increasing walkability	
Campus infrastructure	Street features, street furniture
Campus layout	Building proximity, space connectivity, building permeability, pedestrian pathway networks, open spaces and green areas
Context and services	Destinations, activity type (dining, visiting the library, etc.), service diversity, place vitality, and maintenance
Students' behavior	Safety, way-finding, and walking with friends
Factors having no effect	
Campus infrastructure	Car parks
Campus layout	Student density, building orientation, and building scale
Context and services	Building design and building facades
Students' behavior	Students walking or staying and walking alone
Factors decreasing walkability	
Campus infrastructure	Street intersections, vehicle density, pollution and noise, and public transit
Campus layout	Large university area
Context and services	-
Students' behavior	Hot or cold weather

(Grasser et al., 2016; Vale, 2015). Furthermore, it was found that the destination increased the willingness to walk.

Zhang et al. (2020) found that the variety, frequency, and distance that students travel to and from public facilities improved walkability. Moreover, the study found that activity type (dining, visiting the library, etc.), service diversity, place vitality, and maintenance increase walkability. Pedestrian facilities and diverse community facilities also affect walkability (Grasser et al., 2016; McCormack and Shiell, 2011; Taleai and Yameqani, 2018). The results conclude that street furniture and facilities increase students' campus walkability.

Urban features and green spaces are another two factors that affect walkability (Brownson et al., 2009; Dörrzapf et al., 2019; Krenn et al., 2015). The study showed that open spaces and green areas increased students' campus walkability, while street intersections, high vehicle density, and the availability of public transit on the university campus decreased walkability. Car parks had no effect on walkability.

Safety is one of the main factors that enhances students' campus walkability. That is congruent with the results of Azmi and Karim (2012), Dörrzapf et al. (2019), and Peachey and Baller (2015).

Several studies evaluated campus walkability in relation to students' physical activity (Zhang et al., 2020). Others focused on social and individual aspects (Reyer et al., 2014; Dörrzapf et al., 2019). The friendliness of a walkable environment affects walkability (Zhang et al., 2020), and familiarity increases comfort while walking (Azmi and Karim, 2012; Long et al., 2018). It was found that easy way-finding and walking with friends increase walkability.

Frank et al. (2010), Grasser et al. (2016), McCormack and Shiell (2011), and Peachey and Baller (2015) proposed a walkability index considering student density. The results found that the density of students increased walkability. Additionally, when students walk or gather in groups along pedestrian paths, this also increases walkability.

King et al. (2020) used a different method to assess campus walkability by combining campus participants' perceptions with environmental factors. Forsyth et al. (2008) listed over 200 factors that influence walkability, including attractions and aesthetics (Long et al., 2018; Dörrzapf et al., 2019). Researchers also used a walkability measurement metric based on block length, street connectivity, and facility layout (McCormack and Shiell, 2011; Zhang et al., 2020). It was found that building design, building orientation, building facades, and building scale have no effect on walkability.

Another method was used to assess walkability based on environmental conditions (Dörrzapf et al., 2019; King et al., 2020). The results showed that pollution, noise, and hot or cold weather decreased the students' willingness to walk.

Conclusion

This study examines several issues related to students' campus walkability, including the average frequency of the campus services use by students, and determines the benchmarks needed to classify students' campus walkability as well as students' campus walkability factors. The AABU University in Mafraq, Jordan, was selected as a case study.

The average frequency of using various facilities per week was grouped into high-frequency, medium-frequency, and low-frequency categories. The bus station has a high frequency of use as it is used more than five times a week. The engineering cafeteria has a medium frequency of use as it is used from one to four times per week, while other facilities have a low frequency of use.

The study used the time benchmarks acquired from the survey to categorize walkability into three groups: convenient walkability, tolerable walkability, and weary walkability. The time benchmarks include: walking for 15 minutes from the start, which is considered convenient since students can walk comfortably; from 15 to 30 minutes, which is tolerable walkability since students can walk even when they feel tired; and after 30 minutes, weary walkability, when students cannot walk anymore.

The study examines the effect of several factors on students' campus walkability. The factors were categorized into four groups: campus infrastructure factors, campus layout factors, context and service factors, and students' behavior factors.

The factors that increase students' campus walkability include street features, proximity of buildings, space connectivity, building permeability, pedestrian pathway network, open spaces and green areas, street furniture, destinations, activity type, service diversity, place vitality, maintenance, safety, way-finding, and walking with friends.

The factors that decrease students' campus walkability include street intersections, vehicle density, pollution and noise, public transit, large university areas, and hot or cold weather. The factors that have no effect on students' campus walkability include building design, student density, building orientation, building scale, car parks, students' walking or staying, building facades, and walking alone.

References

Abley, S. (2005). *Walkability Scoping Paper*, sa001 3523. Christchurch New: Abley Transportation Consultants, 62 p.

Al al-Bayt University Annual Report 2020/2021, 2021. https://www.aabu.edu.jo/AR/Centers/QADC/Departments/SAP/Documents/annual_report 2020-2021.pdf.

Akomolafe, C. O. and Adesua, V. O. (2016). The Impact of physical facilities on students' level of motivation and academic performance in senior secondary schools in South West Nigeria. *Journal of Education and Practice*, Vol. 7, No. 4, pp. 38–42.

Azmi, D. I. and Karim, H. A. (2012). Implications of walkability towards promoting sustainable urban neighbourhood. *Procedia - Social and Behavioural Sciences*, Vol. 50, pp. 204–213. DOI: 10.1016/j.sbspro.2012.08.028.

Brownson, R. C., Hoehner, C. M., Day, K., Forsyth, A., and Sallis, J. F. (2009). Measuring the built environment for physical activity: state of the science. *American Journal of Preventive Medicine*, Vol. 36, Issue 4, pp. S99–S123.e12. DOI: 10.1016/j.amepre.2009.01.005.

Dörrzapf, L., Kovács-Győri, A., Resch, B., and Zeile, P. (2019). Defining and assessing walkability: a concept for an integrated approach using surveys, biosensors and geospatial analysis. *Urban Development Issues*, Vol. 62, pp. 5–15. DOI: 10.2478/udi-2019-0008.

Eshruq Labin, A. M. J. (2020). The relation between way-finding and built environment legibility "Effects of architectural design elements on spatial behaviour". *International Journal of Humanities and Social Science*, Vol. 10, No. 2, pp. 43–58. DOI: 10.30845/ijhss.v10n2p6.

Eshruq Labin, A., Sqour, S., Rjoub, A., Al Shawabkeh, R., and Al Husban, S. (2022). Sustainable neighbourhood evaluation criteria-design and urban values (Case study: Neighbourhoods from Al-Mafraq, Jordan). *Journal of Sustainable Architecture and Civil Engineering*, Vol. 31, No. 2, pp. 21–38. DOI: 10.5755/j01.sace.31.2.30953.

Ewing, R. and Handy, S. (2009). Measuring the unmeasurable: Urban design qualities related to walkability. *Journal of Urban Design*, Vol. 14, Issue 1, pp. 65–84. DOI: 10.1080/13574800802451155.

Forsyth, A., Hearst, M., Oakes, J. M., and Schmitz, K. H. (2008). Design and destinations: Factors influencing walking and total physical activity. *Urban Studies*, Vol. 45, No. 9, pp. 1973–1996. DOI: 10.1177/0042098008093386.

Frank, L. D. and Engelke, P. (2005). Multiple impacts of the built environment on public health: Walkable places and the exposure to air pollution. *International Regional Science Review*, Vol. 28, Issue 2, pp. 193–216. DOI: 10.1177/0160017604273853.

Frank, L. D., Sallis, J. F., Saelens, B. E., Leary, L., Cain, K., Conway, T. L., and Hess, P. M. (2010). The development of a walkability index: application to the Neighbourhood Quality of Life Study. *British Journal of Sports Medicine*, Vol. 44, Issue 13, pp. 924–933. DOI: 10.1136/bjsm.2009.058701.

Glazier, R. H., Weyman, J. T., Creatore, M. I., Gozdyra, P., Moineddin, R., Matheson, F. I., and Booth, G. L. (2012). *Development and validation of an Urban Walkability Index for Toronto, Canada.* Toronto: Toronto Community Health Profiles Partnership, 21 p.

Grasser, G., Titze, S., and Stronegger, W. J. (2016). Are residents of high-walkable areas satisfied with their neighbourhood? *Journal of Public Health*, Vol. 24, Issue 6, pp. 469–476. DOI: 10.1007/s10389-016-0744-5.

Iakimovich, D., Sukhinina, E., Sirotkin, V., Usmanov, B., and Kuleshov, A. (2022). Comparative analysis of environmental assessment systems of universities in Russia and China (using the example of greenzoom " universities and campuses" and GB/T51356-2019). *Urbanism. Architecture. Constructions/Urbanism. Arhitectura. Constructii,* Vol.13, No. 1.

King, S. B., Kaczynski, A. T., Knight Wilt, J., and Stowe, E. W. (2020). Walkability 101: A multi-method assessment of the walkability at a university campus. *SAGE Open*, Vol. 10 (2), 215824402091795. DOI: 10.1177/2158244020917954.

Knapskog, M., Hagen, O. H., Tennøy, A., and Rynning, M. K. (2019). Exploring ways of measuring walkability. *Transportation Research Procedia*, Vol. 41, pp. 264–282. DOI: 10.1016/j.trpro.2019.09.047.

Koschinsky, J. and Talen, E. (2015). Affordable housing and walkable neighbourhoods: A national urban analysis. *Cityscape*, Vol. 17, No. 2, pp. 13–56.

Krenn, P. J., Oja, P., and Titze, S. (2015). Development of a bikeability index to assess the bicycle-friendliness of urban environments. *Open Journal of Civil Engineering*, Vol. 5, No. 4, pp. 451–459. DOI: 10.4236/ojce.2015.54045.

Lee, C. and Moudon, A. V. (2006). Correlates of walking for transportation or recreation purposes. *Journal of Physical Activity and Health*, Vol. 3, Issue s1, pp. S77–S98. DOI: 10.1123/jpah.3.s1.s77.

Li, X., Maghelal, P., Tso, Y.-E., Ryan, M., Durodoye, J., Wangpatravanich, P., and Jensen, K. (2016). Evaluating walkability and bikeability in a campus setting. *Politics, Bureaucracy, and Justice*, Vol. 5, No. 2, pp. 11–29.

Long, Y., Zhao, J., Li, S., Zhou, Y., and Xu, L. (2018). The large-scale calculation of 'walk score' of main cities in China. *New Architecture*, Vol. 3, pp. 4–8.

McCormack, G. R. and Shiell, A. (2011). In search of causality: A systematic review of the relationship between the built environment and physical activity among adults. *International Journal of Behavioural Nutrition and Physical Activity*, Vol. 8 (1): 125. DOI: 10.1186/1479-5868-8-125.

Mohamaddan, S. (2010). Human walking behaviour based on different layout design using computer animation. Master Thesis, Sarawak: Universiti Malaysia Sarawak.

Peachey, A. A. and Baller, S. L. (2015). Perceived built environment characteristics of on-campus and off-campus neighbourhoods associated with physical activity of college students. *Journal of American College Health*, Vol. 63, Issue 5, pp. 337–342. DOI: 10.1080/07448481.2015.1015027.

Peiravian, F., Derrible, S., and Ijaz, F. (2014). Development and application of the Pedestrian Environment Index (PEI). *Journal of Transport Geography*, Vol. 39, pp. 73–84. DOI: 10.1016/j.jtrangeo.2014.06.020.

Pikora, T., Giles-Corti, B., Bull, F., Jamrozik, K., and Donovan, R. (2003). Developing a framework for assessment of the environmental determinants of walking and cycling. *Social Science & Medicine*, Vol. 56, Issue 8, pp. 1693–1703. DOI: 10.1016/S0277-9536(02)00163-6.

Ramli, A. and Mohd Zain, R. (2018). The impact of facilities on student's academic achievement. *Science International*, Vol. 30 (2), pp. 299–311.

Resch, B., Puetz, I., Bluemke, M., Kyriakou, K., and Miksch, J. (2020). An interdisciplinary mixed-methods approach to analyzing urban spaces: The case of urban walkability and bikeability. *International Journal of Environmental Research and Public Health,* Vol. 17, Issue 19, 6994. DOI: 10.3390/ijerph17196994.

Reyer, M., Fina, S., Siedentop, S., and Schlicht, W. (2014). Walkability is only part of the story: Walking for transportation in Stuttgart, Germany. *International Journal of Environmental Research and Public Health,* Vol. 11, Issue 6, pp. 5849–5865. DOI: 10.3390/ijerph110605849.

Saghapour, T., Moridpour, S., and Thompson, R. G. (2017). Measuring walking accessibility in metropolitan areas. *Transportation Research Record*, Vol. 2661, Issue 1, pp. 111–119. DOI: 10.3141/2661-13.

Sarkar, C., Webster, C., and Gallacher, J. (2018). Neighbourhood walkability and incidence of hypertension: Findings from the study of 429,334 UK Biobank participants. *International Journal of Hygiene and Environmental Health*, Vol. 221, Issue 3, pp. 458–468. DOI: 10.1016/j.ijheh.2018.01.009.

Silitonga, S. (2020). *Walkability;* The relationship of walking distance, walking time and walking speed. *Jurnal Rekayasa Konstruksi Mekanika Sipil*, Vol. 3, No. 1, pp. 19–26.

Sisson, S. B., McClain, J. J., and Tudor-Locke, C. (2008). Campus walkability, pedometer-determined steps, and moderate-to-vigorous physical activity: A comparison of 2 university campuses. *Journal of American College Health*, Vol. 56, Issue 5, pp. 585–592. DOI: 10.3200/JACH.56.5.585-592.

15

Taleai, M. and Yameqani, A. S. (2018). Integration of GIS, remote sensing and Multi-Criteria Evaluation tools in the search for healthy walking paths. *KSCE Journal of Civil Engineering*, Vol. 22, Issue 1, pp. 279–291. DOI: 10.1007/s12205-017-2538-x.

Vale, D. S. (2015). Transit-oriented development, integration of land use and transport, and pedestrian accessibility: Combining node-place model with pedestrian shed ratio to evaluate and classify station areas in Lisbon. *Journal of Transport Geography*, Vol. 45, pp. 70–80. DOI: 10.1016/j.jtrangeo.2015.04.009.

Wu, J. and Shen, N. (2017). Walk score method-based evaluation of social service function of urban park green lands in Futian district, Shenzhen, China. *Acta Ecologica Sinica*, Vol. 37, pp. 7483–7492. DOI: 10.5846/stxb201609191882.

Zhang, Z., Fisher, T., and Feng, G. (2020). Assessing the rationality and walkability of campus layouts. *Sustainability*, Vol. 12, Issue 23, 10116. DOI: 10.3390/su122310116.

Zhou, Y. and Long, Y. (2017). Large-scale evaluation for street walkability: Methodological improvements and the empirical application in Chengdu. *Shanghai Urban Planning Review*, Vol. 1, pp. 88–93.

ПОВЫШЕНИЕ ПЕШЕХОДНОЙ ДОСТУПНОСТИ ТЕРРИТОРИИ УНИВЕРСИТЕТА КАК ПОКАЗАТЕЛЬ УСТОЙЧИВОГО РАЗВИТИЯ

Ахлам Эшрук Лабин

Архитектурно-инженерный факультет, Университет Аль аль-Байт, Мафрак, Иордания

E-mail: ahlam.labin@aabu.edu.jo

Аннотация
Введение: В последнее время ходьба стала важным и экологичным способом передвижения для студентов университетов в их повседневной жизни. На пешеходную доступность студентов влияют характеристики и среда застройки кампуса. **Цель данного исследования** — определить временные ориентиры, необходимые для классификации пешеходной доступности территории университета, а также изучить факторы, влияющие на пешеходную доступность территории университета, которые включают четыре следующие группы: инфраструктура территории университета, планировка территории университета, среда и услуги, а также поведение студентов. **Методы:** Студентам инженерного факультета Университета Аль аль-Байт в Мафраке, Иордания, было предложено заполнить анкету. Для анализа данных и получения результатов использовалась программа SPSS. В соответствии с полученными **результатами** пешеходная доступность для обучающихся подразделяется на следующие категории: комфортная, приемлемая и утомляющая. Соответствующие факторы подразделяются на факторы, увеличивающие, уменьшающие и не оказывающие влияния на пешеходную доступность территории университета. Значимость исследования обусловлена изучением пешеходной доступности в связи с одним из основных способов передвижения по территории университета. Она считается важным компонентом устойчивого развития и используется при проектировании для определения доступности различных услуг, необходимых студентам университета.

Ключевые слова: устойчивое развитие; пешеходная доступность; поведение пешеходов; пешеходная доступность территории университета.

EVALUATION OF SHIPPING CONTAINER USE AS HOUSING SOLUTIONS FOR GENERATION Z AS CHANGING CONSUMERS

Burcu Erdal*, Çiğdem Tekin

Mimar Sinan Fine Arts University
Meclisi Mebusan Cad. No. 24. Findikli, Beyoglu, 34427, Istanbul, Turkey

*Corresponding author's e-mail: burcuerdal78@outlook.com

Abstract

Introduction: The architectural demands of the near future will have very different characteristics from those of the recent past. With the change in means of communication and transportation, the possibilities of rapid relocation and easy communication have altered many concepts and traditions associated with place. This change will alter the utilization and scale of space. Architecture is undergoing significant changes with Industry 4.0. The consumer of the near future who will demand this today is Generation Z. In parallel, the architectural environment has inherited many environmental problems that started in the recent past and continue to increase in severity. In this rapid change/transformation, environmental problems require sustainable solutions that can be in harmony with nature, which is much more natural than developing technology.

The basis of this study is using shipping containers as a sustainable solution and determining the approach of Generation Z as changing consumers to this solution. **The study aims** to determine how Generation Z, living in Turkey, evaluates the use of shipping containers as an alternative to housing. **Methods:** In the course of the study, a survey was conducted with participants who are both members of Generation Z and architecture students. The purposive sampling method was used in the research.

Keywords: shipping container house; sustainable architecture; generations; Gen Z.

Introduction

With the global environmental problems that started in the 1970s and continue today, solutions have been sought through national and international cooperation, regulations, and structural changes. The construction sector's priority is to reduce the use of primary resources and energy consumption, and to change the approach to architectural production in a way that supports this goal, such as through recycling, reuse, and re-purposing.

For example, aside from re-purposing an existing building, incorporating systems that have been produced for a different purpose into architectural production offers an alternative source of re-purposing. The changing user/consumer plays a crucial role in evaluating the effectiveness of these reused resources. While industrialization and subsequent technology have provided benefits in many areas that can facilitate life, the user/consumer has also undergone significant changes during this period. These changes have also transformed the architectural needs and desires of consumers.

Each country has different national characteristics, with technology developing within the social, cultural, and political environment, as well as the needs and behaviors of the users and consumers. Technology, architectural environment, and consumer behavior have different approaches and scales of development within the unique conditions of each country. On the other hand, each country interprets the global environmental problem experienced by the world today differently within its own conditions and takes different measures. Within these measures, the construction sector also adopts various approaches.

The rapid changes in technology not only offer new construction systems and material options to the architectural production environment, but also alter the factors that influence architecture, with expanding and diversifying stakeholders, as well as changing consumers/users/generations, changing needs and comfort requirements, as well as exploring different spatial concepts within the production/design environment.

Changing consumers/generations have started to have a say in the production environment, especially in post-Fordism after 1980. The fast pace of the industry, coupled with individual preferences, has led to mass customization, where design and production are tailored to the individual. This has created a growing demand for personalized products in the neoliberal market. This situation implies that consumers/generations will take on a more active role in the near future.

In the near future, it will be more efficient to understand the different generations and plan the production environment in line with their preferences. While consumers/generations form

the basis of near-future scenarios, it is also important to consider the environmental dimension of the solutions to be produced and the diminishing world resources. For this reason, it is very important to understand the preferability and environmental impact of the solutions being developed for consumers/generations.

This study focuses on Generation Z, the consumers of the near future, taking into account the changing consumer/generation characteristics. Therefore, it is important to determine the consumption characteristics and architectural preferences of Generation Z. The prominent characteristics of Generation Z in the research conducted are being mobile, easily bored, digitally addicted, and sensitive to the environment. Given these characteristics, the preferability of shipping containers as housing for Generation Z has been questioned.

The fact that the issue of consumption will be quite important in the near future, especially for Generation Z, and that the economy is based on continuous consumption, will necessitate taking precautions. Due to the recyclable structure, the use of shipping containers in architecture can contribute to sustainable architecture with economical, minimal, portable structures as an alternative solution to traditional building materials.

There are many architectural examples designed and constructed using shipping containers. Although there are few examples in Turkey, both academically and practically, a significant amount of shipping container waste is regularly generated. Containers manufactured for international transportation are melted down at the end of their useful life (seven years) in order to be recycled since their material is steel. Considering the energy, labor, and cost spent on this process, it is more appropriate to use it as a building material. Due to their robust construction and dimensions that are suitable for humans, it is possible to use shipping containers as standalone buildings or as building materials in a modular system by stacking them on top of each other or placing them side by side. It should be noted that their use is rapidly increasing.

Generations as Changing Consumers

With the dynamic nature of industrialization and its evolution over time, production methods and consumption preferences have undergone significant changes from the past to the present.

Starting in the 18th century, mechanization and Fordism, which developed at the end of the 19th century, met basic needs through mass production. Until the third industrial revolution, manufacturers managed and directed consumer demands. The effects of Fordism continued until the 1970s, when the understanding of post-Fordism supporting production in line with the demands of the consumer started developing. Since 2000, consumers have

been increasingly involved in the production and design process.

Technologies, political systems, and social institutions have changed in the three industrial periods, and this change has been effective not only in the field of industry but also in people's perspectives, their relations with each other, and their interactions with the world (Halis, 2012). Consumer changes became more evident, especially after the First World War, leading to the emergence of the concept of "generation" and the classification into generations. Although it is commonly believed that generations change every twenty years, it is not simply a matter of being born in the same period; they also need to experience common political, economic, and sociological events together and develop shared ways of thinking, experiences, and reactions (Mannheim, 1952).

The social structure has been influenced by significant historical events, wars, and economic crises, leading to changes in the behaviors, values, and attitudes of individuals within that society (Arslan and Staub, 2015). These events shape the attitudes and behaviors of individuals within the same generation, as well as their common reactions to events within the same period (Akdemir et al., 2013).

The behaviors exhibited by each generation have changed depending on the dynamics of the period they live in, and this is reflected in their consumption habits based on the conditions of the period they live in. Production and consumption have become interdependent (Table 1).

Political, economic, and development policies, as well as culture and traditions, have led to the emergence of different consumer behaviors in each country, based on its unique historical period and social structure. It is necessary to examine and assess the production and consumption environment in Turkey within the particular conditions (Table 2).

For a consumer, consumption implies not only nutrition, healthcare, and clothing, but also demands for architectural structures and material preferences. Architectural structures are also changing depending on the preferences and needs of the consumer.

With the changing consumer/user (generation) and world conditions, the main idea of designs in future housing production has evolved from the past to the present. In particular, the concepts of sustainability and mobility have come to the forefront.

The consumption behavior and architectural preferences of each generation differ from one another. The consumer/user of the near future is Generation Z. When we look at the distribution of this generation in Turkey, Generation Y and Generation Z constitute a significant portion of the population. The highest proportion in Turkey's population is 31.16 % of Generation Y individuals between the ages of 19 and 40, while the proportion of Generation Z,

Table 1. **Generations and Their Characteristics (Demirler, 2019; Saygın, 2021; Yazıcı, 2019)**
(developed based on these sources)

Period	Generations	Generation Characteristics	Important Developments in the Generation Period	Cultural Elements	Consumption Behavior
1925–1945	Traditionalists / Silent Generations	Dislikes taking risks, complies with social requirements, respectful, self-restrained, disciplined, stable, works for a living	World Wars I and II, economic difficulties, and the Great Depression	large family, strong neighborhood	Consuming necessities
1946–1964	Baby Booming	Rule-oriented, hardworking, leader, patient, loyal, lives to work, respects authority, finds change risky, bohemian, values art	Post-war mobilization, migration, economic relief, human rights, transition to a multi-party era	Extended family, the generation that first raises their children and then takes care of their elders in the same household	Careful, conscious consumer, information addict, willing to be informed about products and make choices in line with core values
1965–1979	Generation X	Careful, conscious consumer, information addict, willing to be informed about products and make choices in line with core values	Oil crisis, introduction of household appliances into daily life, rise of radio and TV rapid changes development and sale of the first personal computer	Decrease in the marriage rate, shrinking and disintegration of the family, individualistic structure	The first generation where the impact of mass consumption is dominant and brand loyalty is present
1980–1999	Generation Y	Effective use of technology being the center of attention, having high expectations, having clear goals, socializing, valuing freedom, and being independent individuals who are not loyal to authority. Focused on getting rich, consuming, spending, and constantly being on the move, traveling	Global high competition global brand value is important, digital media, economy, and intercultural relations are intense	Complex family structure with elderly parents, nuclear family, prevalence of divorce	Quickly bored, consumption-oriented; the telephone is an important tool for consumption. Internet shopping is widespread, and people see consumption as entertainment or a game. Desire to be special and unique, with a high tendency to consume products and brands that will make them feel special. High brand awareness, people are conformist while being conscious and questioning. Active in sustainability, ethics, and social problems
2000–	Generation Z	Internet generation, remote socialization, intense desire for independence. No geographical boundaries, the idea that everything should be their own. Open to change, can quickly give up conditions	Technology, communication tools, transportation facilities	Poor family relations and communication	They want to be producers rather than consumers of what is offered to them They influence consumption trends There is no brand loyalty. They have a tendency to buy, consume, and then re-consume immediately They have a transient and changeable nature They can take on different roles as consumers: sustainable, ecological consumers

Table 2. **20th Century Consumption and Production Environment**

Period	Generations	Economic Regime	Production System	Role of the Consumer	Consumption Behavior	Efficiency in Production
1925–1945	Traditionalists / Silent Generations	Statism/ Liberalism	Fordism (mass production)	Consumers are homogeneous and passive	Passive, resistant to change, loyal	Design enabled by the manufacturer
1946–1964	Baby Booming	Liberalism				
1965–1979	Generation X	Liberalism				
1980–1999	Generation Y	Neo-liberalism	Post-Fordism (flexible production, mass customization)	Consumers are heterogeneous and active	Adventurous, brave, easily bored, always ready to move to new places	Design enabled by the consumer
2000–	Generation Z	Neo-liberalism				

which consists of individuals under the age of 19, is 30.71 % (Yıldız, 2021). Therefore, it is Generation Z that will be effective in shaping the architectural production environment of the near future.

Generation Z and Their Preferences

Twenge (2006) coined the term "iGeneration" for the generation born in the period when the Internet and mobile phones were widely used. This term comes from the initials of the words "iPhone", "Internet", and "individualism". Referring to Generation Z, who cannot imagine life without the Internet, Acılıoğlu (2015) stated that the devices they use to connect to the Internet and social media are almost like a limb. This generation, which constantly checks their mobile phones, continues to live their lives in virtual environments (Acılıoğlu, 2015; Twenge, 2018).

This generation has the ability to perform many tasks simultaneously and develop a specific focus for each of them, as rapidly advancing technology provides the ability to easily use various digital tools. With these abilities, it will have the potential to adapt to a different working order by creating a new working system in case of a possible encounter with artificial intelligence in the future. The ability to perform almost all their work through computers leads this generation to have a marked tendency to laziness, and these living conditions cause them to socialize in a virtual environment, that is, through computers (İnce, 2018)

In addition, seeking their rights to the end, being able to express their wishes and demands easily, establishing social relations with different social groups, and being creative are the characteristics of this generation (Aydın and Başol, 2014).

This generation, for whom speed is important, is affected by consumption, and their consumption tendencies are influenced by the discourses of "must have now" and "buy now" (Batı, 2015).

In research on the future of Generation Z, it can be observed that their incomes will be higher compared to other generations. They will not want to be subject to geographical restrictions, and social roles will change in male-female relationships.

Additionally, there will be an intense desire to live alone (Şenbir, 2004).

In Turkey, Generation Z is also referred to as the Crystal Generation. Generation Z in Turkey can quickly adapt to global trends thanks to the Internet and new technologies, which align with the characteristics of the period in which they were born. Compared to other generations, they have almost all the opportunities for consumption. For this reason, shopping malls became one of the favorite places for consumption in the 2000s (Başcı, 2015). However, nowadays, they can easily access all products via the Internet. This consumption shows that the need for space has diminished.

Generation Z can be described as a creative generation. They want to be producers instead of being consumers of the goods offered to them. In this context, they create their own content (Kuran, 2018). The generation born on the Internet can be called the speed generation, and the words "right now» are associated with them. They are heavily influenced by consumption, but they also have a profile that affects consumption trends (Altuntuğ, 2012). This generation, which is very active in using technology, is addicted. They can make instant, simultaneous, and multiple decisions. Generation Z is oriented towards new consumption products, desiring immediate access to the products they want to consume (Altuntuğ, 2012). Generation Z, which is not reliable in brand loyalty, exhibits variable and temporary attitudes (Özel, 2017).

In recent years, there has been an observed increase in places such as cafes and restaurants that directly target consumers. The rapidly increasing new-generation coffee chains are among these examples. These spaces, which offer the opportunity to work, relax, and socialize, provide Internet access services and comfortable furniture choices to ensure that customers spend more time there. Generation Z, which exhibits more individualistic behaviors compared to other generations, makes up a significant portion of the market in these areas. While they may not currently have the opportunity to express their architectural preferences directly,

the participants in the consumption environment play a significant role in shaping their social spaces, particularly through the trends of their generation. Generation Z has started to involuntarily actively participate in shaping, decorating, and implementing tools in the architecture of social spaces.

While individual behavior is an important issue for Generation Z, digital platforms have allowed them to create their own avatars, design their homes, and socialize in a new world where their freedom is unlimited, and they can choose the city they live in. There are opinions that this situation may create the problem of loneliness for this generation in the future (Table 2) (Demirler, 2019; Saygın, 2021; Yazıcı, 2019).

On the other hand, "digital addiction", which is seen as the plague of the age, has made individuals lonely. Loneliness resulting from digital addiction was identified in young people aged 16–24 who took part in the "Loneliness Study" conducted by the University of Manchester, which involved 55,000 participants. Prof. Dr. Nevzat Tarhan, who believes that the situation is no different for Turkey and that digital addiction causes social isolation in young people, stated that this situation is also reflected in divorces (Milliyet, 2019).

The events that took place in the world and in Turkey during the period in which they live have behaviorally influenced this generation, causing it to be more aware and sensitive.

However, in this new world, the decline in physical activity, the decrease in physical labor, and the fact that they only view the world from behind a screen significantly affect their spatial preferences. It should also be taken into consideration how the change in the social environment, the concept of family, the disappearance of the concept of "home" and the sense of belonging attributed to houses will affect this generation psychologically and sociologically. This may lead to them becoming semi-robots in the future.

Generation Z and Mobility

Man is naturally inclined to move. Thanks to this feature, people should not be confined to one place. This aspect of humanity has been a source of inspiration for architects and designers. Thanks to the advancements in technology, the concepts of power, speed, intelligence, and beauty have gained significant importance. When we examine movable structures, we are referring to structures that can be moved from one place to another. Thanks to this feature, they should respond positively to the needs of users over time in order to maintain their functionality in everyday life (Ekmekçi, 2005).

Today, the concept of mobile housing is being discussed more frequently. The goal is to maximize the use of these spaces by reducing their size through the shrinking and streamlining of their internal equipment. The concept of mobility can be exemplified by the fact that a dwelling can be produced in one place and transported to the region where it will be located. Additionally, the dwelling can be transported without being in a specific place by attaching wheels or a similar device to it. In order for these features to be realized, the material should be lightweight, flexible, and the modular parts should be removable (Kronenburg, 2002).

Mobile housing can be used on land as well as on water. They can be a permanent or non-permanent structure. Today, examples of these include caravans, prefabricated houses, modular houses, container houses, tiny houses, disaster houses, sea vehicles, and floating houses (Tuncel, 2007).

In the information age, it has become possible for employees to be mobile. Thanks to portable technological devices such as mobile phones, tablets, and computers, it is now possible to manage work life from anywhere. While mobile architecture was previously seen as a temporary solution that rejected the economic alternative concept or disposable logic, today it has evolved into a building alternative to fixed structures with ecological consciousness. It has also been defined as an experimental resource for fixed structures, with its flexible application and economy (Kronenburg, 2002).

Generation Z can perceive the world not only physically but also virtually, as they have no spatial boundaries. They spend an average of more than three hours a day on the computer outside of work or school, and the fact that this time continues to increase indicates that the physical environment is not as significant (Stillman and Stillman, 2018).

The fact that they were born into a mobile world and do almost all of their work with digital tools, such as mobile phones and tablet computers, indicates that the needs of this generation should be taken into account. They may prefer a more ecological lifestyle due to their awareness, involvement in social responsibility projects, and sensitivity to issues such as the climate crisis, which is greater than that of previous generations.

As the pace of mobile working increases, it is predicted that residences and lifestyles will also become more mobile. In the research conducted by the International Data Corporation (IDC) to measure the number of mobile workers worldwide, it was stated that the number of mobile workers would reach 1.3 billion by 2015. The ratio of this data to the world population constitutes 37.2 % of the total labor force (Abh, 2024).

It is observed that the mobile-collar population is also on the rise in Turkey. This new working model, which appears to be more comfortable, also seems to be a more cost-effective option for companies (Adıgüzel et al., 2014).

Mobile and Sustainable Solution: Shipping Containers

80 % of global trade is facilitated by maritime transportation. Containers produced in standard

sizes are used to facilitate transportation and ensure quick and efficient loading and unloading with minimal labor. Containers, whose main purpose is to carry cargo, are manufactured from robust and lightweight materials for transporting heavy tonnage loads in various types and sizes to accommodate all kinds of cargo. They have flexible features for purposes such as transportation, relocation, and stacking.

A container used in the international transport sector completes its service life in terms of transportation in a short period of seven years. This situation creates a large amount of high-quality waste every year (ISBU Association, 2017). Containers, whose main raw material is steel, are produced using a technology that is difficult to implement and requires high energy. For this reason, the raw materials from containers that have completed their service life can be reused. However, 8000 kWh of electrical energy must be consumed for the melting process of this 3.5-ton steel box. The energy required to recycle this material and use it for a container house is approximately 400 kWh. This accounts for 5 % of the total energy to be consumed (Islam et al., 2016). For this reason, the fact that containers generate high-quality waste as well as the continuous waste generation in high volumes annually attract the attention of designers with an environmentally sensitive and sustainable approach.

These wastes constitute an important resource for re-purposing. It is a valuable resource that can be especially useful in architectural space production. For this reason, when considering containers as an alternative to existing building materials for sustainable architecture, many architects and companies have focused on this issue.

The existence of different types of containers designed for transporting different types of cargo

Fig. 1. Construction Elements of Shipping Containers (Shen, J., Copertaro, B., Zhang, X., Koke, J., Kaufmann, P., & Krause, S, 2019)

allows each to be evaluated for distinct architectural purposes. Their most widely recognized advantages, including construction time, portability, stackability, recyclability, and low cost, are also viewed disadvantageously due to high thermal conductivity.

In architecture, the most preferred containers are 20-foot, 40-foot, and 40-foot HC (High Cube) containers, which are extensively used in international trade. These containers, commonly used for general cargo transportation, can accommodate various types of cargo, whether palletized or non-palletized, that can pass through their doors (Demirlioğlu, 2008) (Fig. 1).

Re-purposing containers provides a sustainable solution that offers various living space possibilities in mobile or fixed configurations at different scales. While this solution may not cater to the comfort preferences of every consumer, it does address the consumer's desire for excitement and action.

Although there are numerous examples of architectural container use, it has not yet become widespread in Turkey. However, considering the significant volume of maritime trade in Turkey and the substantial amount of container waste generated, the utilization of these containers in architecture could offer a solution.

Survey and Results

During the research, it was decided to focus on Generation Z, as this demographic is crucial for the near future and possesses distinct characteristics compared to other generations. Furthermore, given that this generation comprises aspiring architects who have begun their architectural education, it was decided that the survey would include participants from Generation Z as well as architecture students. This approach may offer insights into future architectural trends.

In the research, a survey was conducted with Generation Z, which consists of first- and second-year students at Mimar Sinan University, Faculty of Architecture, Department of Architecture.

Before the survey, information about shipping containers was provided, along with visuals of various plan solutions designed on the subject. Three-dimensional designs were prepared using different container types, and visuals related to their application on different types of land were shared. Therefore, it was ensured that the participants could visually understand the different container layout solutions and their relationship with the immediate environment (Fig. 2).

A total of 22 questions, divided into three main sections, were directed to the Generation Z students of the Department of Architecture at Mimar Sinan University. The survey was conducted among approximately 175 people born after 2000.

Study Sample Definition

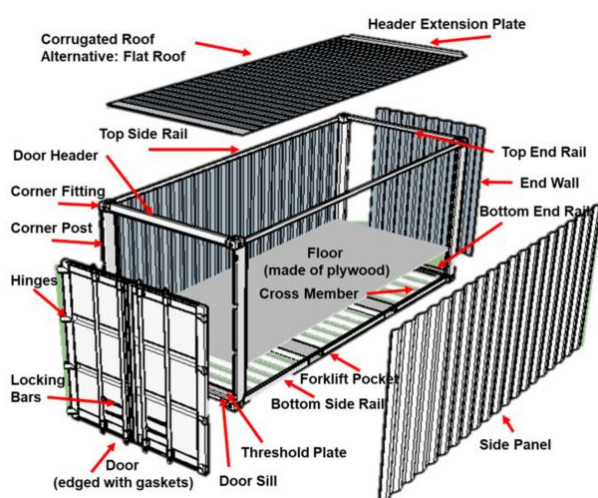The population of the study consisted of first- and second-year students of the Department

of Architecture at Mimar Sinan Fine Arts University. The total number of the two classes was 200. The sample consisted of 175 people who voluntarily participated in the study. The questionnaires were conducted using Google Forms.

The purposive sampling method was used in the study. Purposive sampling allows for in-depth research by selecting information-rich situations based on the purpose of the study. It is preferable when you want to work in one or more specific cases that meet certain criteria or have certain characteristics. Since Generation Z was the target of this study, the purposive sampling method was appropriate.

The number of samples to be drawn from the specific population was determined to be 80 people for p = 0.50 and q = 0.50 (Table 3), with a 0.05 sampling error, as developed by Yazıcıoğlu and Erdoğan (2004).

The formula used to determine the sample size from the determined universe is as follows:

- Sample size;
- Main population (universe) (200 people);
- Probability of occurrence of the event (0,5);
- Probability that the event will not occur (0,5);
- t test level (1,96);
- Margin of error (5 %).

With a 5 % margin of error, it was calculated that the minimum sample size to represent the main population should be 80 people.

In addition to the classical approach to sample selection given above, another approach is to determine the number of samples according to power analysis. Power analysis reveals at least how many samples are required in any analysis. In other words, it determines the number of samples with a different approach.

Since relationship analysis was to be performed in the study, the minimum number of samples required was determined by obtaining the results of power analysis for these two methods. Power analysis was conducted using G*POWER 3.1. According to Cohen (1988) and Prajapati et al. (2010), a statistical power of 1-β = 0.80 is considered sufficient. The results were obtained by calculating correlations and group differences. Statistical significance α = 0.05.

Fig. 2. Shipping Container House Design

Table 3. **Sample Sizes (Yazıcıoğlu and Erdoğan, 2004)**

Population Size	± 0.03 sampling error (d)			± 0.05 sampling error (d)			± 0.10 sampling error (d)		
	p=0.5 q=0.5	p=0.8 q=0.2	p=0.3 q=0.7	p=0.5 q=0.5	p=0.8 q=0.2	p=0.3 q=0.7	p=0.5 q=0.5	p=0.8 q=0.2	p=0.3 q=0.7
100	92	87	90	80	71	77	49	38	45
500	341	289	321	217	165	196	81	55	70
750	441	358	409	254	185	226	85	57	73
1000	516	406	473	278	198	244	88	58	75
2500	748	537	660	333	224	286	93	60	78
5000	880	601	760	357	234	303	94	61	79
10000	964	639	823	370	240	313	95	61	80
25000	1023	665	865	378	244	319	96	61	80
50000	1045	674	881	381	245	321	96	61	81
100000	1056	678	888	383	245	322	96	61	81
100000	1066	682	896	384	246	323	96	61	81
100 million	1067	683	896	384	245	323	96	61	81

Based on the power analysis, the validity of the study was determined to require a minimum of 115 samples for the relationship analysis. In this study, compliance was achieved with 175 people (Fig. 3).

Data Collection Tool

This subject was organized under three main headings. In the questionnaire, general questions were initially asked. The first part began with inquiries about age, gender, type of residence, and previous experience with container-style housing.

In the first part, the spatial preferences of Generation Z were questioned. In this context, first of all, the questionnaire addressed their working space, living preferences, and housing preferences. After gathering this information, the participants were asked to rank their spatial priorities. An attempt was made to determine the connection between the priorities of items in space and the spaces themselves.

In the second part, the economic perspectives of Generation Z on housing were examined. First, information about the family structure was gathered. Then the connection between this structure and economic conditions was analyzed. An attempt was also made to determine if the housing they live in is a choice or a necessity. The study also aimed to determine whether they would continue with this arrangement in the future, despite their preference to live with their families. In addition, their perspectives on whether they see housing as a commercial tool or for shelter purposes were analyzed. The goal was to determine whether housing is an economically beneficial element and whether it can be considered a life choice. Additionally, as architecture students, they were asked about their perspective on building the houses they design under current economic conditions.

In the third and final part, information was collected about their preferences for sustainable architecture, mobile architecture, and modular architecture, considering their future housing preferences and their perspectives on the global climate crisis. For this purpose, efforts were made to gather information about the preferences for mobile, addable, and removable houses in line with current conditions, as well as to explore the potential for adopting this style in response to evolving family structures and future lifestyles. The importance of comfort, along with the principle of sustainable housing preferences, was questioned, and efforts were made to gather information about the conditions and limits under which this could be achieved. Efforts were also made to understand the conditions under which the preferences for recyclable materials, an important aspect of sustainability, can be prioritized.

Research Method

The data obtained were analyzed using the IBM SPSS 27.0 software package. At the first stage, percentage and frequency distributions
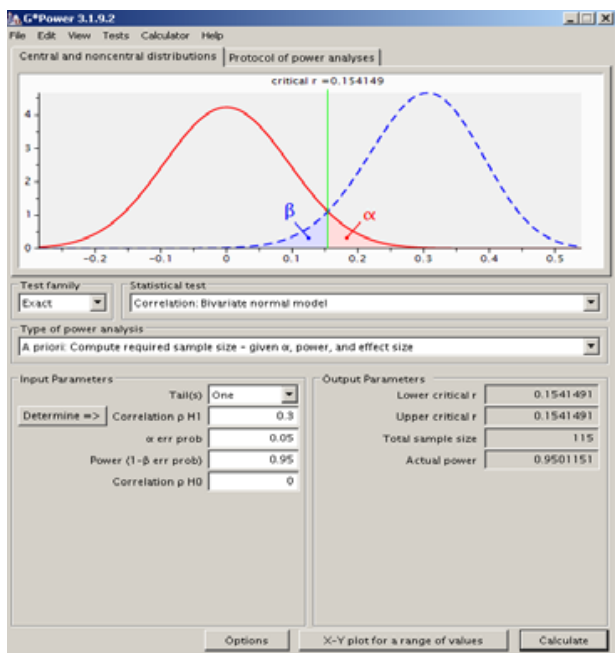

Fig. 3. Power Analysis Results for Relationship Analysis Screen Output

of demographic and general information were presented.

Findings Related to the Demographic Characteristics of the Participants

When the genders of the participants were analyzed, it was observed that 72.0 % were female and 28.0 % were male. When the living arrangements of the participants were analyzed, it was observed that 58.9 % of them lived with their families, 10.3 % lived alone, 8.0 % lived in dormitories, and 22.9 % lived temporarily in student housing.

When the participants were asked about their previous experiences with housing such as containers, caravans, bungalows, and tiny houses, it was found that 30.3 % of them had such experience, while 69.7 % had not.

When the preferred working environments were analyzed (Table 4), it was observed that 28.6 % of the participants would prefer working from home (home office), 34.3 % would prefer working from an office, 28 % would prefer co-working or working independently in an open office, and 9.1 % would prefer a corporate space or cafe.

When the participants were asked where they would prefer their residence to be located, it was observed that 78.3 % of them preferred the city center, while 21.7 % preferred the city outskirts. When the participants' preferences for a second residence

in the future, such as a summer house or weekend residence, were analyzed, it was observed that 78.2 % would prefer that, 2.9 % would not prefer that, and 18.9 % would consider it depending on the conditions.

Table 5 presents information on the priorities of the individuals participating in the study in terms of housing characteristics preferences. Safety for 4.0 % of the participants, comfort for 5.7 %, functionality for 32.6 %, accessibility for 24.6 %, proximity to social life for 35.4 %, mobility/portability for 96.0 %, space dimensions for 60.0 %, and design for 46.3 % were not among the priorities.

Table 6 presents information on the priorities of the individuals participating in the study in terms of housing type preferences. Apartment units for 31.4 % of the participants, detached housing for 1.1 %, residences for 30.3 %, housing estates for 22.3 %, public housing for 65.1 %, container buildings for 72.6 %, caravans for 55.4 %, and tiny houses for 36.6 % were not among the priorities.

Table 7 presents information on the priorities of the individuals participating in the study in the terms of the number of rooms. Studio apartments for 56.0 % of the participants, 1+0 houses for 58.9 %, 1+1 houses for 31.4 %, 2+1 houses for 14.9 %, 2+2 houses for 38.3 %, 3+1 houses for 17.7 %, 3+2 houses for 64.6 %, 4+1 houses for 59.4 %, and 4+2 houses for 80.6 % were not among the priorities.

Table 4. **Values of Generation Z's Spatial Preferences in Housing**

	n	%	
What kind of working environment do you find close to you?			
Home Office	50	28.6	
Office	60	34.3	
Co Working	49	28.0	
Corporate Area or Cafe	16	9.1	
Where would you prefer your residence to be located?			
City Center	137	78.3	
Out of the City	38	21.7	
Would you prefer a second home in the future, such as holiday home, weekend residence, etc?			
Yes	137	78.2	
No	5	2.9	
Depending on the conditions	33	18.9	

Table 5. **(Section I) Spatial Preferences of Generation Z in Housing / Percentage Distribution of Priorities in Housing Characteristics Preferences**

	1st Preference		2nd Preference		3rd Preference		4th Preference		5th Preference		Do not prefer	
	N	%	n	%	n	%	n	%	n	%	N	%
Safety	102	**58.3**	27	15.4	15	8.6	12	6.9	12	6.9	7	4.0
Comfort	34	19.4	67	**38.3**	40	22.9	17	9.7	7	4.0	10	5.7
Functionality	8	4.6	30	17.1	29	16.6	22	12.6	29	16.6	57	**32.6**
Accessibility	15	8.6	27	15.4	39	22.3	34	19.4	17	9.7	43	**24.6**
Proximity to social life	9	5.1	11	6.3	25	14.3	36	20.6	32	18.3	62	**35.4**
Mobile/Portable	1	0.6	0	0	0	0	1	0.6	5	2.9	168	**96.0**
Space dimensions	1	0.6	5	2.9	9	5.1	24	13.7	31	17.7	105	**60.0**
Design	5	2.9	8	4.6	17	9.7	26	14.9	38	21.7	81	**46.3**

Table 6. **(Section I) Spatial Preferences of Generation Z in Housing / Percentage Distribution of Priorities in Housing Type Preferences**

	1st Preference		2nd Preference		3rd Preference		4th Preference		5th Preference		Do not prefer	
	N	%	n	%	N	%	n	%	n	%	n	%
Apartment unit	8	4.6	29	16.6	22	12.6	35	20.0	26	14.9	55	31.4
Detached housing	132	75.4	19	10.9	13	7.4	7	4.0	2	1.1	2	1.1
Residence	15	8.6	44	25.1	28	16.0	21	12.0	14	8.0	53	30.3
Housing estate	10	5.7	39	22.3	43	24.6	25	14.3	19	10.9	39	22.3
Public housing	1	0.6	6	3.4	9	5.1	20	11.4	25	14.3	114	65.1
Container building	3	1.7	1	0.6	15	8.6	15	8.6	14	8.0	127	72.6
Caravan	4	2.3	13	7.4	17	9.7	17	9.7	27	15.4	97	55.4
Tiny house	2	1.1	23	13.1	25	14.3	26	14.9	35	20.0	64	36.6

Table 8 presents information on the priorities of the individuals participating in the study in terms of space preferences. The living area for 2.9 % of the participants, kitchen for 4.0 %, bedroom for 2.9 %, toilet/bathroom for 29.1 %, study for 18.9 %, pantry for 97.1 %, laundry room for 95.4 %, hobby room for 56.0 % were not among the priorities.

Table 9 presents information on the priorities of the individuals participating in the study in terms of housing items. An armchair/couch for 15.4 % of the participants, dining table/chairs for 57.7 %, bed for 10.9 %, refrigerator for 26.9 %, TV set for 82.9 %, washing machine for 54.9 %, oven/microwave for 82.9 %, work desk for 37.1 %, coffee table for 96.0 %, wardrobe for 50.9 %, dryer for 97.1 %, iron / ironing board for 96.6 % were not among the priorities.

Table 10 presents information on the respondents' perception of housing as a commercial commodity.

Table 11 presents information on the approaches of the individuals participating in the study to their future residences.

Results

Based on the results of the questionnaire in Section I, which aimed to determine the spatial preferences of Generation Z in housing, the following can be concluded.

Even though the participants have not yet experienced working life, when we consider their working environment preferences, they show equal interest in working from home (home office), public space, or independent co-working place. Due to their digital predisposition, they have the ability to work from anywhere.

In terms of their housing preferences, it is evident that safety is of primary importance, followed by comfort. It should also be noted that the fact that safety is the top priority for Generation Z living in Turkey, whose behavior is influenced by the events in the country, reflects the atmosphere they live in. The fact that safety comes before design shows that the impact of the conditions they live in is quite essential for a Generation Z member who is a future architect.

This generation prefers a detached house (75.4 %), but they want to stay close to the city without leaving urban life.

Once again, the housing preferences of this generation are influenced by the country's economic conditions. The responses "depending on the conditions" suggest that the situation may change depending on the economy.

When choosing a house, 2+1 houses are the first preference (28 %). Preferences for 1+1 and 3+1 houses are close in percentage. The participants preferred small-scale housing, such as 1+1 and 2+1 units. This indicates the preference for living in smaller, minimal spaces is coming to the forefront.

When we look at the data on space priorities when choosing a house, it can be noted that

Table 7. **(Section I) Preferences of Generation Z in Housing / Percentage Distribution of Priorities in the Number of Rooms**

	1st Preference		2nd Preference		3rd Preference		4th Preference		5th Preference		Do not prefer	
	N	%	N	%	n	%	n	%	n	%	n	%
Studio apartment	10	5.7	6	3.4	13	7.4	18	10.3	30	17.1	98	56.0
1+0 house	4	2.3	10	5.7	21	12.0	24	13.7	13	7.4	103	58.9
1+1 house	31	17.7	29	16.6	33	18.9	14	8.0	13	7.4	55	31.4
2+1 house	49	28.0	44	25.1	21	12.0	24	13.7	11	6.3	26	14.9
2+2 house	7	4.0	20	11.4	24	13.7	22	12.6	35	20.0	67	38.3
3+1 house	32	18.3	28	16.0	25	14.3	37	21.1	22	12.6	31	17.7
3+2 house	6	3.4	13	7.4	22	12.6	9	5.1	12	6.9	113	64.6
4+1 house	16	9.1	19	10.9	9	5.1	13	7.4	14	8.0	104	59.4
4+2 house	18	10.3	4	2.3	2	1.1	2	1.1	8	4.6	141	80.6

Table 8. (**Section I) Spatial Preferences of Generation Z in Housing / Percentage Distribution of Priorities in Spatial Preferences in Housing**

	1st Preference		2nd Preference		3rd Preference		4th Preference		5th Preference		Do not prefer	
	N	%	N	%	N	%	n	%	n	%	n	%
Living space	85	48.6	23	13.1	25	14.3	24	13.7	13	7.4	5	2.9
Kitchen	10	5.7	46	26.3	53	30.3	35	20.0	24	13.7	7	4.0
Bedroom	38	21.7	48	27.4	43	24.6	29	16.6	12	6.9	5	2.9
Toilet/bathroom	18	10.3	22	12.6	22	12.6	37	21.1	25	14.3	51	29.1
Study	19	10.9	25	14.3	19	10.9	25	14.3	54	14.3	33	18.9
Pantry	0	0	0	0	2	1.1	1	0.6	2	1.1	170	97.1
Laundry room	0	0	0	0	0	0	3	1.7	5	2.9	167	95.4
Hobby room	5	2.9	11	6.3	10	5.7	17	9.7	34	19.4	98	56.0

Table 9. **(Section I) Spatial Preferences of Generation Z in Housing / Percentage Distribution of Priorities in Housing Items**

	1st Preference		2nd Preference		3rd Preference		4th Preference		5th Preference		Do not prefer	
	N	%	n	%	n	%	n	%	n	%	n	%
Armchair/couch	46	26.3	46	26.3	26	14.9	16	9.1	14	8.0	27	15.4
Dining table / chairs	0	0	13	7.4	21	12.0	24	13.7	16	9.1	101	57.7
Bed	85	48.6	36	20.6	17	9.7	8	4.6	10	5.7	19	10.9
Refrigerator	8	4.6	37	21.1	27	15.4	34	19.4	22	12.6	47	26.9
TV set	4	2.3	3	1.7	8	4.6	8	4.6	7	4.0	145	82.9
Washing machine	1	0.6	8	4.6	20	11.4	17	9.7	33	18.9	96	54.9
Oven/microwave	2	1.1	1	0.6	5	2.9	11	6.3	11	6.3	145	82.9
Work desk	26	14.9	20	11.4	28	16.0	18	10.3	18	10.3	65	37.1
Coffee table	0	0	0	0	0	0	6	3.4	1	0.6	168	96.0
Wardrobe	3	1.7	8	4.6	21	12.0	25	14.3	29	16.6	89	50.9
Dryer	0	0	1	0.6	0	0	2	1.1	2	1.1	170	97.1
Iron / ironing board	0	0	0	0	0	0	2	1.1	4	2.3	169	96.6

the living space is the first preference (48.6 %), and the bedroom is the second preference (21.7 %). This indicated that this iGeneration may prioritize the bedroom since it is easier to use an iPad or iPhone in this area. The kitchen and bedroom are close in terms of preference distribution. After the living space, bedroom, and kitchen, the toilet comes next.

When it comes to furniture preferences, 48.6 % of the respondents preferred a bed. This is followed by an armchair/couch and a desk. This shows that this generation can spend a long time using comfortable furniture such as a bed, sofa, or chair, with mobile devices in their hands. Their second preference includes an armchair/couch, desk, and refrigerator.

These results show that Generation Z is more inclined towards small-scale, independent dwellings. They are not fully committed to the working life yet, but they prioritize their home and independent space options. They also prefer environments and items that offer comfort and solitude in residential space.

Table 10. **(Section II) Percentage Distribution of Generation Z's View of Housing as a Commercial Commodity**
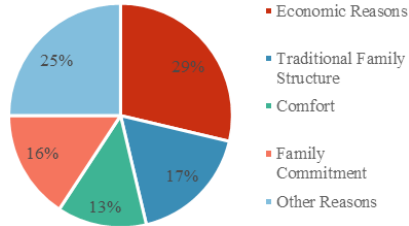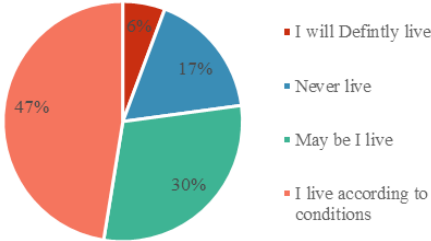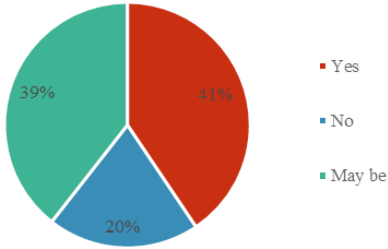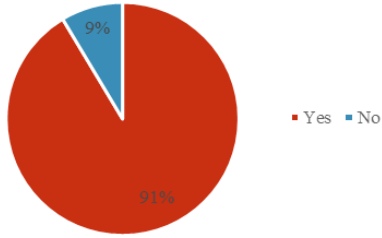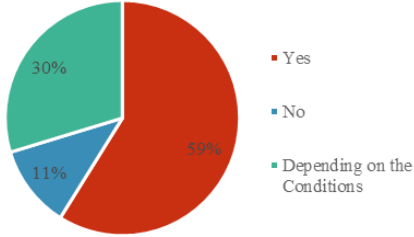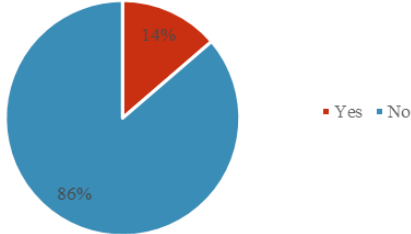
			n	%	
Do you live with your parents?					
Yes	What is the reason living with your family?	Economic Reasons	31	24.2	
		Traditional Family Structure	39	30.5	
		Comfort	14	10.9	
		Family Commitment	17	13.3	
		Other Reasons	27	21.1	
		TOTAL	128	73.1	
No			47	26,9	
Would you consider continuing your life in the house where you live with family house offered to you (such as inheritance, investment)?					
I will defintly live			10	5.7	
Never live			30	17.1	
Maybe I will live			52	29.7	
I live according to conditions			83	47.4	
Dou you want to allocate a budget for spatially unused or underused parts of the house?					
Yes			71	40.6	
No			35	20.0	
Maybe			69	39.4	
Dou you like to design and build your home yourself with the DIY(Do It Yourself) technique?					
Yes			160	91.4	
No			15	8.6	
Dou you see housing as an investment instrument?					
Yes			103	58.9	
No			20	11.4	
Depending on the Conditions			52	29.7	
Would you consider owning a house by borrowing (20 years)?					
Yes			24	13.7	
No			151	86.3	

Table 11. **(Section III) Percentage Distribution in terms of Generation Z's Future Housing Approach**

Dou you prefer your home to be portable or mobile?				
Yes		28	16.0	
No		42	24.0	
Depending on the Conditions		105	60.0	
Would you like your home to be expandable or demolish in the future, depending on whether your family increase or decrease?				
Yes		118	67.4	
No		57	32.6	
Would you prefer sustainable housing for the future?				
Yes	Dou you compromise on comfort when choosing sustainable housing?	Yes	14	8.1	
		No	79	45.7	
		Depending on the Conditions	80	46.2	
		Total	173	98.8	
No			2	1.2	
Dou you prefer the use of recycled, industrial or steel materials in housing?				
I definitely prefer		51	29.1	
I never prefer		0	0	
Maybe I would prefer		30	17.1	
Depending on the conditions or design I prefer		94	53.7	

In Section II, Generation Z's views on housing as a commercial commodity were evaluated.

It should be noted that 31 % of the participants stated that they live with their parents for economic reasons, while 27 % chose "other reasons" for their answer. Additionally, 39 % of the participants chose the traditional family structure as the reason for staying with their parents. This indicates that the traditional structure of their parents' generation and Turkish society in general is still influential, and the country's economic level has its impact on their preferences too.

Besides, 47.4 % of the respondents chose the option "depending on the conditions" as their preference for continuing to live in the house where they live with their family or the family house offered to them (such as inheritance, investment, etc.). In addition, 5.7 % of the participants preferred the option "I would definitely live here".

As for the next question, 91.4 % of the respondents answered "yes" to the idea of designing and building their own house using the DIY (Do It Yourself) technique. Since they are still aspiring architects, they are keen on the idea of designing and building their own houses. While shipping containers are designed to facilitate the creation of solutions in limited spaces, their light weight and portability align with this preference. This system can be easily assembled by individuals, making construction with the DIY technique quick and convenient.

The percentage of those who view housing as an investment instrument is 58.9 %. Depending on the economic conditions of the country, many people view housing as an investment instrument due to its potential for future security. Owning a title deed is highly valued in this country. However, the survey showed that 86.3 % of the respondents are not inclined to borrow money to own a house within the next 20 years.

Based on the findings of Section II, this generation, due to the traditional family structure and economic reasons, tends to live with their families. They do not prioritize inheritance or living in the family home to a great extent. Instead, they view housing as an investment instrument but are reluctant to take on long-term loans to own a house, preferring to build their own homes. This situation shows that the desire to live in a separate house is predominant if economic conditions and traditional family structure allow it. People see housing as an

29

investment instrument due to traditional attitudes and for reasons of feeling safe. On the other hand, this generation grew up during the period of urban transformation. The subject has become more valuable through the transformation. Witnessing this process also justifies the view of housing as an investment instrument.

Section III aimed to determine the future housing approach.

Ad for housing mobility, 24 % would not prefer their house to be mobile, and 60 % responded that it would depend on the conditions. These results show that they are more favorable to the idea of mobility. In Section I, 30 % of the participants stated that they had experienced living in a tiny house, caravan, or container building. The result shows that inexperienced individuals are actually favorable to this idea, depending on the conditions.

As for other findings, 67.4 % of the participants answered "yes" to the question of whether they would prefer their house to be added or removed in the future, depending on the expansion or reduction of their family. This result shows that, in addition to fixed solutions, various options are favorable for removable systems.

As for preferences for sustainable housing in the future, 98.8 % of the respondents stated that they would prefer it. However, about half of them also mentioned that they would not be willing to compromise on comfort. The concept of comfortable and sustainable housing is a positive one.

When it comes to using recycled, industrial, or steel materials in housing, 29.1 % stated that they would definitely use those, while 53.7 % answered that they would consider it depending on the conditions. It is evident that they are favorable towards recycling and open to using different materials other than reinforced concrete.

Conclusions

The purpose of this study was to determine the approach of Generation Z, the consumer of the near future, which has a significant population in Turkey, towards the use of shipping containers as a sustainable solution. Both architect students and Generation Z members living in Turkey were surveyed to determine their opinions on the use of shipping containers as housing solutions.

Studying the inclinations of Generation Z members, who are mobile, fast-paced, easily bored, and value home life, based on their generational traits, in relation to the use of shipping containers, which is considered a viable solution, will provide insights into the approach to housing production in the near future.

The architectural preferences of this generation, which is also sensitive to environmental issues, are being questioned, and there is an attempt to determine sustainability sensitivity through the use of reusable shipping containers. Shipping containers offer significant advantages as a housing choice for Generation Z due to their mobility, cost-effectiveness, eco-friendliness, and recyclable features.

Many social, cultural, traditional, and political factors in Turkey, from the past to the present, primarily determine consumer/generation characteristics. An appropriate consumption demand environment is formed accordingly. For this reason, the same results will not be obtained if this study is conducted in a different country. In this study of Generation Z, while Generation Z exhibits similar characteristics globally, it is common for them to have different traits, consumption habits, and preferences based on social, economic, and political factors in Turkey. Additionally, the experiences and generation characteristics of the parents raising them also have a significant impact.

The use of idle shipping containers as a sustainable and environmentally friendly solution, with the re-purposing approach, offers positive solutions to reduce resource use, energy consumption, and negative environmental impacts.

Shipping containers are a valuable resource generating a high amount of waste due to geopolitical location of the country, surrounded by seas on three sides, and also associated with the high volume of maritime trade as well as characterized by limited lifespan (seven years). Shipping containers are recyclable, easy to obtain, and can be added, removed, and used side by side or stacked on top of each other. With re-purposing, the transformation/construction time is very short, and economic solutions are flexible. The fact that their lifespan is as short as seven years is important for the continuity of this resource. It offers a fast, economical, and sustainable option for housing production.

Approaches of the participants, both Generation Z members and architecture students, to the use of shipping containers for sustainable housing solutions are as follows:

- Generation Z, who are economically strong, tend to not prefer to live with their families.

- They tend to not prefer living in a family house or inherited house.

- Safety and economic conditions have a dominant influence on housing preferences.

- They want to have small-scale, detached, and independent housing still remaining part of the social life of the city.

- They have the option to work independently or from home.

- Comfort in residential spaces is essential, with preferences for beds and armchairs/couches taking center stage.

- They support the sustainability approach but do not want to compromise on comfort and favor the idea of a predominantly conventional mobile home.

- They prefer using recycled materials.

When we consider the housing preferences of Generation Z, the criteria of safety, independence, small scale, sustainability, portability, proximity to the city but in nature, and proximity to social areas come to the forefront. The preferences of Generation Z, who will be the consumers/users of the near future, contain important information for both architects and non-architects. It is concluded that the desired features in residences are not multi-story and large-scale, but rather detached/independent, in nature, close to the city, environmentally friendly, and sustainable due to the use of recycled materials and systems.

References

Abh (2024). [online] Available at: www.abh.com.tr [Date accessed December 01, 2023].

Acılıoğlu, İ. (2015). *İş'te Y Kuşağı*. Ankara: Elma, 144 p.

Adıgüzel, O., Batur, H. Z., and Ekşili, N. (2014). Kuşakların Değişen Yüzü ve Y Kuşağı İle Ortaya Çıkan Yeni Çalışma Tarzı: Mobil Yakalılar. *Journal of Süleyman Demirel University Institute of Social Sciences*, No. 19, pp. 165–182.

Akdemir, A., Konakay, G., Demirkaya, H., Noyan, A., Demir, B. Ağ, C., Pehlivan, Ç., Özdemir, E., Akduman, G., Eregez, H., Öztürk, İ., and Balci, O. (2013). Y Kuşağının Kariyer Algısı, Kariyer Değişimi ve Liderlik Tarzı Beklentilerinin Araştırılması. *Journal of Economics and Management Research*, Vol. 2, No. 2, pp. 11–42.

Altuntuğ, N. (2012). Kuşaktan Kuşağa Tüketim Olgusu ve Geleceğin Tüketici Profili. *Organizasyon ve Yönetim Bilimleri Dergisi*, Vol. 4, Issue 1, pp. 203–212.

Arslan, A. and Staub, S. (2015). Kuşak Teorisi ve İç girişimcilik Üzerine Bir Araştırma. *The Journal of KAU IIBF*, Vol. 6, Issue 11, pp. 1–24.

Aydın, G. Ç. and Başol, O. (2014). X ve Y Kuşağı: Çalışmanın Anlamında Bir DeğişmeVar Mı? *Electronic Journal of Vocational Colleges*, Vol. 4, Issue 4, pp. 1–15. DOI: 10.17339/ejovoc.41369.

Başcı, E. (2015). *Pazarlama ve Tüketim Toplumuna Eleştirel Bir Bakış: Tüketim Karşıtlığına İlişkin Nitel Bir Model*. DSc Thesis.

Batı, U. (2015). *Tüketici Davranışları: Tüketim Kültürü, Psikolojisi ve Sosyolojisi Üzerine Şeytanın Notları*. İstanbul: Alfa, 330 p.

Cohen, J. (1988). *Statistical Power Analysis for the Behavioral Sciences*. 2nd Edition. Hillsdale: Lawrence Erlbaum Associates, 567 p.

Demirler, Y. H., (2019). *X ve Z Kuşağında Yer Alan Tüketicilerin Sembolik Tüketim ve Marka Bağlılığı Açısından Karşılaştırılması*. MSc Thesis.

Demirlioğlu, H. (2008). *Türkiye Denizyolu Konteyner Taşımacılıpının Kombine Taşımacılık Ile Geliştirilmesi*. MSc Thesis.

Ekmekçi, Ç. (2005). *Mimari Yapılarda Hareket Çeşitlerinin Incelenmesi ve Hareketin Mimari Tasarımda Kullanılması*. MSc Thesis.

Halis, B. (2012). Tüketimin Değişen Yüzü: Elektronik Ticaret Uygulamaları ve Sosyal Paylaşım Ağlarının Rolü. *Journal of History Culture and Art Research*, Vol. 1, Issue 4, pp. 149–160. DOI: 10.7596/taksad.v1i4.102.

ISBU Association (2017). *The History of ISO Shipping Containers*. [online] Available at http://www.isbu-association.org/history-of-shipping-containers.htm [Date accessed January 21, 2017].

Islam, H., Zhang, G., Setunge, S., and Bhuiyan, M. A. (2016). Life Cycle Assessment of Shipping Container Home: A Sustainable Construction. *Energy and Buildings*, Vol. 128, pp. 673–685. DOI: 10.1016/j.enbuild.2016.07.002.

İnce, F. (2018). *Kuşaklar Arası Etkin İletişim ve Davranış*. Konya: Eğitim Yayınevi, 160 p.

Kronenburg, R., (2002). *Houses in Motion: The Genesis, History and Development of the Portable Building*. 2nd edition. Chichester: Academy Press, 168 p.

Kuran, E. (2018). *Telgraftan Tablete. Türkiye'nin 5 Kuşağına Bakış*. Istanbul: Destek Yayınları, 136 p.

Mannheim, K. (1952). The Problem of Generations. In: Kecskemeti, P. (ed.). *Essays on the Sociology of Knowledge*. London: Routledge, pp. 276–320.

Milliyet (2019). ps://www.milliyet.com.tr/gundem/10-yil-sonra-yalnizlik-bakanligi-kurulabilir-2805998 [Date accessed December 6, 2023].

Özel, Ç. H. (2017). Kuşak Kavramı ve Turizme Yansımaları. In: Özkoç, H. H. and Bayrakdaroğlu, F. (eds.). *Kuşak Kavramına Disiplinler Arası Bakış*. Ankara: Nobel Akademik Yayıncılık, pp. 1–25.

Prajapati, B., Dunne, M., and Armstrong, R. (2010). Sample Size Estimation and Statistical Power Analyses. *Optometry Today*, Vol. 16, No. 7, pp. 10-18.

Saygın, E. (2021). *Hofstede'nin Kültürel Boyutları Bağlamında Kuşaklar Arasındaki Tüketim Farklılıklarının Incelenmesi: Kırklareli III Örneği*. DSc Thesis.

Shen, J., Copertaro, B., Zhang, X., Koke, J., Kaufmann, P., and Krause, S. (2019). Exploring the potential of climate-adaptive container building design under future climates scenarios in three different climate zones. *Sustainability*, 12(1), 108.

Stillman, D. and Stillman, J. (2018). *İşte Z Kuşağı*. Istanbul: İKÜ Yayınevi, 232 p.

Şenbir, H. (2004). *Z Son İnsan Mı?* Istanbul: Okuyan Us Yayınları, 362 p.

Tuncel, A. (2007). *Mobil Konutlarda İç Mekan Organizasyonu ve Mobil Mekanların Tarihsel Gelişim Süreci*. MSc Thesis.

Twenge, J. M. (2006). *Generation Me: Why Today's Young Americans Are More Confident, Assertive, Entitled—and More Miserable Than Ever Before*. New York: Free Press, 292 p.

Yazıcı, B. (2019). Yeni Lüks Kavramı Bağlamında Y Kuşağı ile Evrilen Tüketim ve Y Kuşağının Lüks Kavramına Bakışı. DSc Thesis.

Yazıcıoğlu, Y. and Erdoğan, S. (2004). *SPSS Uygulamalı Bilimsel Araştırma Yöntemleri*. Ankara: Detay Yayıncılık, 433 p.

Yıldız, D. (2021). Türkiye'de Korona Virüs Pandemisi ve Kuşaklar. *Social Sciences Research Journal*, Vol. 10, Issue 1, pp. 1–7.

ОЦЕНКА ИСПОЛЬЗОВАНИЯ МОРСКИХ КОНТЕЙНЕРОВ В КАЧЕСТВЕ ЖИЛЬЯ ДЛЯ ПОКОЛЕНИЯ Z КАК МЕНЯЮЩЕГОСЯ ПОТРЕБИТЕЛЯ

Бурчу Эрдал*, Чигдем Текин

Университет изящных искусств имени Мимара Синана
Меклиси Мебусан, № 24 Фындыклы, Бейоглу, 34427, Стамбул, Турция

*E-mail: burcuerdal78@outlook.com

Аннотация
Введение: Архитектурные требования ближайшего будущего будут иметь совершенно иные характеристики, чем в недавнем прошлом. С изменением средств коммуникации и транспорта, благодаря возможности быстрого перемещения и легкого общения также поменялись и традиционные представления о жилище. Эти изменения повлекут за собой перемены в использовании пространства и его масштабе. Архитектура претерпевает значительные изменения в связи с появлением Индустрии 4.0. В ближайшем будущем непосредственным потребителем, который будет предъявлять такие требования уже совсем скоро, станет поколение Z. Одновременно с этим архитектурная среда унаследовала множество экологических проблем, которые возникли в недавнем прошлом и продолжают обостряться. В условиях стремительных изменений/трансформаций экологические проблемы требуют устойчивых решений, которые вполне могут находиться в гармонии с природой, что гораздо более естественно, чем развитие технологий.
В основе данного исследования лежит использование морских контейнеров в качестве устойчивого решения и определение подхода поколения Z как меняющегося потребителя к этому решению. **Цель исследования** — выяснить, как поколение Z, живущее в Турции, оценивает использование морских контейнеров в качестве альтернативы жилью. **Методы:** В ходе исследования был проведен опрос лиц, которые одновременно являются представителями поколения Z и студентами архитектурных вузов. В исследовании использовался метод целенаправленной выборки.

Ключевые слова: дом из морского контейнера; устойчивая архитектура; поколения; поколение Z.

SENSE OF URBAN AND ARCHITECTURAL ENVIRONMENT

İlker Erkan

Faculty of Architecture, Suleyman Demirel University, Turkey

E-mail: ilkererkan@sdu.edu.tr

Abstract
Introduction: In this study, we aimed to explore how different spaces affect people and influence their emotions from a neuro-architectural perspective. The **purpose of the study** was to investigate how navigating historical and modern architectural environments impacts individuals both cognitively and physiologically. **Methods**: People's reactions to historical and modern environments were explored and then analyzed using quantitative data and various analysis methods. Three different architectural environments were designed, and the participants were allowed to navigate these environments in a virtual reality setting. The participants were asked to select images from modern or historical pictures, and then they were subjected to the Beck Depression Inventory and the Positive and Negative Affect Schedule tests. In addition, physiological data were collected from 164 participants using electroencephalography, eye tracking, and galvanic skin response devices. As a **result**, when the participants were evaluated based on their preferences for modern or historical environments, they were found to prefer a combination of historical and modern environments. It was determined that people exhibit different cognitive responses in different architectural environments. This is an important finding for re-designing the built environment.

Keywords: neuroarchitecture; architectural environment; people's behavior; built environment.

Introduction

The quality of the components that make up the architectural environment also determines the type of environment. The quality of that environment is reflected in all units, from cities to the minuscule elements. A city is defined as an artificial physical environment that represents an organized system far beyond the natural and primitive life mechanisms (Kuban, 1994). Social, economic, and administrative elements play a role in the formation of a city, starting with social memory. In addition, it is necessary to discuss the role of fabric in shaping the city from ancient times to the present, as it reflects the character of a city. The factors such as the adjacent or separate arrangement of buildings, their distribution across the topography, and parcel sizes make the character of the city visible. The diverse street layout in a residential area, the quality of the structures, and the way they interact reflect the character of a city. The basic elements that reflect the original architecture, repetitive urban objects, monumental structures, and groups of buildings are among the elements that make up the city skyline. Over time, cities become modern as they evolve with the development of technology and the changing needs of humans. Since the industrial revolution, the ongoing modernization movement has been spreading into the historical fabric, and even encroaching upon the historical urban fabric in some parts of the city.

Due to its form, the historical urban fabric can be defined as the environment built by humans over a long period of time. If we look at the city

from this perspective, it offers a wealth of important information, including archaeology, architecture, and art history.

The expectations, desires, and even relationships of users in urban life define the identity of that city. The built environment, shaped by the tangible (concrete) and intangible (abstract) interactions of city dwellers, generates urban values through the formal and structural characteristics of buildings. These urban values differentiate cities from each other and create their unique atmospheres. Urban values include the environment and events in which city dwellers share a common memory, integrating with nature, space, and objects. In addition to the main structures that have survived from ancient times to the present day, historical sites that are not monumental but have a documentary character and have witnessed a certain period or social development also gain importance as cultural treasures.

Another important issue is how to make sense of the environments and events that contribute to urban identity. Many restorers and architectural historians have worked on this subject. However, what is missing is an understanding of what people expect in the historical fabric of the city and what kind of urban fabric they want to see. This is because the expectations of people from urban fabric, both in their place of residence and during their visits for tourism purposes, have been widely discussed (Edwards et al., 2008; Selby, 2004). Studies have progressed from various perspectives. Various studies, ranging from urban design strategies (Alawadi, 2017; Yang and Yamagata, 2020) to crowd behavior (Li et al.,

2009), and from the design of recreational areas (Rathnayake, 2015) to urban policies (Al-kheder et al., 2009; Bartolini, 2014; Popp, 2012), were conducted. However, cognitive studies on people's navigation behavior within the city were found to be incomplete. This is because when people visit a city, they sometimes experience something that goes beyond physical or sensory features. Ebejer (2014) refers to this phenomenon as the "sense of place". In urban design literature, the sense of place is often attributed to three elements: the physical environment, activities, and meaning (Salah Ouf, 2001; Soini et al., 2012). The meaning of buildings, spaces, and even cities is subjective and can be read and interpreted differently by different people based on their past and culture. As a result of a comprehensive review of the literature, the study proposes two different hypotheses:

• H1: There is a relationship between gender and preferences for navigating modern or historic urban areas.

• H2: In a modern + historical city, the navigation behavior exhibited by the same participants will not change.

Methods

The basic requirement for inclusion in the research is that the participants selected for the study should not have any history of taking depression medication. The participants were required to sleep for at least 8 hours the night before the experiment and to refrain from smoking or consuming alcohol and stimulant beverages. A total of 164 people participated in the experiment (88 males, 76 females), and the average age of the participants was 22.78 years. All participants started the experiment after all the devices were installed. However, 4 participants were unable to complete the experiment due to the dizziness they experienced. Therefore, these 4 participants were excluded from the experiment.

The experiment was conducted using both psychological and neurophysiological measurement methods, along with a virtual reality application. Three different areas within the city were designed for the experiment. The first area features modern architecture, the second area showcases historical

buildings, and the third area is a modern + historical area (Fig. 1).

In these three areas, the participants could navigate through the virtual reality application using the Wii controller. The participants were allowed to navigate all three areas for particular time. However, none of the participants exceeded the allocated time. The experiment was conducted in stages, with approximately 2–3 hours allocated for each participant, and the necessary permissions were obtained from the dean of the faculty. The experiment was completed in a total of 11 months. The flow of the experiment is shown in Fig. 2.

In the experiment, the Beck Depression Inventory scores of the participants were initially determined. The goal was to determine the participants' depression scores before they participated in the experiment. The Positive and Negative Affect Schedule (PANAS) test was performed immediately after the Beck Depression Inventory. In the second stage, the select-a-visual application prepared for the experiment was launched. At this stage, the participants were shown pictures on the computer screen and asked to rate them on a scale of 1 to 10. In the third stage, the participants were asked to navigate a virtual reality environment after attaching the GSR, EEG, and eye-tracking devices. The basic tests and the equipment used in the experiment were as follows:

Stage 1 — Beck Depression Inventory and PANAS Scale: The first stage of the experiment was to determine the participants' depression scores. The Beck Depression Inventory (BDI), developed by Beck (1963), measures somatic, motivational, emotional, and cognitive symptoms associated with depression. The purpose of the scale is to objectively determine the extent of depression symptoms, rather than to diagnose depression. Each item is scored between 0 and 3 points. The depression score is obtained by summing up these scores. The highest possible score is 63. A high score indicates a high level of depression. The cutoff point of the scale was determined to be 17. This score and higher scores indicate clinical depression, and an increase in the score indicates increased depression severity.

Fig. 1. Images from the areas visited by the participants in the modern, historical, and modern + historical environments
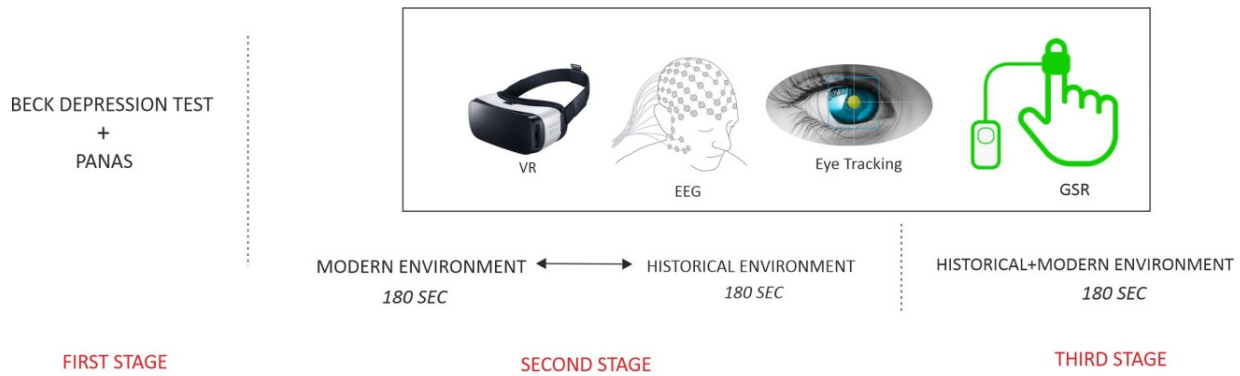
Fig. 2. Simple flowchart of the experiment

In the research, based on the conducted studies (Lasa et al., 2000; Steer et al., 1999), 30–63 points indicate severe depression, 17–29 points indicate moderate depression, 10–16 points indicate mild depression, and 0–9 points indicate no depression. Cronbach's Alpha analysis was used to determine the reliability of the responses given in the Beck Depression Inventory. Cronbach's Alpha of the Beck Depression Inventory was 0.945 (if $0.80 ≤ α < 1.00$, the scale is highly reliable).

After completing the Beck Depression Inventory, the participants took the PANAS test. On a scale of 10 positive and 10 negative feelings, Watson et al. (1988) determined the reliability of the positive emotion scale as 0.88 and the negative emotion scale as 0.87. The researchers used the PANAS test across various disciplines to determine the current moods of the participants. The participants responded to these feelings using a 7-point Likert-type scale based on the frequency of their general encounters (1 = Never, 2 = Very rarely, 3 = Rarely, 4 = Sometimes, 5 = Frequently, 6 = Mostly, 7 = Always). The scores that can be obtained on the scale range from 10 to 70 for both sub-scales. In this study, Cronbach's Alpha calculated for positive affectivity was 0.81, and Cronbach's Alpha calculated for negative affectivity was 0.76. The Cronbach's alpha method was used to assess the reliability of the responses to the PANAS test. PANAS total mood Cronbach's Alpha was found to be 0.79 (the scale is quite reliable if $0.60 ≤ α < 0.80$). The main goal of the PANAS test was to determine the moods of the participants before they embarked on their trips in a virtual reality environment.

Stage 2 — Select-a-Visual: The participants were asked to sit in front of the computer screen immediately after completing the Beck Depression Inventory and PANAS test. They were then instructed to give a score (1 being the lowest and 10 being the highest) to 30 different images shown to them. The software used in this study was developed with the assistance of the Visual Basic program, and the scores given by the participants were recorded.

A screenshot of the software prepared for the study is shown in Fig. 3.

All the images shown to the participants are presented in Appendix 1. To help the participants distinguish between modern and historical images, the images were shown at 5-second intervals. The main purpose of the select-a-visual software is to enable participants to express their modern or historical preferences through visual arts. Therefore, an attempt was made to determine historical and modern tendencies. In the study, individuals with a high classical visual score were defined as inclined towards historical, while those with a high modern score were defined as inclined towards modern.

Stage 3 — VR-1: At this stage, GSR, EEG, eye tracking, and VR goggles were used for the participants. Thanks to virtual reality, participants can take trips as if they were in a real environment. Researchers working in different disciplines have noted that VR systems have several advantages. At this stage, the participants were able to navigate two different settings designed using VR technology. Some of the participants first navigated through the modern environment, while others first explored the historical fabric of the city. In other words, it was randomly determined which participants would start from the modern urban fabric and which would start from the historical urban fabric. All the participants were allowed to navigate for 180 seconds, which means that the experiment took 360 seconds at this stage.

Stage 4 — VR-2: At this stage, the virtual environment was designed in an urban setting with both modern and historical structures, and was referred to as a historical + modern urban environment. Additionally, the VR-2 stage was intended to provide a different experience for the subjects, and, therefore, this stage took place 1 hour after the standard experimental procedure. In other words, the volunteers who participated at the VR-1 stage of the study were also invited to VR-2. At this stage, EEG, VR, GSR, and eye tracking stages were also applied in the same manner. Unlike the VR-1 environment, the VR-2 environment can be
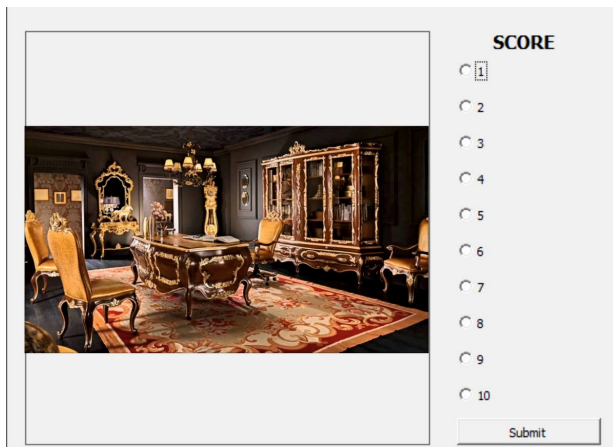
Fig. 3. Interface of the select-a-visual program as seen by the participants

described as historical + modern, designed in 3D. The environment, both with modern fabric and historical fabric, was tested with the same participants.

In the experiment, data were recorded from the participants using physiological measurement methods. The details of these measurement methods are as follows.

Galvanic Skin Response: Galvanic Skin Response is a type of data used to measure the response to stimuli in individuals. The GSR device was attached to the participants to measure a type of response caused by changes in the electrical conductivity of the skin. Minor changes in the electrical properties of the skin are measured using electrodes attached to the fingers. These physiological changes are caused by changes in the person's psychological state, such as stress and relaxation. Galvanic skin response (GSR), also known as skin conductivity or electrodermal activity response, is a reliable indicator of stress (Healey and Picard, 2005; Labbé et al., 2007). It is the measurement of electric current flow in an individual's skin. Skin conductivity increases due to the increased moisture on the surface of the skin when an individual is under stress (Sharma and Gedeon, 2012). The GSR values tend to decrease as time passes during a period of rest. This change can indicate that the person is experiencing a sense of relief at that moment. In the study, a statistically significant difference was found in the average skin conductivities during the rest and navigation states ($p = 0.005 < 0.05$). Over time, the conductivity values increase from their minimum to their maximum. The difference between the maximum and minimum values refers to the amplitude.

Electroencephalography (EEG): EEG is measured by recording the electrical activity in the brain, specifically the cerebral cortex, with the help of electrodes on the scalp. In other words, the change in electrical potential defines the signal of electroencephalography. EEG electrodes are placed according to the 10/20 electrode layout, standardized by the International Federation of Electroencephalography and Clinical Neurophysiology (Jasper, 1958). The frequency range of electroencephalography signals varies between 0.1 and 100 Hz, depending on the dominant regions. In order to regularly examine these changes, electroencephalography signals are divided into five main classes based on their frequency. These are called alpha, beta, theta, delta, and gamma. The study focused on the FP1, FP2, F3, F4, FZ, C3, C4, CZ, P3, P4, and PZ channels. Moreover, this study focused on alpha, beta, and gamma. EEG was used to measure changes in the neurophysiological states of the participants' emotions.

Eye Tracking (ET): The basic principle of the eye tracking technique is based on recording infrared light projected onto the retina and corneal layer of the eye. Although it depends on the specifications of the device used, light is typically reflected to the pupil at a frequency ranging from 120 to 1000 Hz on average. As a result of this process, the recorded data are processed using special computer programs. The eye-tracking system is integrated into the virtual reality goggles to measure where and for how long participants are looking.

Results

In the study, the reactions of people to historical and modern environments were analyzed using quantitative data and various analysis methods. The hypotheses put forward were investigated in detail.

• H1: There is a relationship between gender and preferences for navigating modern or historic urban areas.

Based on the hypothesis, the navigation preferences of the participants were determined. First, the participants were shown 15 modern and 15 classic images in the select-a-visual software developed for this study. They were asked to rank the images shown on a scale of 1 to 10 (with 10 being the highest). Statistical analysis was then performed on the participants' scores. The main goal was to determine people's preferences for visual art (modern/historical). The responses of the participants were recorded. The statistical values of the recorded responses are shown in Table 1.

As shown in Table 1, the select-a-visual test found that women prefer classical visuals, while men prefer modern visuals. After the select-a-visual test, the Beck Depression Inventory and PANAS test were used (Table 2).

Based on Table 2, it was found that the Beck Depression Inventory score differed significantly by gender and that the scores of the females were higher than those of the males ($p < 0.05$). Positive and negative mood levels were also found to differ significantly depending on gender, and the positive mood score of the males was higher ($p < 0.05$). As a result, the depression scores and PANAS

Table 1. **Data on the participants' responses to the select-a-visual test**

	Modern Picture Scores	Historical Picture Scores
Male (Avg)	6.78	3.58
Female (Avg)	4.54	7.12
SD	2.54	2.78

negative mood scores of the females participating in the study were higher than those of the males.

Modern and classical preferences of the females (N = 61) with higher depression scores and PANAS negative mood scores were examined. The results showed that these females preferred classical works in the select-a-visual test, indicating that their scores for classical visuals were higher than their scores for modern visuals. In the eye-tracking recordings of the same 61 female participants in modern city navigation, the heat maps analyzed were found to have fewer highlighted areas compared to the historical urban fabric (Fig. 4).

This may indicate that they don't really look at the details in the modern city. For an overview of the information obtained in the two tasks, some general eye-tracking measures were calculated (Table 3).

The number of dwells, total time, and the number of options attended to were all pieces of information acquired from the two urban settings. The mean dwell time and the total dwell time were collected from each city setting. GSR signals for 61 tested female participants are shown in Fig. 5.

61 female participants first navigated the historical city and then the modern urban fabric, as shown in their GSR records in Fig. 5. As shown in the figure, the GSR signals are above a certain level when navigating the historical urban fabric, but tend to decrease as soon as they move to the modern urban fabric (from the 180th second onward). In addition, the GSR value graphs of the participants with high scores for modern and classic pictures were overlapped, as shown in Fig. 6.

The data shown in Fig. 6 confirm data in Fig. 5. It was observed that the GSR records of the participants with a modern tendency increased during their navigation in the modern urban fabric, while the GSR records of the participants with a classical

tendency increased during their navigation in the historical urban fabric. Furthermore, this finding confirms the findings of Erkan (2021), which state that increased GSR signals indicate people's excitement in that environment. In the study, EEG bands were examined with a focus on beta and gamma waves. The beta bands of EEG signals are known to be associated with stimulation, stress, active thinking, and active attention (Sanei and Chambers, 2013). In addition, Güntekin and Başar (2010) stated that people exhibit excessive responses to stimuli that trigger negative emotions. Erkan (2021) reported that the EEG amplitude of higher beta bands (21–30 Hz) was relatively high in participants with negative mood. When examining the EEG plots of 56 out of the 61 females mentioned earlier, it is evident that there are significant differences in beta EEG amplitudes during the navigation of modern urban environments. In this case, it can be assumed that people with a historical inclination may experience a heightened state of anxiety, as evidenced by the increase in beta bands during a modern urban trip. The amplitudes of electroencephalography in historical and non-historical (modern) environments were determined using the measured beta bands, as shown in Fig. 7.

Moreover, the gamma power spectrum of the participants was also found to be different. The EEG activity of gamma bands can be easily observed along with beta band activity in sensory analysis and negative emotional analysis (Luijcks et al., 2015; Newson and Thiagarajan, 2019). Furthermore, the EEG activity in the gamma band is related to higher-level cognitive processing in the sensory system, including auditory and visual systems (Bhattacharya et al., 2001; Müller et al., 2000). In this study, there was a significant difference in the EEG power spectrum of gamma bands during the navigation in modern and historical environments among the participants who selected modern visuals in the select-a-visual section and had a high modernity score. A higher EEG power spectrum in the gamma bands was observed during historical environment trips of the participants with a high modernity score, and vice versa. In other words, the participants with high classical scores were also found to have high EEG

Table 2. **Relationship between the Beck Depression Inventory score, the PANAS test score, and gender**

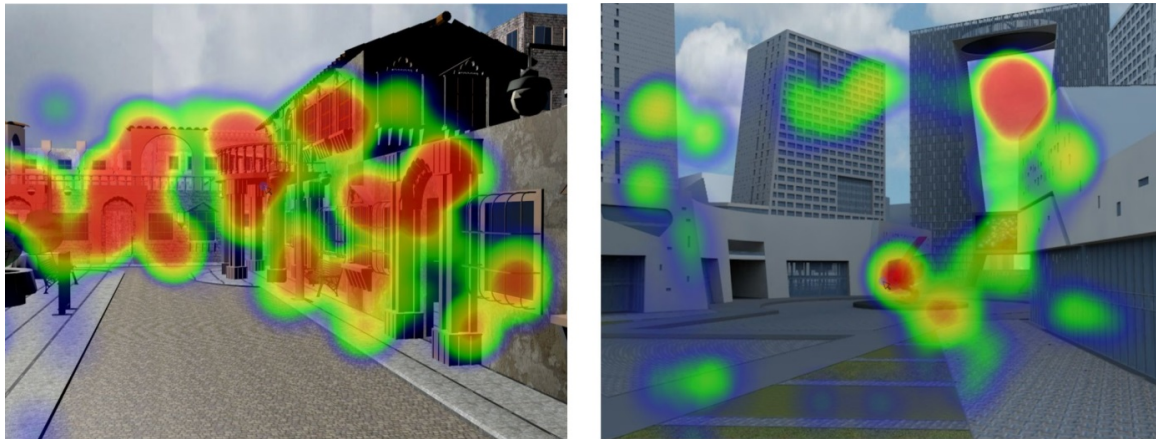| Score	Gender	N	X	S.S	t	S.D	p
Beck Depression Score	M	88	0.148	0.324	–8.789	157.147	0.000
	F	76	0.389	0.329	–	–	–
Positive Emotional State Score	M	88	2.789	0.287	7.778	189.879	0.000
	F	76	2.147	0.301	–	–	–
Negative Emotional State Score	M	88	2.145	0.678	–7.457	201.145	0.000
	F	76	3.147	0.699	–	–	–

Fig. 4. Heat maps revealed in the eye-tracking analysis in the modern and historical urban fabric as viewed by the female participants with high depression scores and high classical scores in the select-a-visual test

Table 3. **Measures of information acquired in the different tasks (SD in parentheses; all times are in ms)**

	Modern City Environment	Historical City Environment
Total Duration	17,589.4 (16,788.7)	29,086.4 (20,559.2)
No. of dwells	34.64 (30.73)	39.48 (33.78)
No. of options attended to	21.14 (15.89)	27.78 (78.99)
Mean dwell time on each option	400.45 (124.67)	700.78 (211.88)
Total dwell time on each option	641.78 (245.47)	997.78 (456.45)

gamma bands compared to the other groups in the modern environment (Fig. 8).

Environmental psychologists have proposed the concept of attention restoration in contrast to the concepts of stress and mental fatigue. They have noted that the relaxing benefits of natural landscapes can stimulate brain activity associated with positive moods (Tilley, 2017; Ulrich, 1981). Based on this, the alpha bands of the same participants were also studied by adding FP1 and FP2 channels. The alpha value of the participants with a positive mood was found to be significantly higher in both the historical city trip and the modern city trip compared to other
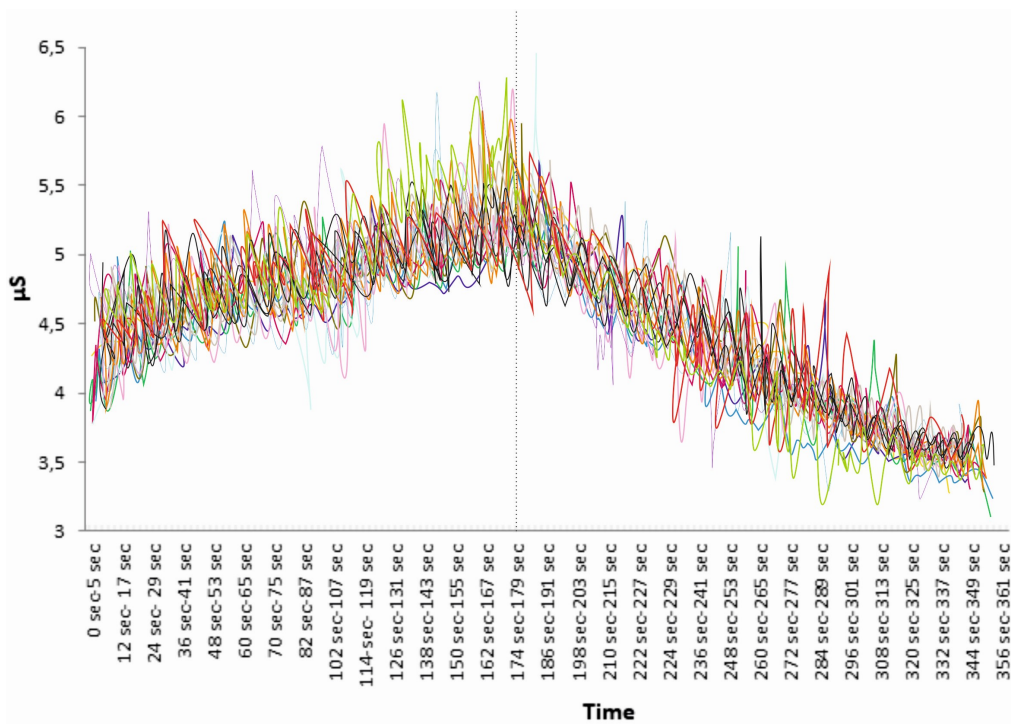
Fig. 5. GSR responses of 61 female participants as they navigated the modern urban environment following the historical city
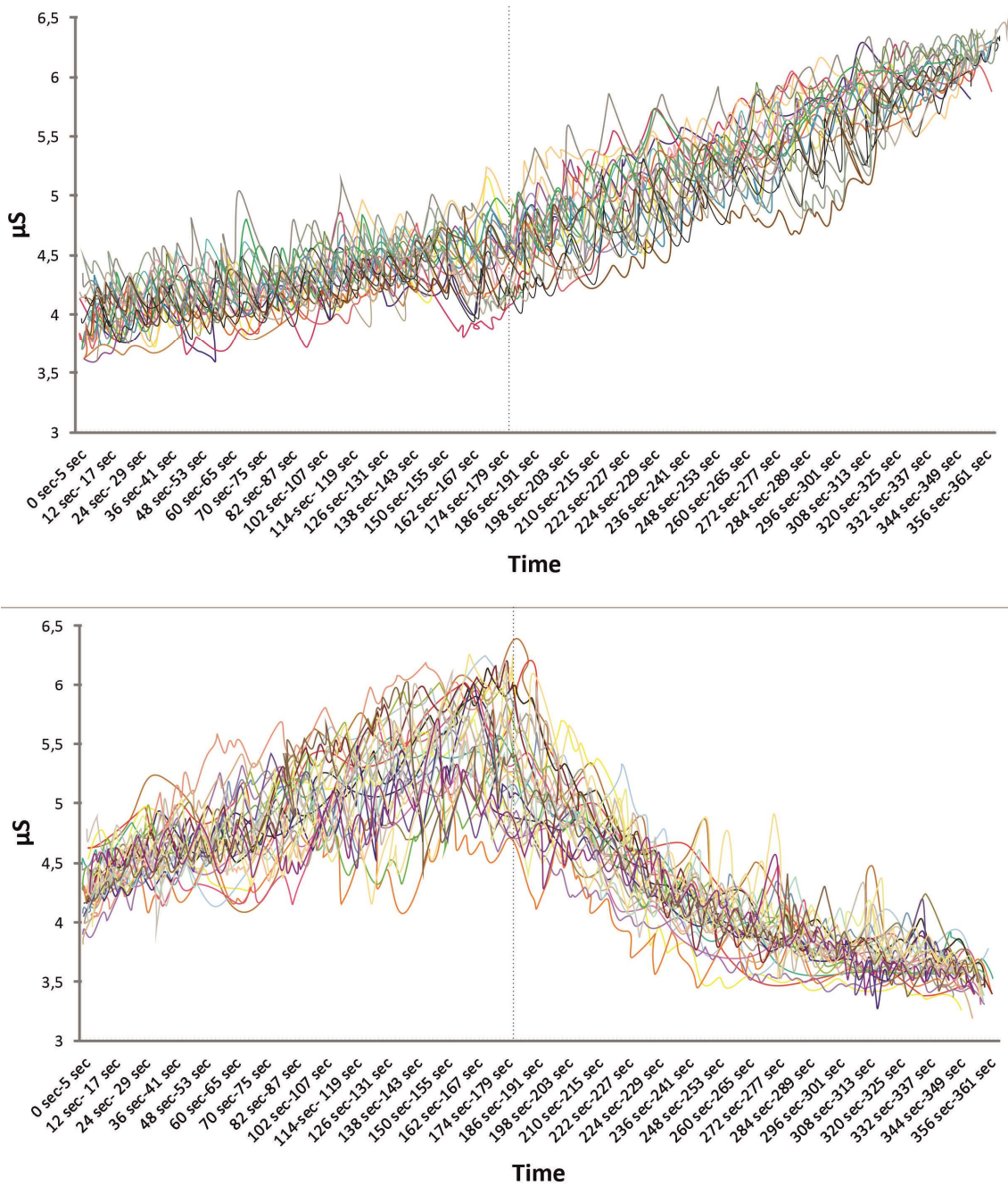
Fig. 6. (1) Schematic view of the GSR plots for the participants with a high modern score, navigating from the historical city to the modern city; (2) Schematic view of the GSR plots for the participants with a high modern score navigating from the modern city to the historical city

participants (who had a higher Beck Depression score and a higher PANAS negative score) (Fig. 9). This result confirms the findings of Shaw (2003) and Hugdahl and Davidson (2004).

In the first 60 seconds, the higher alpha power spectrum is remarkable in the right frontal lobes of the participants with higher classical or modern visual scores, navigating respective historical or modern environments. This is consistent with Tilley's (2017) study, which indicates that participants are relieved in these environments, albeit for a while.

In contrast to the activities of beta and gamma bands, in stressful situations, the EEG power spectrum of alpha bands is known to increase in a steady state, such as meditation or relaxation (Erkan, 2017a; Erkan, 2017b Lagopoulos et al., 2009). Given the positive relationship between alpha power and comfort (Sammler et al., 2007), it can be concluded that the participants were comfortable in both environments. However, when examining the modern-classical visual tendencies of the same participants, it is noteworthy that the modernity score was higher. This is in line with the results of the 61 participants mentioned above.
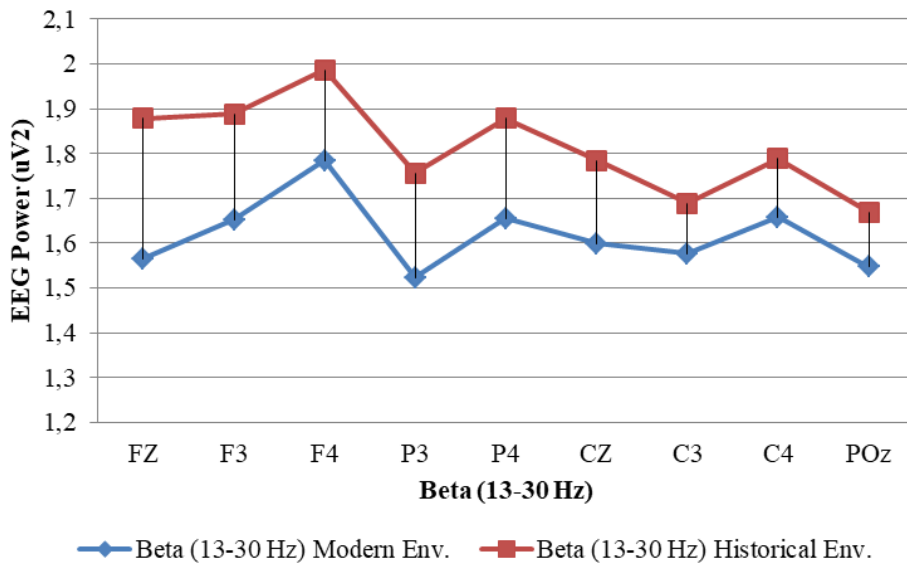
Fig. 7. Distribution of the electroencephalography (EEG) power spectrum beta waves measured in different architectural environments
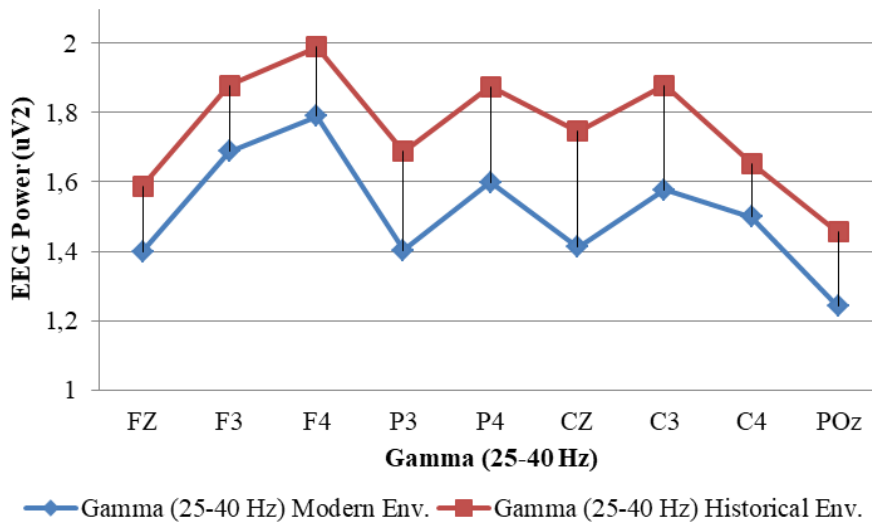
Fig. 8. Gamma bands of the participants with higher modernity scores in modern and historical environments

Alpha (8-12 Hz)
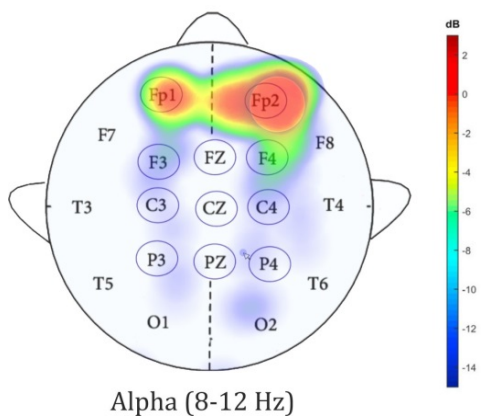
Fig. 9. Brain map of the alpha value of the participants with positive/negative moods during both the historical city trip and the modern city trip

Discussion

When all of these findings are carefully examined, it is neurocognitively confirmed that there is a relationship between gender and preferences for navigating modern or historical urban fabric, as mentioned in Hypothesis 1.

• H2: In a modern + historical city, the navigation behavior exhibited by the same participants will not change.

Stage-VR-2 was used to test this hypothesis. This stage was tested unlike any other stages.

First, eye tracking data from the participants with a historical-modern tendency in Stage-VR-2 were analyzed in a historical-modern environment, and compared with Stage-VR-1 data. The fixation duration data are shown in Fig. 10.

Fig. 10 shows the participants' fixation duration on modern or historical environmental fabric. The total fixation scores of the participants who navigated both the modern and historical environments seem to be close to each other. Interestingly, the total fixation scores in the historical + modern environments were quite high. GSR analyses were performed on the same participants, and instant rises and falls in the GSR records were observed during the modern + historical urban trip. A logarithmic increase/decrease was observed in the GSR signals obtained from both modern and historical settings.

The right temporal lobe of the brain, among other functions, is responsible for visual attention, interpreting visual information, pictorial memory, and processing visual scenes (Milner, 1968). As expected, more beta signals were recorded in the right temporal lobe (Fig. 11).

In this experiment, it was observed that brain activity (greater right temporal beta activity) induced by stimuli in both historical and modern fabric may be associated with the mechanism of involuntary attention. However, this effect was more intensively recorded in the modern + historical urban fabric. This was significantly more powerful in the modern + historical environment compared to both modern and historical environments. This may indicate that participants perceive the holistic aspect of the setting more intensively while navigating the environments, recognizing and processing the general spatial relationships between the elements. This is because, during the modern + historical urban trip, the participants were found to be more focused, as evidenced by the activity in the right temporal lobe of the brain (Fig. 11).

Upon careful examination of all these findings, the hypothesis positing that "in a modern + historical city, the navigation behavior exhibited by the same participants will not change" was neurocognitively rejected, and behavioral changes were observed compared to the case of the modern + historical environment.

Given the unique nature of human behavior, it is quite difficult to identify the causes of any behavior. This study focused on identifying people's preferences for historical and modern urban fabric and investigating the reasons behind these preferences.

At the first stage of the study, the select-a-visual test was conducted, revealing that the males scored higher in modern pictures while the females scored higher in classic pictures. In other words, the modern/classical preferences of the participants were determined at this stage of the study.

At the second stage of the study, PANAS and psychological tests were conducted to assess the participants' depression scores. It was found that the females had higher depression scores and PANAS negative mood scores compared to the males. When the Beck Depression Inventory and PANAS scale results were evaluated together, it was found that the average score of 61 out of the 76 female participants indicated a depressive level. The select-a-visual test results of these 61 female participants were analyzed, and all of them were found to prefer classical works. When examining the GSR records of the same participants, it is observed that the GSR signals above a certain level during navigation in the historical urban fabric tend to decrease in the modern urban fabric. This decrease can be interpreted as a reduction in excitement when transitioning to the modern fabric, aligning with other results.

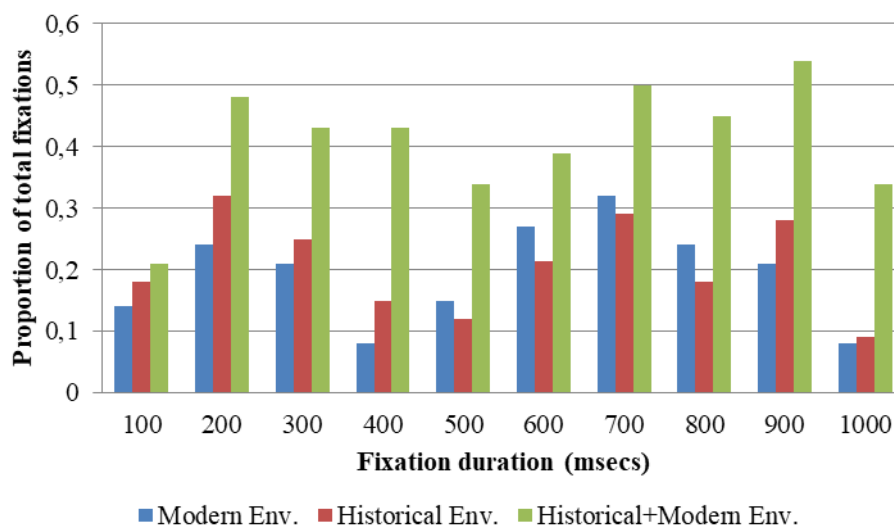When all participants' GSR records were examined, it was observed that those with a high

Fig. 10. Heat map analysis of participants with high modern and historical scores
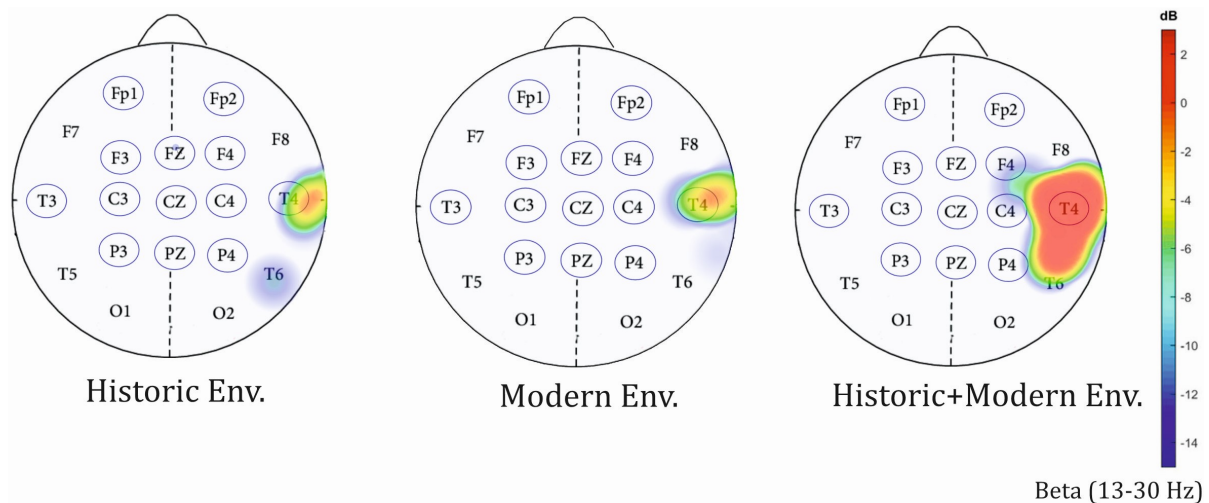in a historical + modern urban environment

Fig. 11. Activation of beta signals observed in brain mapping

modern tendency in the select-a-visual test had higher GSR levels during their navigation in the modern urban fabric. Similarly, the participants with a high classical tendency had higher GSR levels when navigating the historical urban fabric. It is believed that this indicates that people tend to become more excited when they navigate in their preferred historical or modern urban fabric.

At the third stage of the study, the alpha, beta, and gamma bands of the participants with high modernity scores during their navigation in modern and historical environments were examined, and a significant difference in EEG levels was observed.

It was found that the alpha value of the participants who had positive emotions was significantly higher than that of other participants (with high Beck Depression scores and high PANAS negative scores) in both the historical and modern city navigations.

Nohl (2001) proposed a conceptual framework for a better understanding of future landscapes as aesthetic objects, investigated various aesthetic aspects of development, and outlined the most important aesthetic prototypes of tomorrow's landscape. This study supports the study by Noh (2001) from a different perspective and concludes that the aesthetic data is better understood within a modern + historical environmental framework.

Based on the techniques used in the study (eye tracking + EEG + GSR) and the characteristics of the participants (gender, PANAS + Beck Depression Inventory), it appears that historical + modern environmental design is superior in all aspects. In the

analysis of all the test results, it was found that all the participants, whether they preferred a modern or historical environment, spent a longer period of time exploring the historical + modern environment. This was determined through eye-tracking analysis, which also showed higher cognitive awareness as detected by EEG, and elevated skin conductivity according to the GSR results. Considering the reflection of all these findings on the design, it can be stated that designs in the construction of future cities should be shaped by the trips and behavioral decisions of people who live in the city or will visit this habitat.

The study is believed to inspire future space and environmental designs. The study plays an important role in shaping environmental design, utilizing various methods. EEG was used in the study. An fMRI device can also be used to perform more precise and detailed measurements, allowing for the study of changes occurring in the inner regions of the brain in greater detail. The study was conducted in a VR environment. Even though VR environments are considered ideal for such experiments, it may be advisable to use real experimental environments in future studies. Additionally, the factors/stimulants that affect decision-making mechanisms are a separate issue projected for future study.

Appendix 1
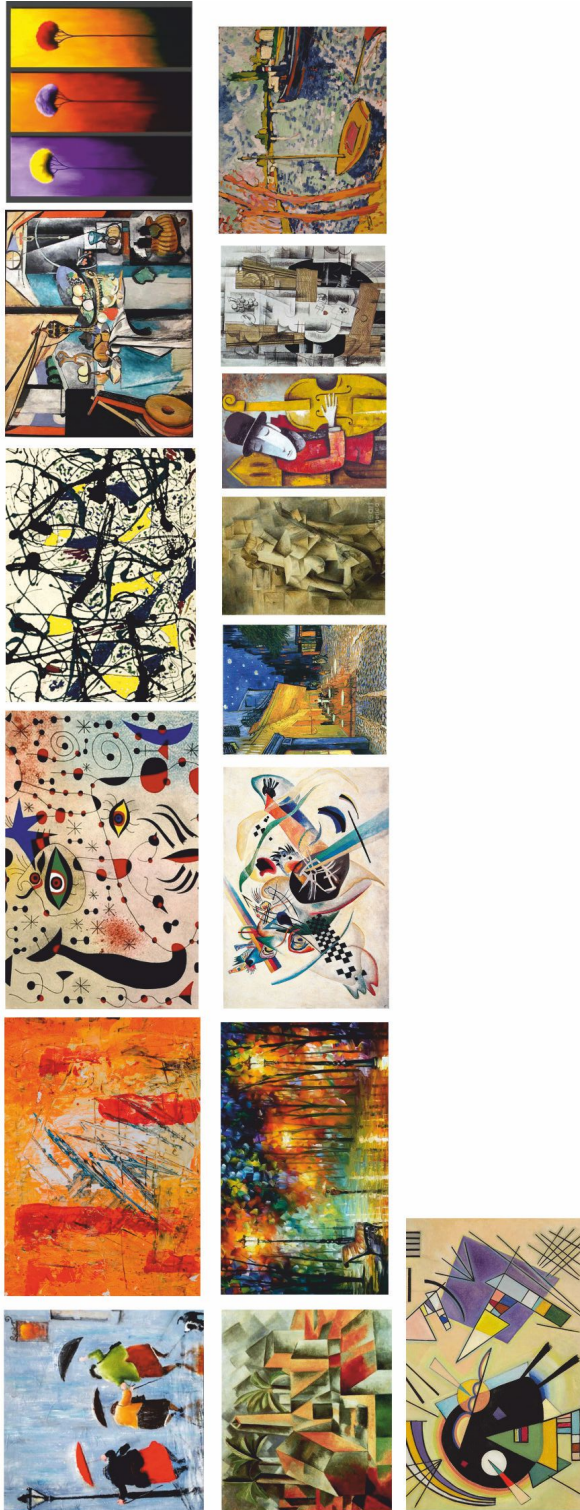

Modern Pictures

Classic Pictures
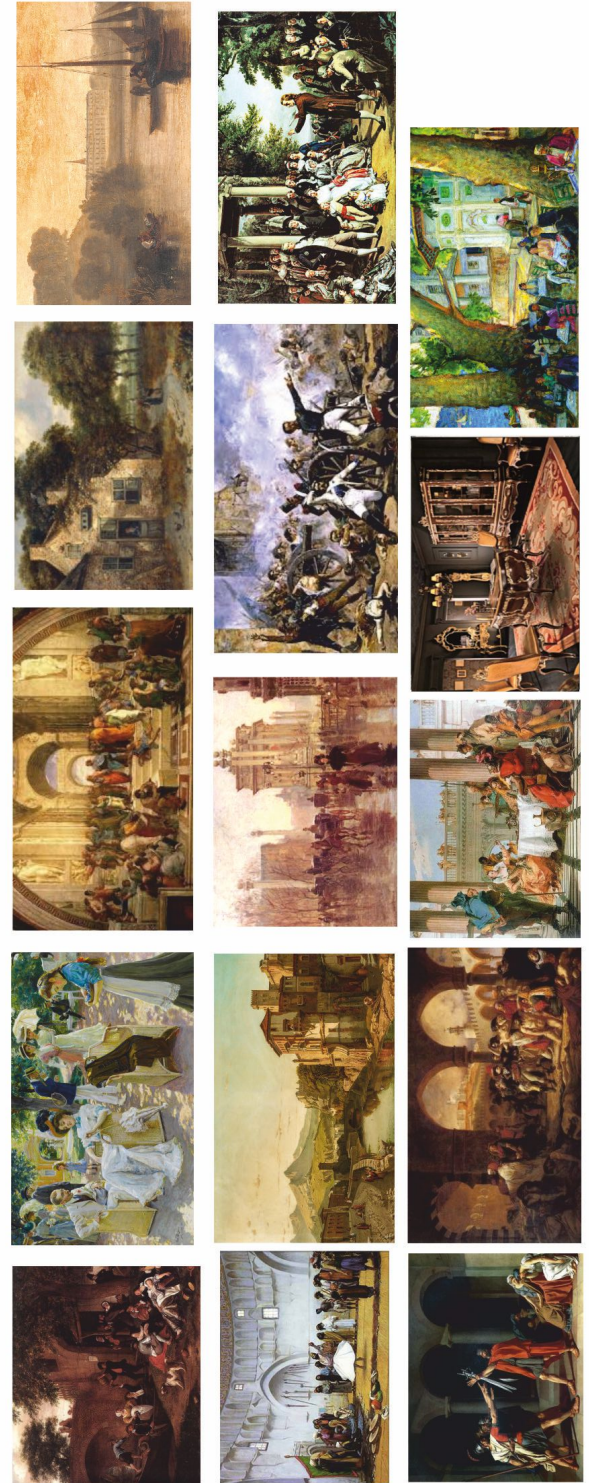
References

Alawadi, K. (2017). Rethinking Dubai's urbanism: Generating sustainable form-based urban design strategies for an integrated neighborhood. *Cities*, Vol. 60, Part A, pp. 353–366. DOI: 10.1016/j.cities.2016.10.012.

Al-kheder, S., Haddad, N., Fakhoury, L., and Baqaen, S. (2009). A GIS analysis of the impact of modern practices and polices on the urban heritage of Irbid, Jordan. *Cities*, Vol. 26, Issue 2, pp. 81–92. DOI: 10.1016/j.cities.2008.12.003.

Bartolini, N. (2014). Critical urban heritage: From palimpsest to brecciation. *International Journal of Heritage Studies*, Vol. 20, Issue 5, pp. 519–533. DOI: 10.1080/13527258.2013.794855.

Beck, A. T. (1963). Thinking and depression: I. Idiosyncratic content and cognitive distortions. *Archives of General Psychiatry*, Vol. 9, Issue 4, pp. 324–333. DOI: 10.1001/archpsyc.1963.01720160014002.

Bhattacharya, J., Petsche, H., Feldmann, U., and Rescher, B. (2001). EEG gamma-band phase synchronization between posterior and frontal cortex during mental rotation in humans. *Neuroscience Letters*, Vol. 311, Issue 1, pp. 29–32. DOI: 10.1016/s0304-3940(01)02133-4.

Ebejer, J. (2014). Meaning of place and the tourist experience. In: *Tourism Research Symposium*, July 16–17, 2014, Floriana, Malta, 13 p.

Edwards, D., Griffin, T., and Hayllar, B. (2008). Urban tourism research: developing an agenda. *Annals of Tourism Research*, Vol. 35, Issue 4, pp. 1032–1052. DOI: 10.1016/j.annals.2008.09.002.

Erkan, İ. (2017a). Cognitive analysis of pedestrians walking while using a mobile phone. *Journal of Cognitive Science*, Vol. 18, No. 3, pp. 301–319. DOI: 10.17791/jcs.2017.18.3.301.

Erkan, İ. (2017b). Effects on the design of transport systems of pedestrian dynamics. In: Yaghoubi, H. (ed.). *Highway Engineering*, pp. 17–33. DOI: 10.5772/intechopen.70496.

Erkan İ. (2021) Cognitive response and how it is affected by changes in temperature. *Building Research & Information*, Vol. 49, Issue 4, pp. 399–416. DOI: 10.1080/09613218.2020.1800439.

Güntekin, B. and Başar, E. (2010). Event-related beta oscillations are affected by emotional eliciting stimuli. *Neuroscience Letters*, Vol. 483, Issue 3, pp. 173–178. DOI: 10.1016/j.neulet.2010.08.002.

Healey, J. A. and Picard, R. W. (2005). Detecting stress during real-world driving tasks using physiological sensors. *IEEE Transactions on Intelligent Transportation Systems*, Vol. 6, Issue 2, pp. 156–166. DOI: 10.1109/TITS.2005.848368.

Hugdahl, K. and Davidson, R. J. (eds.). (2004). *The asymmetrical brain*. Cambridge: MIT Press, 810 p.

Jasper, H. (1958). Report of the committee on methods of clinical examination in electroencephalography. *Electroencephalography and Clinical Neurophysiology*, Vol. 10, pp. 370–375.

Kuban, D. (1994). Kentin Gelişmesi. *Dünden Bugüne İstanbul Ansiklopedisi*, Vol. 4, pp. 533–545.

Labbé, E., Schmidt, N., Babin, J., and Pharr, M. (2007). Coping with stress: the effectiveness of different types of music. *Applied Psychophysiology and Biofeedback*, Vol. 32, Issue 3–4, pp. 163–168. DOI: 10.1007/s10484-007-9043-9.

Lagopoulos, J., Xu, J., Rasmussen, I., Vik, A., Malhi, G. S., Eliassen, C. F., Arntsen, I. E., Saether, J. G., Hollup, S., Holen, A., Davanger, S., and Ellingsen, Ø. (2009). Increased theta and alpha EEG activity during nondirective meditation. *The Journal of Alternative and Complementary Medicine*, Vol. 15, No. 11, pp. 1187–1192. DOI: 10.1089/acm.2009.0113.

Lasa, L., Ayuso-Mateos, J. L., Vázquez-Barquero, J. L., Dıez-Manrique, F. J., and Dowrick, C. F. (2000). The use of the Beck Depression Inventory to screen for depression in the general population: a preliminary analysis. *Journal of Affective Disorders*, Vol. 57, Issues 1–3, pp. 261–265. DOI: 10.1016/S0165-0327(99)00088-9.

Li, J.-G. T., Kim, J.-O., and Lee, S. Y. (2009). An empirical examination of perceived retail crowding, emotions, and retail outcomes. *The Service Industries Journal*, Vol. 29, Issue 5, pp. 635–652. DOI: 10.1080/02642060902720121.

Luijcks, R., Vossen, C. J., Hermens, H. J., van Os, J., and Lousberg, R. (2015). The influence of perceived stress on cortical reactivity: a proof-of-principle study. *PLoS ONE*, Vol. 10, No. 6, e0129220. DOI: 10.1371/journal.pone.0129220.

Milner, B. (1968). Visual recognition and recall after right temporal-lobe excision in man. *Neuropsychologia*, Vol. 6, No. 3, pp. 191–209. DOI: 10.1016/0028-3932(68)90019-5.

Müller, M. M., Gruber, T., and Keil, A. (2000). Modulation of induced gamma band activity in the human EEG by attention and visual information processing. *International Journal of Psychophysiology*, Vol. 38, Issue 3, pp. 283–299. DOI: 10.1016/S0167-8760(00)00171-9.

Newson, J. J. and Thiagarajan, T. C. (2019). EEG frequency bands in psychiatric disorders: a review of resting state studies. *Frontiers in Human Neuroscience*, Vol. 12, 521. DOI: 10.3389/fnhum.2018.00521.

Nohl, W. (2001). Sustainable landscape use and aesthetic perception–preliminary reflections on future landscape aesthetics. *Landscape and Urban Planning*, Vol. 54, Issues 1–4, pp. 223–237. DOI: 10.1016/S0169-2046(01)00138-4.

Popp, M. (2012). Positive and negative urban tourist crowding: Florence, Italy. *Tourism Geographies*, Vol. 14, Issue 1, pp. 50–72. DOI: 10.1080/14616688.2011.597421.

Rathnayake, R. M. W. (2015). How does 'crowding' affect visitor satisfaction at the Horton Plains National Park in Sri Lanka? *Tourism Management Perspectives*, Vol. 16, pp. 129–138. DOI: 10.1016/j.tmp.2015.07.018.

Salah Ouf, A. M. (2001). Authenticity and the sense of place in urban design. *Journal of Urban Design*, Vol. 6, Issue 1, pp. 73–86. DOI: 10.1080/13574800120032914.

Sammler, D., Grigutsch, M., Fritz, T., and Koelsch, S. (2007). Music and emotion: electrophysiological correlates of the processing of pleasant and unpleasant music. *Psychophysiology*, Vol. 44, Issue 2, pp. 293–304. DOI: 10.1111/j.1469-8986.2007.00497.x.

Sanei, S. and Chambers, J. A. (2013). *EEG signal processing*. Chichester: John Wiley & Sons, 312 p.

Selby, M. (2004). Consuming the city: conceptualizing and researching urban tourist knowledge. *Tourism Geographies*, Vol. 6, Issue 2, pp. 186–207. DOI: 10.1080/1461668042000208426.

Sharma, N. and Gedeon, T. (2012). Objective measures, sensors and computational techniques for stress recognition and classification: A survey. *Computer Methods and Programs in Biomedicine*, Vol. 108, Issue 3, pp. 1287–1301. DOI: 10.1016/j.cmpb.2012.07.003.

Shaw, J. C. (ed.). (2003). *The brain's alpha rhythms and the mind: a review of classical and modern studies of the alpha rhythm component of the electroencephalogram with commentaries on associated neuroscience and neuropsychology*. Amsterdam: BV Elsevier Science, 360 p.

Soini, K., Vaarala, H., and Pouta, E. (2012). Residents' sense of place and landscape perceptions at the rural–urban interface. *Landscape and Urban Planning*, Vol. 104, Issue 1, pp. 124–134. DOI: 10.1016/j.landurbplan.2011.10.002.

Steer, R. A., Cavalieri, T. A., Leonard, D. M., and Beck, A. T. (1999). Use of the Beck depression inventory for primary care to screen for major depression disorders. *General Hospital Psychiatry*, Vol. 21, Issue 2, pp. 106–111. DOI: 10.1016/S0163-8343(98)00070-X.

Tilley, S., Neale, C., Patuano, A., and Cinderby, S. (2017). Older people's experiences of mobility and mood in an urban environment: a mixed methods approach using electroencephalography (EEG) and interviews. *International Journal of Environmental Research and Public Health*, Vol. 14, Issue 2, 151. DOI: 10.3390/ijerph14020151.

Ulrich, R. S. (1981). Natural versus urban scenes: Some psychophysiological effects. *Environment and Behavior*, Vol. 13, Issue 5, pp. 523–556. DOI: 10.1177/0013916581135001.

Watson, D., Clark, L. A., and Tellegen, A. (1988). Development and validation of brief measures of positive and negative affect: the PANAS scales. *Journal of Personality and Social Psychology*, Vol. 54, No. 6, pp. 1063–1070.

Yang, P. P. J. and Yamagata, Y. (2020). Urban systems design: Shaping smart cities by integrating urban design and systems science. In: Yang, P. P. J. and Yamagata, Y. (eds.). *Urban Systems Design*. Amsterdam: Elsevier, pp. 1–22. DOI: 10.1016/B978-0-12-816055-8.00001-4.

ОЩУЩЕНИЕ ГОРОДСКОЙ И АРХИТЕКТУРНОЙ СРЕДЫ

Илькер Эркан

Факультет архитектуры, Университет Сулеймана Демиреля, Турция

E-mail: ilkererkan@sdu.edu.tr

Аннотация
Введение: В рамках данного исследовании изучено, как различные пространства влияют на людей и на их эмоции с точки зрения нейроархитектуры. **Цель исследования**: изучить, как перемещение в исторической и современной архитектурной среде влияет на людей как когнитивно, так и физиологически.. **Методы**: изучены реакции на историческую и современную среду, которые затем были проанализированы с помощью количественных данных и различных методов анализа. Разработаны три различные архитектурные среды. Участникам эксперимента было предложено перемещаться по ним в виртуальной реальности. Участникам было также предложено выбрать изображения в современном или историческом стиле, после чего они проходили тесты по шкале депрессии Бека и по шкале позитивного и негативного аффекта. Кроме того, с помощью приборов для электроэнцефалографии, отслеживания движений глаз и кожно-гальванического рефлекса были собраны физиологические данные 164 участников эксперимента. В **результате**, когда участников эксперимента оценивали по их предпочтениям в отношении современной или исторической среды, оказалось, что они предпочитают сочетание исторической и современной среды. Установлено, что в разных архитектурных средах люди демонстрируют различные когнитивные реакции. Это важный вывод для перепланировки окружающей среды.

Ключевые слова: нейроархитектура; архитектурная среда; поведение людей; застройка.

Civil Engineering

EXPERIMENTAL STUDY OF A WOODEN GIRDER TRUSS WITH COMPOSITE CHORDS

Mikhail Lisyatnikov*, Anastasia Lukina, Mikhail Lukin, Svetlana Roschina

Vladimir State University named after Alexander and Nikolay Stoletovs, Vladimir, Russia

*Corresponding author's e-mail: mlisyatnikov@mail.ru

Abstract

Introduction: Beam is one of the most common wooden structures. The use of beam structures is relevant in the flooring and roofing of buildings. A disadvantage of using wooden beams is the impossibility to cover a span of more than 6 m without expensive factory-made structures (glued beams, composite beams, metal-and-wood beams, LVL beams, etc.). The study proposes a wooden structure of a composite girder truss with a span of 9 m, assembled from planks with the use of steel dowels directly at the construction site. The **purpose of the study** was to experimentally determine the strength and deformability of wooden girder trusses with a span of 9 m. The following **methods** were used: experimental investigations of the stress-strain state of beams. As a **result**, brittle fracture was noted in the area of the support chord junction with the span chords under the action of breaking load equal to 14.52 kN/m. The values of tensile and compressive strength of wooden girder trusses were experimentally determined to be 35.35 MPa and 25.14 MPa, respectively. The developed wooden girder trusses are recommended for use in the flooring of buildings with a span of 9 m.

Keywords: construction; timber; beam; strength; girder truss; stress-strain state; composite chords.

Introduction

Construction grade timber is one of the most valuable products in engineering. Timber can have economic benefits for construction, as modern timber products are mainly factory-made and brought to the site for rapid assembly. The environmental benefits of using timber structures have been demonstrated in a significant number of projects around the world (Lukina et al., 2022b).

Studies on microstructure and mechanical properties (Lukina et al., 2022ba) show that the molecular and cellular structure of wood is fundamental to its use as a building material.

The use of wooden beam structures in the flooring and roofing of buildings is especially relevant in low-rise individual housing construction (IHC). Such structures can reduce the load from horizontal bearing structures on the walls and foundations of a building since wood is lighter than reinforced concrete cast-in-place and prefabricated slabs in terms of specific weight. This is especially in demand in wall structures when not engineering bricks but less durable light-weight energy-efficient blocks made of expanded clay aggregate, aerated concrete, wood concrete, etc. are used, currently utilized in the construction of more than 85 % of all IHC buildings. However, the use of wooden structures in the flooring and covering of IHC buildings is limited by a number of features. These include issues of structural specifics (anisotropy, flaws,

etc.), durability, biological resistance, fire hazard, etc. The main factor leading to an end user's refusal to use wooden structures in the flooring and roofing of buildings is the impossibility to construct spans of more than 6.0 m without additional supports, i.e., limitations in the assortment of solid wood lumber. If steel and reinforced concrete structures are not taken into account, then premises with a width exceeding 6.0 m can be constructed with the use of glued wooden structures, composite wooden structures, metal-and-wood beams, LVL beams, etc.(Nadir et al., 2016). However, the use of such structures results in higher construction costs since all of the above products are manufactured at factory. Among other disadvantages of these structures, their massiveness can be mentioned, which inevitably leads to aesthetic discomfort (pressure on a person) if these structures are arranged in an open form (without lining) in the roofing.

Beam is one of the most common building structures made of timber (Koshcheev et al., 2018; Lukina et al., 2021). Depending on the production method, there are the following types of these structures: beams of solid section made of logs, bars or boards (Autengruber et al., 2021; Ianasi, 2015; Keenan, 1974; Li et al., 2017; Mungwa et al., 1999; Song and Lam, 2010); composite beams made of logs, bars or boards connected on pliable joints (dowels, nails, dowel plates, keys, etc.) (Jiao et al., 2017; Pulngern et al., 2010; Qi et al., 2017); glued

beams made of boards (Asyraf et al., 2020; Foliente and McLain, 1992; Xu et al., 2024) [14,15,16]; wood-composite structures combined from different materials: (wood-and-metal) HTS I-beam; beams reinforced with steel elements, carbon and glass fiber materials, etc.) (Borri et al., 2005; De Jesus et al., 2012; Issa and Kmeid, 2005).

The use of wooden beam structures in the flooring and roofing of buildings is especially relevant in low-rise individual housing construction due to their physical and mechanical properties, relatively low price, and no need to use lifting and transportation equipment during installation (Anshari et al., 2012; Bocquet et al., 2007). However, these structures also have a number of disadvantages: structural specifics (anisotropy, flaws, etc.), durability, biological resistance, fire hazard, etc. The main factor leading to an end user's refusal to use wooden structures in the flooring and roofing of buildings is the impossibility to construct spans of more than 6 m without additional supports, i.e., limitations in the assortment of solid wood lumber (El-Houjeyri et al., 2019; LeBorgne and Gutkowski, 2010). If we consider only wood-based structures, it is possible to cover a span of more than 6 m only with glued wooden structures, composite wooden structures, metal-and-wood beams, LVL beams, etc. However, the use of such structures results in higher construction costs since all of the above products are manufactured at factory. Among other disadvantages of these structures, their massiveness can be mentioned, which inevitably leads to aesthetic discomfort (pressure on a person) if these structures are arranged in an open form (without lining) in the roofing (Ehtisham et al., 2024; Karelskiy et al., 2015).

This study proposes a structure of a composite lattice girder truss with a span of 9 m, assembled from planks with the use of steel dowels directly at the construction site. The structural design of the girder truss was based on the behavior of structures in bending, to ensure resistance to the maximum forces at all sections. The beam structure makes it possible to use lumber with almost no residue: in 48 m (8 planks of 6 m each), only 18 cm are not used in the structure. Depending on the quality of wood and its processing, pine (*Pinus sylvestris L.*) lumber of grades I–II can be used in the girder truss. Besides, due to its lattice structure, the girder truss has an artistic and aesthetic appearance, which makes it possible to use it in an open form in the roofing.

The use of such a structure in the flooring and roofing of buildings is quite a new direction and requires special studies to determine the strength and deformability of the beam.

The purpose of the study was to determine the strength and deformability of wooden lattice girder trusses by conducting experiments on structure models. The subject of the study is the stress-strain state of a wooden lattice girder truss.

The results of the study make it possible to justify the use of wooden beam structures in the flooring and roofing of buildings with spans of more than 6 m.

Methods

The structural design of the girder truss was based on the behavior of structures in bending, to ensure resistance to the maximum forces at all sections. The girder truss with a span of 9 m (Fig. 1) represents a lattice structure similar in appearance to a wooden truss with parallel chords. Due to the small construction height, this element is considered a beam element (Cao et al., 2020), but for convenience, hereinafter the elements are called truss elements (chord, post, brace).

The girder truss consists of 4 span chords, 4 support chords, 18 braces, and 4 posts. It should be noted that the beam is assembled from eight 6000x150x50 mm planks with almost no residue, which is 176x150x50 mm. This implies that the lumber is 99.96 % utilized.

Between the span chords, braces are installed in the middle of the section at a 3 m long section at an angle of 50°. In the remaining space (1.5 m each) between the span chords, support chords are installed. At the free ends of the 1.5 m long support chords, braces in the form of a lattice at an angle of 50° are installed on both sides. At the ends of the girder truss, paired posts are installed between the chords. The structural elements are connected by dowels: Ø 8 in the support part of the truss, and Ø 12 in the braces. The connection uses paired washers, i.e., washers installed on two opposite sides of the connected element, which ensures high bearing capacity and low deformability of the structure. Flat washers are grouped in sets on both sides coaxially. Due to this, the metal to be joined is pressed evenly into the outer washer around the perimeter. Otherwise, skewing of the bolt body and, as a consequence, incomplete metal pressing-through around the perimeter are possible (Prosyanikov, 2016).

The action of the maximum bending moment in the middle of the span is taken up by the double section of the span chord, the action of the maximum shear stresses in the near-support areas is taken up by the double wall of cross braces, and the action of the support reactions is taken up by the double braces at the ends of the truss.

To confirm the results of the previously conducted engineering and numerical calculations for the wooden girder truss, it was necessary to conduct an experimental study (Alekseytsev et al., 2019), which makes it possible to identify the features of the stress-strain state, reveal the nature of the failure of such structures, and determine the breaking load.
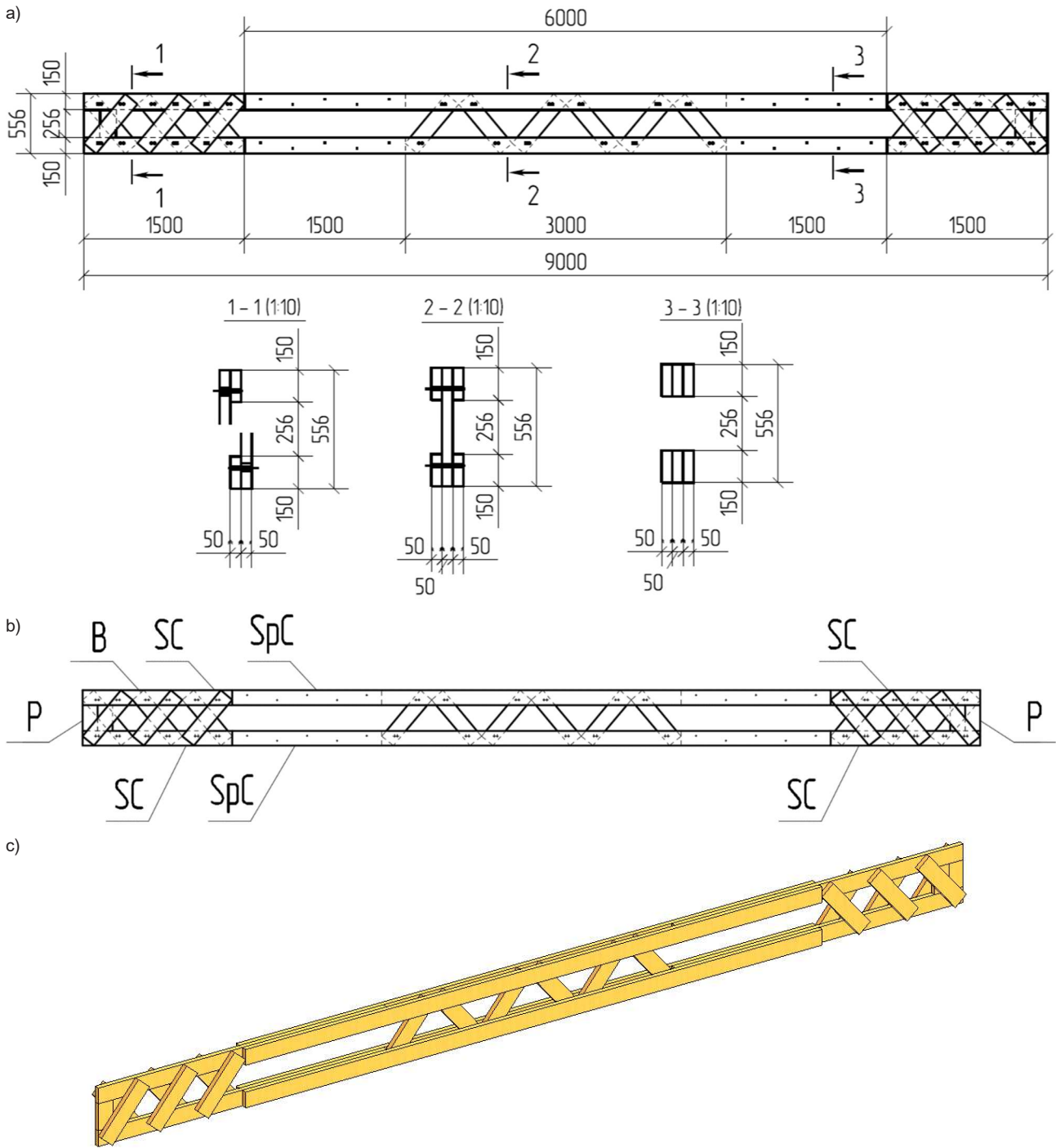
Fig. 1. Lattice girder truss: (a) geometric dimensions; (b) description of the beam elements; (c) 3D view.
SC — support chord; B — brace; P — post; SpC — span chord

The test rig (Fig. 2) developed at the Department of Building Structures and Architecture (Vladimir State University, Vladimir) is designed for testing models of building structures with a maximum span of 4.5 m. Eight-point loading with 0.5 m spacing is performed, which simulates load uniformly distributed over the entire span. Load is directly applied to the structure by means of a system of rods and flexible hangers connected via a shaft/reel to the basket with weights. Load conversion ratio n = 8.5.

Based on recommendations for testing wooden structures, the loading increment can be set within 0.2–0.25 of the design load. This loading corresponds to stress increase in bending in the range of 2–3.25 MPa and relative strains of 26×10^{-5}–32.5×10^{-5}. A TDS-530 multi-channel measuring complex was used to record relative strains with high accuracy. This complex makes it possible to record edge strains of materials by using strain gauges with a base of 20 mm. The latter are glued to the pre-
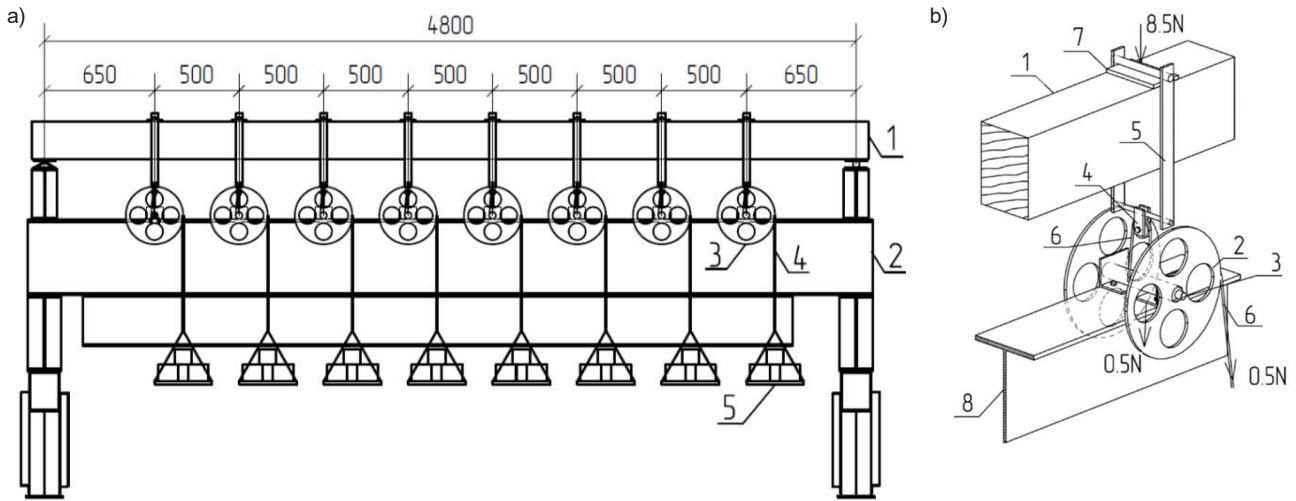
Fig. 2. Diagram of the test rig for testing beams with a span of 4.5 m: a) geometric dimensions; b) principle of the shaft/reel operation. (a) 1 — full-scale beam model; 2 — reactive beam: I-beam No. 45 + I-beam No. 30B1; 3 — connection shaft/reel; 4 — steel cables ø 6 mm; 5 — baskets with weights; 6 — dial gauges, 7 — PAO-6 deflection meters to measure rotation angles of support sections, 8 — PAO-6 deflection meter to determine beam deflections. (b) Design of the shaft/reel to transfer loads to the composite beam with conversion ratio n = 8.5: 1 — beam; 2 — connection reel ø 340 mm; 3 — connection shaft ø40 mm; 4 — single block for cable ø50 mm; 5 — rod made of rolled plate δ = 5 mm; 6 — steel cables ø 6 mm; 7 — distributing plate δ = 16 mm; 8 — reactive beam: I-beam No. 45 + I-beam No. 30B1)

cleaned and treated surface of wooden elements using cyanoacrylate-based adhesive.

The theoretical basis of modeling is the theory of similarity (Mastachenko, 1974), which establishes certain relationships between geometric dimensions, material properties, loads and deformations of the model and the full-scale structure. Simple and extended similarity can be distinguished. In case of simple (linear) similarity, the ratios of all dimensionless quantities are equal to 1, in case of extended (non-linear) similarity, they can differ from 1, and different quantities of the same dimension can have different ratios.

Since the wooden lattice girder truss has a span of 9 m, and the test rig allows for testing structures with a maximum span of 4.5 m, it was was required to perform modeling of the girder truss. The essence of theory of similarity is that a full-scale object is replaced by an analog (its model) based on that theory (Murata et al., 2007). The study addresses large-scale modeling of the structure with simple similarity at 1/2 ratio. All girder truss and fastening dowel elements are reduced in half. The transition from a full-scale object to a model takes place by introducing a system of proportionality coefficients or conversion ratios.

The moduli of elasticity of the model and the full-scale structure are as follows:

$$E_r = \frac{E_m}{E_n}, \qquad (1)$$

where E_m — modulus of elasticity of the model; E_n — modulus of elasticity of the full-scale structure.

Since all geometric dimensions are reduced in half, the following equality applies:

$$L_r = \frac{L_m}{L_n} = \frac{1}{2}, \qquad (2)$$

where L_m — model span; L_n — full-scale structure span.

We will load the large-scale model with eight concentrated forces. Then the value of the transformed load on the full-scale structure will be as follows:

$$P_n = \frac{P_m}{P_r} = \frac{P_m}{E_r L_r^2} = 4P_m, \qquad (3)$$

where P_m — concentrated force applied to the model; P_n — concentrated force applied to the full-scale structure; E_r — modulus of inelastic buckling; L_r — reduced span.

The deflections of the full-scale structure relative to the model can be determined by the following equation:

$$f_n = f_m \frac{L_n}{L_m} = 2f_m, \qquad (4)$$

where L_m — model span; L_n — full-scale structure span.

Results and discussion

The tests were conducted at the laboratory of building structures of Vladimir State University (Vladimir, Russia).

The wooden lattice girder trusses were studied in two stages:

• At the first stage, the stress-strain state of the wooden girder trusses was studied and the nature of failure was determined.

• At the second stage, the integral modulus of elasticity was determined, which, unlike the

calculated modulus of elasticity, takes into account the heterogeneity of wood, the influence of flaws, etc.

Fig. 3 shows the arrangement of strain gauges on the structure.

The air temperature in the room during the tests was in the range of 18–22°C, relative humidity — in the range of 50–60 %. Wood moisture content was measured with a Testo 616 electronic moisture meter with a measuring range for wood <50 % with an absolute measurement accuracy of 1.2 % in the measuring range of 7–10 % and 2 % in the measuring range nore than 10 %.

At the first stage, the trusses were loaded up to 0.8 of the standard load, in steps of 0.1 of the upper limit. At the second stage, they were loaded until failure, in steps of 0.25 of the design load. Loading time at each step is assumed to be 3 minutes, time of holding under the load is 15 minutes according to the requirements of the testing standard.

The design load was determined based on the condition of strength of normal sections in the middle of the span and amounted to 1.5 kN/m. Four identical models of beam structures (WLB 1...4) were tested. The digit in the girder truss marking indicates the serial number of the model.

Figs. 4 and 5 show the general views of the studied girder trusses during the tests and the nature of failure.

Based on the test results, the statistical processing of the experimental data was performed. The test results are summarized in Table 1 and Figs. 6 and 7.

The girder truss failure occurred at the point at the boundary of the upper support chord junction with the span chords in the form of cut fibers of the near-knot cross-grain and along the flaws in the form of knots. The failure occurred in the upper chord as a result of bending forces. It should be noted that tensile and compressive forces occurred in the

upper and lower chords of the girder truss, which was recorded by strain gauges.

Considering the nature of the forces (tension, compression, bending) occurring in the girder truss elements, it can be stated that the developed structure can be classified as a beam although structurally it resembles a truss. The beam showed a quite linear behavior during the tests up to the maximum load achieved during the testing.

The failure was brittle. The average breaking load per unit length was 3.63 kN/m, which exceeds the design load by 2.4 times. To increase the bearing capacity of the girder truss, we propose to install an additional post in the support chord to take up the bending forces. The post will be fastened with metal dowels, similar to the posts in the support part of the structure.

As Figs. 6 and 7 show, the behavior of all tested beams was quite uniform.

Based on the diagram in Fig. 7, we can draw conclusions about the coincidence of the neutral axis of the girder truss with the geometric center of the section. This indicates the symmetrical and simultaneous development of stresses in the compression and tension areas with an increase of the load acting on the structure. Besides, the diagram shows stress points on the top and bottom surfaces of the beam, which lead to the failure of the structure in the tension area under the action of the ultimate load.

The bearing capacity of the tested structures was assessed according to the recommendations for testing wooden structures. The method makes it possible to assess the bearing capacity of wooden beams by calculating the required safety factor depending on the logarithm of reduced time and type of structural failure in a short-term test.

For brittle beam failure, the factor is assumed to be 0.85. Therefore, the design load on the beam will
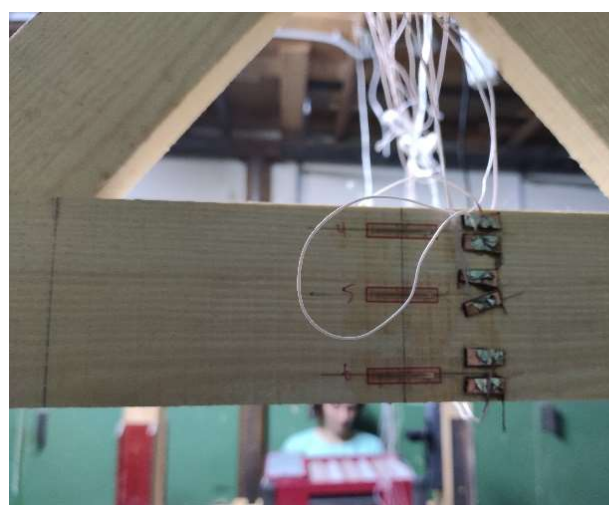

Fig. 3. Arrangement of strain gauges:
a) in the middle of the structure span; b) on the upper and lower span chords, respectively

Fig. 4. General view of wooden lattice beam testing

be 1.275 kN/m instead of 1.5 kN/m, and the maximum allowable load during the design is 3.87 kN/m.

Based on the results of the experimental studies, the breaking load and ultimate deflection of the models of wooden lattice girder trusses were determined. Using Eqs. (3) and (4), it is possible to determine the breaking load and deflection of the full-scale structure during failure, which will amount to 14.52 kN/m and 19.52 cm, respectively.

The tests showed that the joint with the adopted geometric configuration and materials can withstand loads significantly exceeding design ones. The developed girder truss adds versatility to wooden structures and is part of major studies currently conducted around the world to increase the use of structural timber, even in small sizes, obtained as a result of sustainable forestry.

This unique structure was patented in 2022. The use of such structures is possible both in the form of elements in the flooring and roofing of buildings and in the form of temporary elements at the construction site, for example, for formwork construction.

Considering the obtained results, it can be stated that the development and adaptation of scientific and technical solutions to strengthen girder trusses by means of rational reinforcement, mainly in the areas of the support chord junction with the span chords, is a promising approach to improve the performance of the developed wooden beam structure. Composite/reinforced trusses can provide greater strength and stiffness than wooden beam systems, which makes them more suitable for applications with large spans and no columns. Further studies in this direction will contribute to the development of new types of composite building structures with advanced strength and stiffness characteristics.

Conclusions and recommendations

Thus, based on the study of the stress-strain state of wooden lattice girder trusses, the following conclusions can be drawn:

1. A new wooden girder truss with a span of 9 m was developed, which is characterized by easy assembly at the construction site and low installation weight (about 190 kg) at a bearing capacity of 3.87 kN/m.

2. Large-scale modeling (1:2) of the studied wooden girder truss was performed, load and deflection conversion factors (with transition from model to full-scale structures) were determined.

3. Experimental studies of wooden girder truss models under short-term loading on the original test rig were conducted.

4. Tensile and compressive strength of the wooden girder trusses made of pine (*Pinus sylvestris L.*) of grades I–II were determined experimentally, which amounted to 35.35 and 25.14 MPa, respectively.

5. The brittle nature of failure in the area of the support chord junction with the span chords under the action of the breaking load equal to 14.52 kN/m was established, which determines
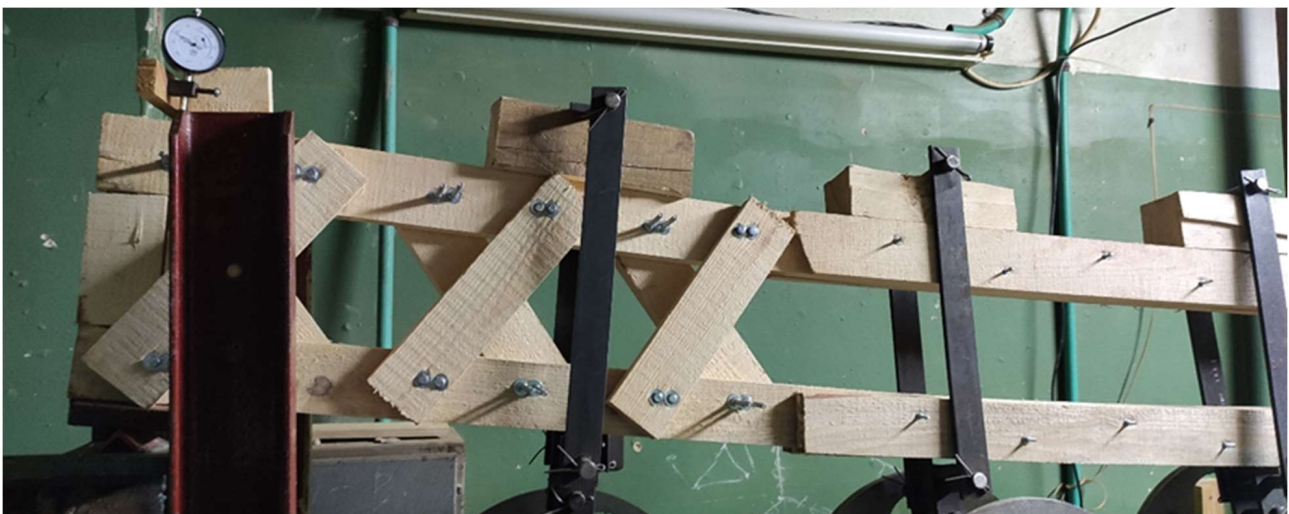

Fig. 5. Fragment of the general view of the failure area and the nature of failure

Table 1. **Results of wooden lattice girder truss testing**

No.	Beam	Design load, kN/m	Strains, $\varepsilon \times 10^{-6}$		Deflections, cm	Breaking load, kN/m
			compression	tension		
1	WLB-1	1.5	2.501	3.587	9.87	3.74
2	WLB-2	1.5	2.439	3.353	9.68	3.52
3	WLB-3	1.5	2.397	3.228	9.53	3.41
4	WLB-4	1.5	2.567	3.760	9.95	3.85
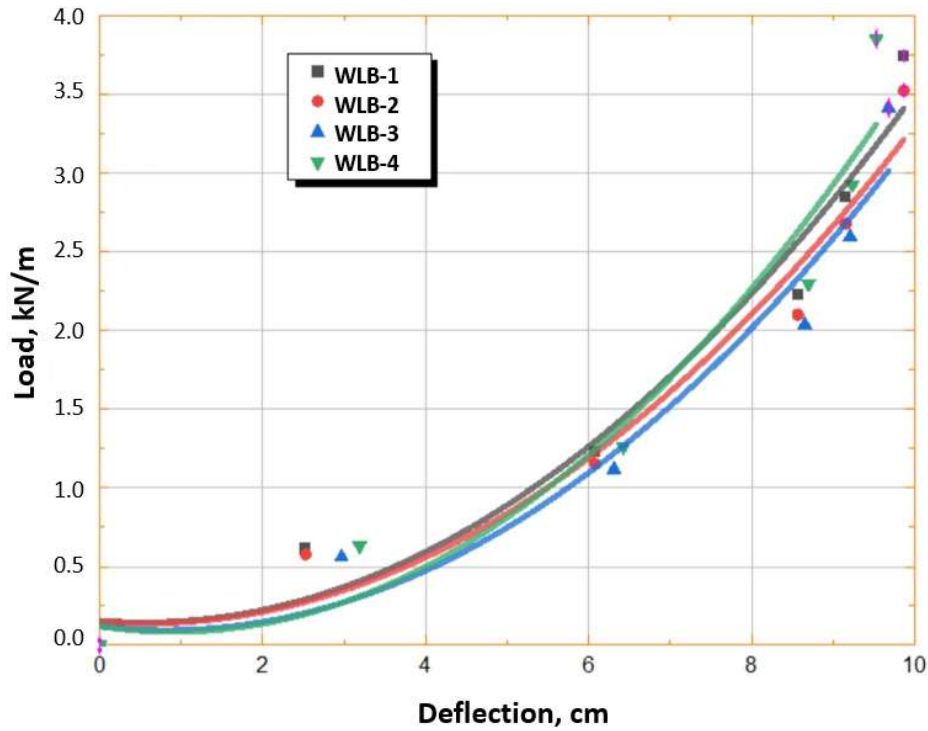
Fig. 6. Load/deflection diagram
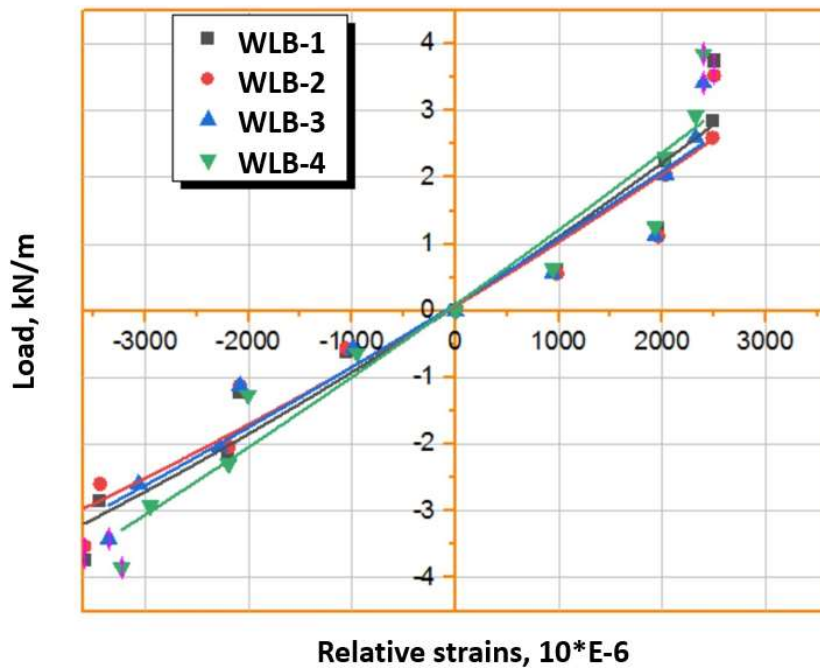
Fig. 7. Load / relative strains diagram

53

the prospects for further search for scientific and technical solutions to improve the rational layout and structural scheme and its analysis, including the assessment of the influence of the pliable joints of node connections on the stress-strain state of the developed girder truss.

The next stage of research will be devoted to the study of the girder truss under long-term loading to ensure comprehensive reliability assessment of the developed structure.

Funding

References

Alekseytsev, A. V., Gaile, L., and Drukis, P. (2019). Optimization of steel beam structures for frame buildings subject to their safety requirements. *Magazine of Civil Engineering*, Issue 7 (91), pp. 3–15. DOI: 10.18720/MCE.91.1.

Anshari, B., Guan, Z. W., Kitamori, A., Jung, K., and Komatsu, K. (2012). Structural behaviour of glued laminated timber beams pre-stressed by compressed wood. *Construction and Building Materials*, Vol. 29, pp. 24–32. DOI: 10.1016/j.conbuildmat.2011.10.002.

Asyraf, M. R. M., Ishak, M. R., Sapuan, S. M., Yidris, N., and Ilyas, R. A. (2020). Woods and composites cantilever beam: A comprehensive review of experimental and numerical creep methodologies. *Journal of Materials Research and Technology*, Vol. 9, Issue 3, pp. 6759–6776. DOI: 10.1016/j.jmrt.2020.01.013.

Autengruber, M., Lukacevic, M., Wenighofer, G., Mauritz, R., and Füssl, J. (2021). Finite-element-based concept to predict stiffness, strength, and failure of wood composite I-joist beams under various loads and climatic conditions. *Engineering Structures*, Vol. 245, 112908. DOI: 10.1016/j.engstruct.2021.112908.

Bocquet, J.-F., Pizzi, A., Despres, A., Mansouri, H. R., Resch, L., Michel, D., and Letort, F. (2007). Wood joints and laminated wood beams assembled by mechanically-welded wood dowels. *Journal of Adhesion Science and Technology*, Vol. 21, Issue 3–4, pp. 301–317. DOI: 10.1163/156856107780684585.

Borri, A., Corradi, M., and Grazini, A. (2005). A method for flexural reinforcement of old wood beams with CFRP materials. *Composites Part B: Engineering*, Vol. 36, Issue 2, pp. 143–153. DOI: 10.1016/J.COMPOSITESB.2004.04.013.

Cao, S., Huo, M., Qi, N., Zhao, C., Zhu, D., and Sun, L. (2020). Extended continuum model for dynamic analysis of beam-like truss structures with geometrical nonlinearity. *Aerospace Science and Technology*, Vol. 103, 105927. DOI: 10.1016/j.ast.2020.105927.

De Jesus, A. M. P., Pinto, J. M. T., and Morais, J. J. L. (2012). Analysis of solid wood beams strengthened with CFRP laminates of distinct lengths. *Construction and Building Materials*, Vol. 35, pp. 817–828. DOI: 10.1016/j.conbuildmat.2012.04.124.

Ehtisham, R., Qayyum, W., Camp, C. V., Plevris, V., Mir, J., Khan, Q. Z., and Ahmad, A. (2024). Computing the characteristics of defects in wooden structures using image processing and CNN. *Automation in Construction*, Vol. 158, 105211. DOI: 10.1016/j.autcon.2023.105211.

El-Houjeyri, I., Thi, V.-D., Oudjene, M., Khelifa, M., Rogaume, Y., Sotayo, A., and Guan, Z. (2019). Experimental investigations on adhesive free laminated oak timber beams and timber-to-timber joints assembled using thermo-mechanically compressed wood dowels. *Construction and Building Materials*, Vol. 222, pp. 288–299. DOI: 10.1016/j.conbuildmat.2019.05.163.

Foliente, G. C. and McLain, T. E. (1992). Design of notched wood beams. *Journal of Structural Engineering*, Vol. 118, Issue 9, pp. 2407–2420. DOI: 10.1061/(ASCE)0733-9445(1992)118:9(2407).

Ianasi, A. C. (2015). On the role of CFRP reinforcement for wood beams stiffness. *IOP Conference Series: Materials Science and Engineering*, Vol. 95, 012015. DOI: 10.1088/1757-899X/95/1/012015.

Issa, C. A. and Kmeid, Z. (2005). Advanced wood engineering: glulam beams. *Construction and Building Materials*, Vol. 19, Issue 2, pp. 99–106. DOI: 10.1016/j.conbuildmat.2004.05.013.

Jiao, P., Borchani, W., Soleimani, S., and McGraw, B. (2017). Lateral-torsional buckling analysis of wood composite I-beams with sinusoidal corrugated web. *Thin-Walled Structures*, Vol. 119, pp. 72–82. DOI: 10.1016/j.tws.2017.05.025.

Karelskiy, A. V., Zhuravleva, T. P., and Labudin, B. V. (2015). Load-to-failure bending test of wood composite beams connected by gang nail. *Magazine of Civil Engineering*, Issue 2 (54), pp. 77–85. DOI: 10.5862/MCE.54.9.

Keenan, F. J. (1974). Shear strength of wood beams. *Forest Products Journal*, Vol. 24, Issue 9, pp. 63–70.

Koshcheev, A. A., Roshchina, S. I., Lukin, M. V., and Lisyatnikov, M. S. (2018). Wooden beams with reinforcement along a curvilinear trajectory. *Magazine of Civil Engineering*, Issue 5 (81), pp. 193–201. DOI: 10.18720/MCE.81.19.

LeBorgne, M. R. and Gutkowski, R. M. (2010). Effects of various admixtures and shear keys in wood–concrete composite beams. *Construction and Building Materials*, Vol. 24, Issue 9, pp. 1730–1738. DOI: 10.1016/j.conbuildmat.2010.02.016.

Li, H., Lam, F., and Qiu, H. (2017). Flexural performance of spliced beam connected and reinforced with self-tapping wood screws. *Engineering Structures*, Vol. 152, pp. 523–534. DOI: 10.1016/j.engstruct.2017.08.032.

Lukina, A., Roshchina, S., and Gribanov, A. (2021). Method for Restoring Destructed Wooden Structures with Polymer Composites. In: Vatin, N., Borodinecs, A., and Teltayev, B. (eds.). *Proceedings of EECE 2020. Lecture Notes in Civil Engineering*, Vol. 150. Cham: Springer, pp. 464–474. DOI: 10.1007/978-3-030-72404-7_45.

Lukina, A., Lisyatnikov, M., Martinov, V., Kunitskya, O., Chernykh, A., and Roschina, S. (2022a). Mechanical and microstructural changes in post-fire raw wood. *Architecture and Engineering*, Vol. 7, No. 3, pp. 44–52. DOI: 10.23968/2500-0055-2022-7-3-44-52.

Lukina, A., Roshchina, S., Lisyatnikov, M., Zdralovic, N., and Popova, O. (2022b). Technology for the restoration of wooden beams by surface repair and local modification. In: Manakov, A. and Edigarian, A. (eds.). *International Scientific Siberian Transport Forum TransSiberia - 2021. TransSiberia 2021. Lecture Notes in Networks and Systems*, Vol. 403. Cham: Springer, pp. 1371–1379. DOI: 10.1007/978-3-030-96383-5_153.

Mastachenko, V. N. (1974). *Reliability of modeling building structures*. Moscow: Stroyizdat, 88 p.

Mungwa, M. S., Jullien, J.-F., Foudjet, A., and Hentges, G. (1999). Experimental study of a composite wood–concrete beam with the INSA–Hilti new flexible shear connector. *Construction and Building Materials*, Vol. 13, Issue 7, pp. 371–382. DOI: 10.1016/S0950-0618(99)00034-3.

Murata, K. and Kanazawa, T. (2007). Determination of Young's modulus and shear modulus by means of deflection curves for wood beams obtained in static bending tests. *Holzforschung*, Vol. 61, No. 5, pp. 589-594. DOI: 10.1515/HF.2007.082.

Nadir, Y., Nagarajan, P., Ameen, M., and Arif M. M. (2016). Flexural stiffness and strength enhancement of horizontally glued laminated wood beams with GFRP and CFRP composite sheets. *Construction and Building Materials*, Vol. 112, pp. 547–555. DOI: 10.1016/j.conbuildmat.2016.02.133.

Prosyanikov, B. D. (2016). Bolted joint with reciprocal punch of connected slender sections. *Journal of Construction and Architecture*, No. 2, pp. 130–138.

Pulngern, T., Chucheepsakul, S., Padyenchean, C., Rosarpitak, V., Prapruit, W., Chaochanchaikul, K., and Sombatsompop, N. (2010). Effects of cross-section design and loading direction on the creep and fatigue properties of wood/PVC composite beams. *Journal of Vinyl and Additive Technology*, Vol. 16, Issue 1, pp. 42–49. DOI: 10.1002/vnl.20227.

Qi, Y., Fang, H., Shi, H., Liu, W., Qi, Y., and Bai, Y. (2017). Bending performance of GFRP-wood sandwich beams with lattice-web reinforcement in flatwise and sidewise directions. *Construction and Building Materials*, Vol. 156, pp. 532–545. DOI: 10.1016/j.conbuildmat.2017.08.136.

Song, X. and Lam, F. (2010). Stability capacity and lateral bracing requirements of wood beam-columns. *Journal of Structural Engineering*, Vol. 136, Issue 2, pp. 211–218. DOI: 10.1061/(ASCE)ST.1943-541X.0000095.

Xu, B., Xia, J., Chang, H., Chen X., Yang, C., and Zhang, L. (2024). Numerical-analytical investigation on bending performance of laminated beams in modular steel buildings. *Journal of Constructional Steel Research*, Vol. 217, 108630. DOI: 10.1016/j.jcsr.2024.108630.

ЭКСПЕРИМЕНТАЛЬНОЕ ИССЛЕДОВАНИЕ ДЕРЕВЯННОЙ БАЛОЧНОЙ ФЕРМЫ С СОСТАВНЫМИ ПОЯСАМИ

Лисятников Михаил Сергеевич*, Лукина Анастасия Васильевна, Лукин Михаил Владимирович, Рощина Светлана Ивановна

Владимирский государственный университет имени Александра Григорьевича и Николая Григорьевича Столетовых

*E-mail: mlisyatnikov@mail.ru

Аннотация
Введение: Одной из самых распространенных деревянных конструкцией является балка. Применение балочных конструкций актуально в перекрытиях и покрытии зданий. Недостатком применения деревянных балок является невозможность перекрыть пролет более 6 м без использования дорогостоящих конструкций заводского изготовления (клееных балок, составных балок, металлодеревянных балок, LVL бруса и т.д.). В исследовании предлагается деревянная конструкция составной балочной фермы пролетом 9 м, которая собирается из досок стальными нагелями непосредственно на строительной площадке. **Цель работы** — экспериментально определить прочность и деформативность деревянных балочных ферм пролетом 9 м. Использованы **методы:** экспериментальные исследование напряженно-деформированного состояния балок. **В результате** установлен хрупкий характер разрушения в месте примыкания опорного пояса к пролетным поясам при действии разрушающей нагрузки, равной 14,52 кН/м. Экспериментально определены значения предела прочности деревянных балочных ферм на растяжение и сжатие, равные 35,35 МПа и 25,14 МПа соответственно. Разработанные деревянные балочные фермы, рекомендуется применять в перекрытиях зданий пролетом 9 м.

Ключевые слова: строительство; древесина; балка; прочность; балочная ферма; напряженно-деформированное состояние; составные пояса.

IMPACT OF LEAD RUBBER BEARING BASE ISOLATION SYSTEMS ON BUILDING STRUCTURES DESIGNED AS PER EUROCODE 8

Mohammed Tamahloult[1], Mouloud Ouanani[2], Boualem Tiliouine[1]*

[1]Laboratory of Earthquake Engineering and Structural Dynamics, Department of Civil Engineering, Ecole Nationale Polytechnique, Algeria
[2]Department of Civil Engineering, University of Djelfa, Algeria

*Corresponding author's e-mail: boualem.tiliouine@g.enp.edu.dz

Abstract
Introduction: Seismic base isolation has been classified as a structural protection system designed to minimize the seismic forces transferred to a structure during an earthquake. This can be achieved through the use of various devices, such as elastomeric bearings, sliding bearings, and hybrid systems. **Purpose of the study**: The study aims to evaluate the impact of using lead rubber bearings (LRB) as a base isolation system in building structures. **Methods:** In order to achieve this, nonlinear dynamic analyses of a seven-story building with and without an isolation device at its base were performed using the Fast Nonlinear Analysis (FNA) algorithm. The building was designed according to Eurocode 8 (EC8) criteria and then subjected to analysis using data from two previous earthquake events. **Results**: It is concluded that the bilinear behavior assumption made in the design stage according to EC8 is appropriate. Additionally, implementing an isolation system with LRBs at the building foundation can significantly enhance building performance by reducing floor accelerations, inter-story drifts, and base shear responses. Furthermore, it is demonstrated that isolating a building at its base with LRBs effectively reduces internal forces due to both gravity and seismic loads.

Keywords: base isolation; LRB system; 3D nonlinear earthquake response analysis; Eurocode 8; bilinear hysteresis.

Introduction

Seismic isolation is an excellent method for passive protection of a building structure. It enhances structural performance and reduces potential earthquake damage by lengthening the fundamental period of vibration and increasing energy dissipation (Naeim and Kelly, 1999). Seismic base isolation systems, including laminated rubber bearings, friction pendulum systems, and Teflon-steel friction bearings, have been utilized to reduce the transmission of seismic forces from the ground to a building structure.

Each of these systems has its own characteristics and advantages. Laminated rubber bearings are known for their durability, cost-effectiveness, and optimal control of their characteristics (Jain et al., 2004).

A laminated rubber bearing consists of alternating thin layers of rubber and steel, giving it the ability to support heavy weights due to its stiffness in the vertical direction. At the same time, it is horizontally flexible, allowing superstructures to move similarly to the motion of a rigid body during an earthquake (Koo et al., 1999). A lead rubber bearing (LRB) is a specific type of the laminated rubber bearing that includes a lead core in its structure, providing high initial rigidity and high damping, with equivalent damping varying from 15 to 35 % (Attanasi et al., 2009). Buildings equipped with LRBs demonstrated excellent performance during past earthquakes

(1994 — Northridge; 1995 — Kobe), confirming the effectiveness of LRBs as suitable base isolators (Asher et al., 1997).

Several mathematical models have been used to characterize the hysteresis behavior of various types of bearings. The idealized hysteresis behavior of bearings has been the subject of extensive studies. Among the various models proposed, the bilinear model is widely used in both research and design practice (e.g. Amanollah et al., 2023). Its simplicity allows for an accurate characterization of the mechanical properties of bearings, making it suitable for both elastomeric-type and sliding-type bearings (Cheng et al., 2008).

According to Mayes (Mayes and Naeim, 2001), any design process must ensure that (i) the bearings will safely withstand the maximum gravity service loads for the lifetime of the structure and (ii) provide period shift and hysteretic damping during one or more design earthquakes.

The current generation of building codes has progressed in two significant ways. Firstly, they provide guidelines for incorporating energy dissipation mechanisms, taking into consideration both the lateral strength method and the type of structural material used. Secondly, these updated codes have expanded their scope to include additional considerations, such as geotechnical aspects. Furthermore, these new regulations incorporate a semi-probabilistic approach to assess safety, in line with the principles defined

in EN 1990 (Elghazouli, 2009). Eurocode 8 (European Committee for Standardization, 2004) includes a dedicated chapter on the seismic isolation of buildings and bridges. In that chapter, the calculation of maximum isolator displacement is carried out in the preliminary design phase using the Equivalent Linear Force (ELF) method (Cavdar and Ozdemir, 2022). In the same context of designing building structures with base isolation, the Chinese code GB50011-2010 (Ministry of Housing and Urban-Rural Development of the People's Republic of China, 2010) recommends a distinct design approach. This approach ensures that the isolation system and superstructure are designed independently, and introduces the concept of horizontal seismic isolation coefficients (Hu et al., 2023).

In this study, we aim to demonstrate the impact of seismic base isolators on building structures during earthquakes. The analyses were carried out on a multi-story building model with a base isolation system with LRBs incorporated at the base, as well as on the same model with a fixed base, both designed according to EC8. The earthquake data included ground motion records from the 1940 El Centro and the 1996 Kobe earthquakes.

Subject, models, and methods

Building model

The subject model is a seven-story frame building with dimensions of 15×8 m². The beam sections are 40×30 cm², and the column sections are 50×50 cm². Each story has a height of 3 m, as shown in Fig. 1a and Fig. 1b. The building is isolated with LRBs placed under each column between the foundation and superstructure, and attached to a 10 cm rigid base slab. The total weight of the building is 14.066 kN. The fundamental period of the building is 0.61 s, and the modal damping ratio is expected to remain constant at 5 % for each mode. The building structure is intended to be located in a highly seismic zone, resting on a soil profile categorized as stiff soil profile type C. The system isolator to be used is a lead rubber bearing (LRB) as shown in Fig. 2. Two LRB profiles are designed for the building because the gravity load transferred to the corner bearings is less than that transferred to the inner and side bearings.

The bearings are labeled as *(A)* for the columns at the corners and *(B)* for those on the sides and inside (Fig. 1b). The force deformation behavior of the isolators (LRBs) in this study is modeled as a nonlinear hysteretic loop directly idealized by the bilinear model (AASHTO, 2010; Kelly, 1997; Mori et al., 1998) as indicated in Fig. 3.

Seismic displacement criteria as per EC8

First, we define the design response spectrum of each isolator (LRB^A, LRB^B) in accordance with the seismic requirements specified by Eurocode 8, Type 1 spectrum (Fig. 4). This applies to areas with high seismicity and near-field earthquakes, relative to a reference peak ground acceleration (PGA) of a_{gR} = 0.4 g. The importance factor for the building g_I = 1; soil type — C, spectral parameters from EC8 (Table 3.2) are as follows:

$T(s)$ is the linear *SDOF* system's vibration period and $Se(T)$ is the elastic response spectrum; the lower and upper limits of the period of the constant spectral acceleration branch are T_B = 0.2 s and T_C = 0.6 s, respectively. Soil factor S = 1.15. Damping correction factor η = 0.7.

The desired effective period (T_{eff}) and effective damping (ξ_{eff}) of the isolation system are assumed to be T_{eff} = 2 s and ξ_{eff} = 0.137, respectively. Following a gravity load analysis, we determine that the vertical reaction is as follows: R^a = 989 kN for the corner columns and R^b = 1.461 kN for the side and inside columns. Subsequently, the effective stiffness of each rubber isolation bearing is defined as follows:

$$K_{eff} = \frac{R4\pi^2}{gT_{eff}^2}, \tag{1}$$

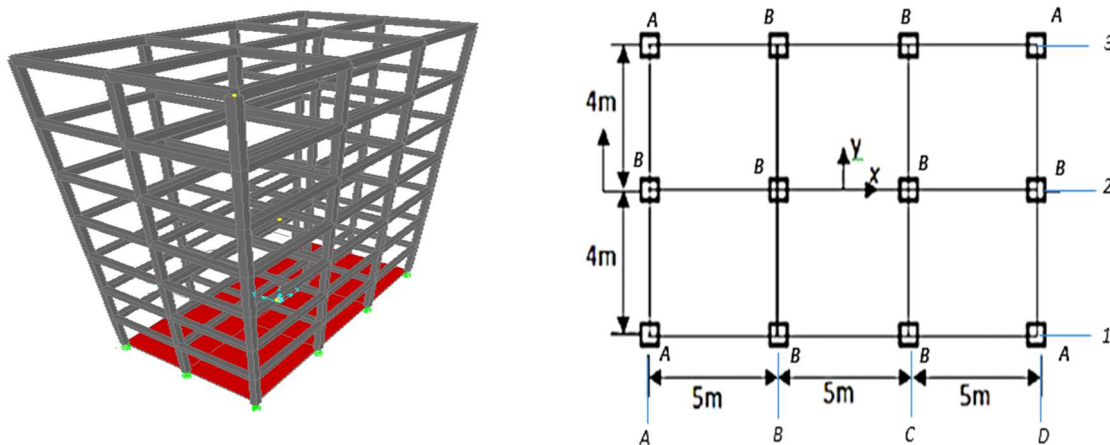where: R is the vertical reaction (R^a, R^b).

Fig. 1: a) 3D frame building, b) plan view of the structural model

Fig. 2. Lead rubber bearing (LRB) (Takenaka Corp., Japan)

For: LRB^A $K_{eff} = \dfrac{989 \times 4 \times \pi^2}{9.81 \times 2^2}$ = 994 kN/m;

LRB^B $K_{eff} = \dfrac{1461 \times 4 \times \pi^2}{9.81 \times 2^2}$ = 1.468 kN/m.

The total effective stiffness of the isolation system can be calculated as follows:

$$\sum K_{eff} = 4 \times K_{eff}^A + 8 \times K_{eff}^B =$$
$$= 4 \times 994 + 8 \times 1468 = 15.720 \text{ kN/m.}$$

The design level damping ratio of the isolation system can be calculated as follows:

$$\xi = \frac{\sum_{eff}^A K_{eff}^A + \sum_{eff}^B K_{eff}^B}{4 K_{eff}^A + 8 K_{eff}^B} = 0.137, \qquad (2)$$

where ξ_{eff}^A and ξ_{eff}^B are damping ratios of individual bearings of 0.10 and 0.15, respectively.

The design displacement d_{dc} of the isolation system along the main horizontal direction is calculated as per EC8 (10.9.3) using the following expression:

$$d_{dc} = \frac{W S_e\left(T_{eff,eff}\right)}{g \sum K_{eff}} = 0.228 \text{ m,} \qquad (3)$$

where:

$$S_e\left(T_{eff}, \varepsilon_{eff}\right) = S_e\left(2 \text{ sec, } 13.7 \%\right) = 0.25 \text{ g;}$$

W is the total weight of the building, i.e., 14.066 kN.

The total eccentricity does not exceed 7.5 % of the length of the superstructure transverse to the horizontal direction, as specified in EC8 (Chapter 10).

$$e = e_{tot,y} = 0.05 \, L_i = 0.4 \text{ m} < 0.075 \, L = 0.6 \text{ m}$$
$$\text{(the condition is met).}$$

L_i is the dimension of the building perpendicular to the direction of the seismic action (EC8, 4.3.2).

The total design displacement d_{db}, including torsional effects, can be calculated for each direction by multiplying the design displacement d_{dc} by given factor δi.

For the action in the x direction:

$$\delta_{xi} = 1 + \frac{e_{tot,y}}{r_y^2} y_i = 1 + \frac{0.4}{36.60} 8 = 1.07 \text{ m,} \qquad (4)$$

where:

$$r_y^2 = \Sigma(x_i^2 K_{yi} + y_i^2 K_{xi}) / \Sigma K_{xi} = 39.18 \text{ m}^2, \qquad (5)$$

where y is the horizontal direction transverse to the x direction under consideration; (x_i, y_i) are the coordinates of the isolator unit i relative to the effective stiffness center (Fig. 5); $e = e_{tot. y}$ = 0.05×8 = = 0.4 m is the total eccentricity in the y direction; r_y is the torsional radius of the isolation system in the y direction.

Total design displacement of the isolator unit:

$$d_{db} = \delta_{xi} x d_{dc} = 1.07 \times 0.228 = 0.24 \text{ m.}$$

Bilinear hysteretic behavior of the isolator

The isolation system may be modeled with bilinear hysteretic behavior, taking into account the conditions required by EC8 (EC8 S10.9.2). The bilinear model of the isolator is essentially described by three parameters: elastic stiffness (K_1), post-yield stiffness (K_2), and characteristic strength (Q). These three parameters are calculated using the convergence procedure as described below (Datta, 2010):

1. Energy dissipation per cycle, or W_D, can be estimated for very small post-yield stiffness as follows:
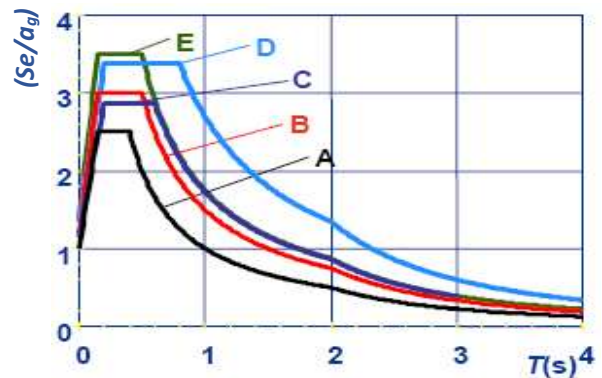

Fig. 3. Idealized force-deflection curve

Fig. 4. EC8 Type 1 spectrum

59

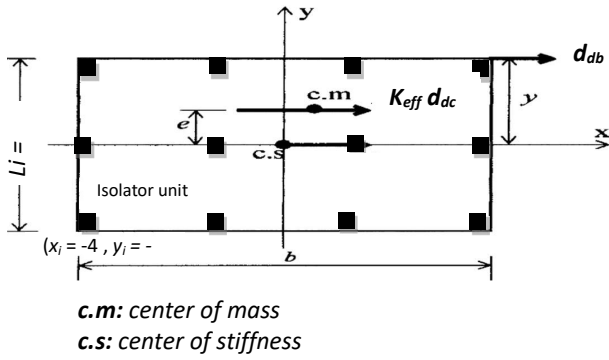c.m: center of mass
c.s: center of stiffness

Fig. 5. Dimensions of the plan to calculate the total eccentricity

$$W_D = 2\pi K_{eff} d_{db}^2 \text{ and } W_D = 4Q(d_{db} - D_y). \quad (6)$$

W_D is also measured by the area bounded by the force-deflection curve loop (Fig. 3).

2. Neglecting the yield displacement D_y, the first approximation for the *short-term yield force Q* is as follows:

$$Q = \frac{\pi}{2} K_{eff} d_{db} \varepsilon_{eff}. \quad (7)$$

3. K_1 and K_2 are the pre- and post-yield stiffness ($K_1 = 10\ K_2$)

$$K_2 = K_{eff} - \frac{Q}{d_{db}}. \quad (8)$$

4. D_y can be estimated as follows:

$$D_y = \frac{Q}{9K_2}. \quad (9)$$

5. Adjusting the first estimate of Q for D_y using the convergence procedure, we obtain the following:

$$Q = \frac{W_D}{4(d_{db} - D_y)}. \quad (10)$$

The properties of the isolators (LRB^A and LRB^B), designed according to EC8, after the convergence procedure are given in Table 1 and Fig. 6.

In addition, EC8 requires that the effective stiffness of the isolation system is not less than 50 % of the effective stiffness at a displacement of $0.2d_{dc}$ (EC8 S10.9.2).

$$F(0.2d_{db}) = \frac{0.2d_{db}Fy + Q(dy - 0.2d_{db})}{d_y}; \quad (12)$$

$$\sum K_{eff}(0.2d_{db}) = 29928 \text{ kN/m};$$

$$\sum K_{eff} = 15720.00 \text{ kN/m} > 50 \%;$$

$$\sum K_{eff}(0.2d_{db}) = 14.964 \text{ kN/m}$$

(the condition required by EC8 is met).

Seismic inputs and numerical analyses

The numerical analysis investigates the performance of nonlinear time history for both fixed and base-isolated building structures under 3D seismic excitations of the 1940 6.9 M_W El-Centro earthquake (PGA = 0.281 g) and the 1995 6.9 M_W Kobe earthquake (PGA = 0.834 g), classified

as far-field and near-field earthquakes, respectively (Gudainiyan and Gupta, 2023; Tamahloult and Tiliouine, 2023). The major components of each earthquake, as shown in Fig. 7, are applied in the longitudinal X direction of the building. The Nonlinear finite element software SAP2000*v.14* (SAP, 2000) is used to obtain the dynamic responses at discrete time intervals. The solutions to the motion equations were obtained using the Fast Nonlinear Analysis method (Wilson, 2002). The isolators were modeled using LINK elements.

Seismic performance evaluation

The seismic criteria for evaluating the performance of the base-isolated building include the following parameters:

1) Peak base displacement (P_1):

$$(P_1) = \max_t(|d_b|),$$

where d_b is relative displacement with respect to the ground.

2) Story drift (P_2): the ratio between the inter-story displacement (top floor displacement d_7 and base floor displacement d_b) and the height of the building H, defined as follows:

$$(P_2) = \max_t(|(d_7 - d_b)|/H),$$

where d_7 is relative displacement of the top floor (7th floor).

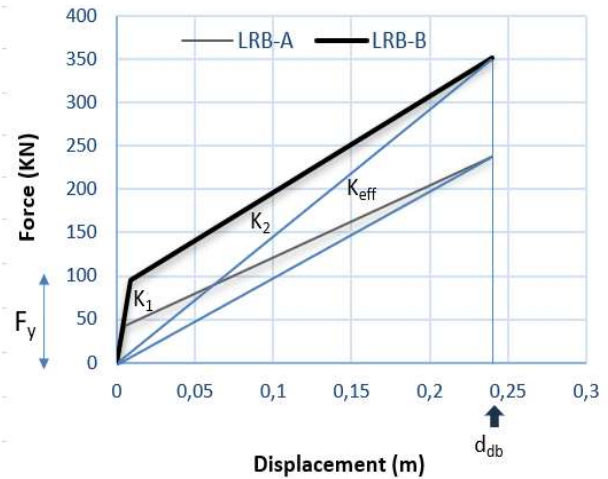3) Maximum base shear (P_3):

$$(P_3) = \max_t(|V_b|).$$

Fig. 6. Bilinear curves for the isolators LRB_A and LRB_B

Table 1. **Isolator characteristics**

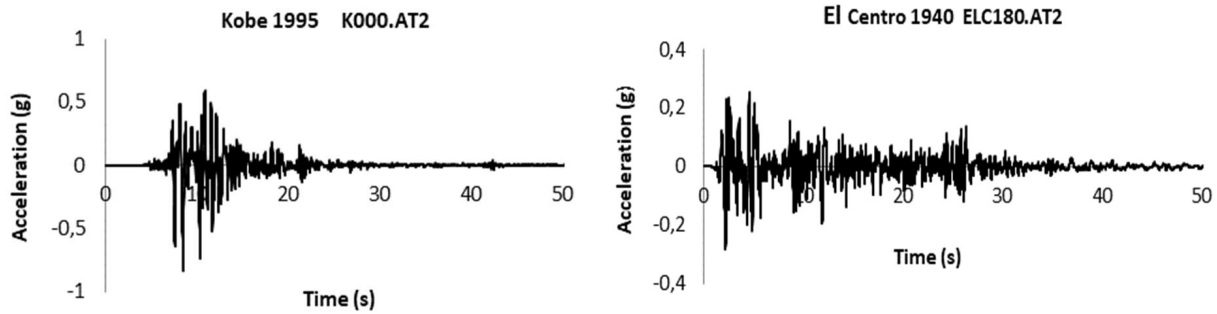| Isolator characteristics	LRB$_A$	LRB$_B$
Characteristic strength, Q (kN)	38.27	86.08
Post-yield stiffness, K_2 (kN/m)	834.55	1109
Pre-yield stiffness, ($K_1 = 10\ K_2$)	8345.5	11090
Yield displacement, D_y (m)	0.0051	0.0086
Yield force, $F_y = K_1\ D_y$ (kN)	42.52	95.64

Fig. 7. Acceleration time history of longitudinal components recorded during the following earthquakes: a) Kobe, b) El-Centro

where V_b is maximum shear at the base of the building.

4) Top floor acceleration (P_4):

$$\left(P_4\right) = \max_t \left(\left|a_7\right|\right),$$

where a_7 is total acceleration of the top floor.

5) Internal forces (bending moment values) (P_5).

Results and discussion

Table 2 summarizes the numerical results obtained from time history analyses of seismic performance for both fixed and base-isolated structures, with comments presented in the following subsections. For the sake of brevity, we only present results in the X direction (similar conclusions are found for the results in the Y direction). The findings illustrate that, in contrast to the ductility-based approach aimed at reducing earthquake damage, seismic base isolation effectively reduces maximum values of seismic inter-story drift, floor acceleration, base shear, and internal forces simultaneously, thus enhancing the structural performance of the building.

Base displacement response

The peak displacement at the base is a very important parameter in the case of base-isolated buildings, which must not exceed the predicted maximum total design displacement calculated according to EC8. The values of peak displacement in the principal direction *X* were found to be P_1 = 2.6 cm and P_1 = 15 cm for the El Centro earthquake and the Kobe earthquake, respectively. It should be noted that the peak base displacement in the case of the Kobe earthquake increased drastically, reaching up to 62 % of the total displacement. The hysteresis curves for the force displacement of LRB^B bearings are presented in Fig. 8a and Fig. 8b for the El-Centro

and Kobe earthquakes, respectively. It is evident that the bilinear behavior assumption according to EC8 is compatible with the force-deformation curves of the seismic isolator obtained from the time history analyses.

Inter-story drift displacement response

The drift ratio in the base-isolated structure shows a minor reduction in the case of the El Centro earthquake but a significant reduction of about 53 % during the Kobe earthquake, as shown in Table 2. However, in the case of the fixed-base building, the drift ratio calculated for the Kobe earthquake is equal to 0.8 %, which is very close to the EC8 requirement limit (0.005/v = 1 %). This result illustrates the effectiveness of the LRB isolation in reducing the drift displacement of the structure and suggests that the superstructure behaves similarly to a rigid body when placed above the isolation system.

Base shear response

The results of the base shear time history demonstrate a significant reduction due to the incorporation of an isolation system. For example, in the case of the El Centro earthquake, the peak base shear values for the base-isolated building and its fixed base are 1.089 kN and 1.290 kN, respectively. In the case of the Kobe earthquake, the base shear values are 2.504 kN and 3.433 kN, respectively, as shown in Fig. 9.

Absolute acceleration response

The comparison of maximum top floor accelerations between fixed-base and isolated-base structures is presented in Table 2. In the X direction, the maximum top floor acceleration decreased from P_4 = 7.77 m/s² to P_4 = 5.25 m/s² for the El Centro earthquake

Table 2. **Seismic performance of fixed and base-isolated buildings**

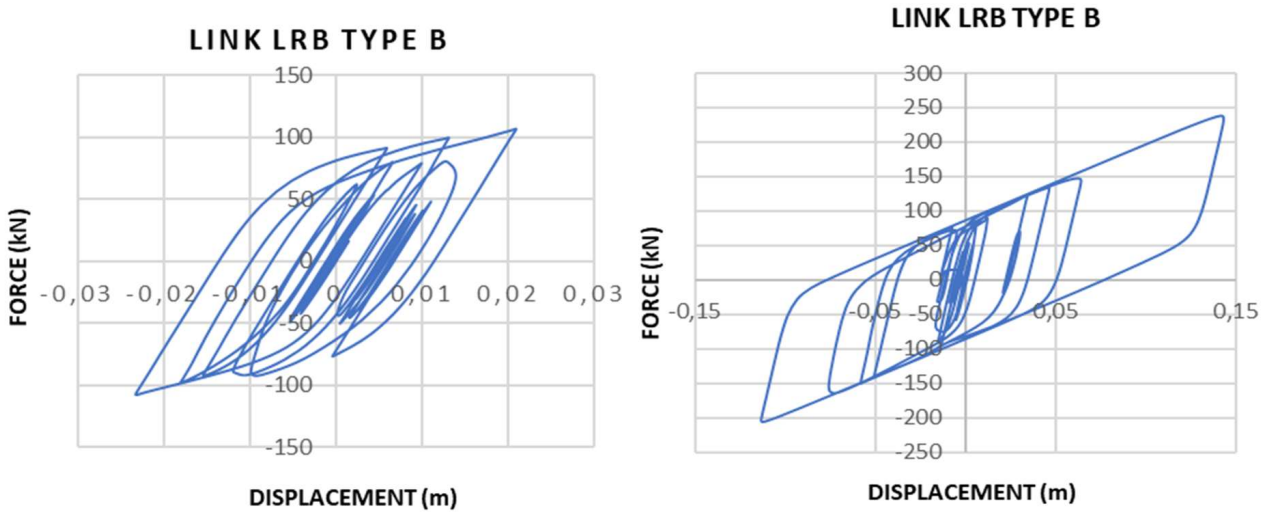| Seismic performance evaluation	El-Centro (PGA = 0.281 g)		KOBE (PGA = 0.834 g)	
	Fixed base	Base-isolated	Fixed base	Base-isolated
Base displacement (P_1) (cm)	–	2.30	–	14.9
Roof drift (P_2)	0.0031	0.0032	0.0085	0.0066
Base shear (P_3) (kN)	1290	1089	3433	2504
Top floor acceleration (P_4) (m²/s)	7.77	5.25	20.23	10.03

Fig. 8. Force-deformation curves of the seismic isolator for 3D input acceleration ground motion components recorded during the El Centro (a) and Kobe (b) earthquakes

(a reduction of 32 %) and from P_4 = 20.23 to P_4 = 10.03 m/s² for the Kobe earthquake (a reduction of 50 %). This decrease in absolute acceleration for the base-isolated structure demonstrates the effectiveness of the isolation system.

Internal forces (bending moment values)

Table 3 presents the calculated values of the maximum bending moments in the fixed-base and base-isolated building structures for both the El-Centro and Kobe earthquakes. It has been observed that for the base-isolated building, there is a significant reduction in bending moment values compared to those of the fixed-base building, as shown in Table 3, for both load cases, the El-Centro and Kobe earthquakes. For example, at the base level, the maximum bending moments decrease from 302 to 222 kN·m and from 829 to 631 kN·m for the El Centro and Kobe earthquakes, respectively. Furthermore, at the top level, a significant reduction of approximately 50 % can be observed. For example, the maximum bending moments decrease from 42 kN·m to 28 kN·m for the El Centro earthquake and from 113 kN·m to 53 kN·m for the Kobe earthquake.

These results once again demonstrate the success of LRB bearings in controlling internal forces under both gravity and seismic loads. As a result, it may be interesting to consider the possibility of resizing the cross-sectional dimensions of structural elements, especially columns and beams (all beams 35×30 cm², all columns 40×40 cm²), within the base-isolated building. This adjustment has the potential to enhance structural efficiency and yield cost savings.

Conclusion

The design of base isolation systems is well defined in EC8 for building structures. The design displacement of an isolator unit is calculated using a formula defined in EC8, depending on the spectral acceleration (type 1 spectrum). This formula includes several parameters such as the reference peak ground acceleration of each seismic zone, the soil factor S, the behavior factor, the importance factor of buildings, effective fundamental period, and effective damping. The dynamic response behavior of a multi-story building structure isolated using an LRB system was evaluated. Seismic response parameters for structures with fixed and isolated
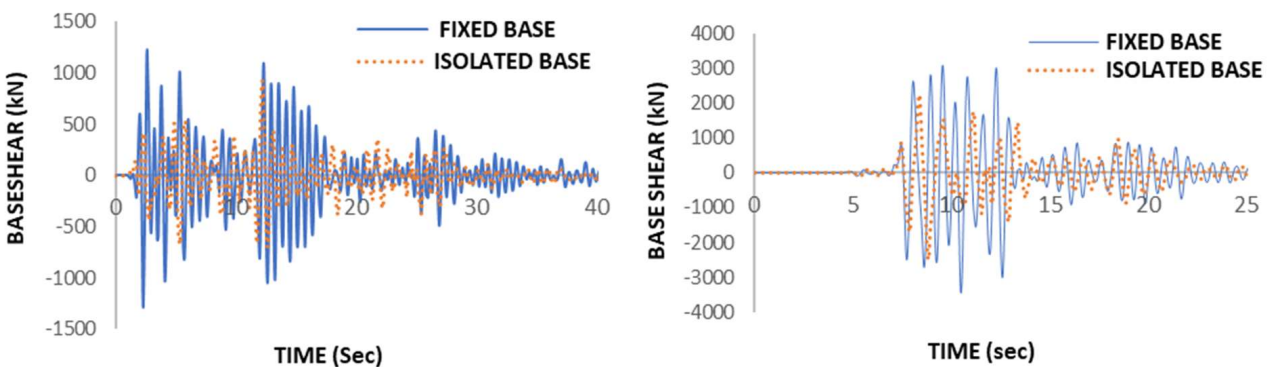

Fig. 9. Comparison of base shear between fixed-base and base-isolated buildings for the El Centro (a) and Kobe (b) earthquakes

Table 3. **Maximum bending moment values**

Maximum bending moment values		El-Centro (PGA = 0.281 g)		KOBE (PGA = 0.834 g)	
		Fixed base	Base-isolated	Fixed base	Base-isolated
1st story	Column	302	222	829	631
	Beam	144	189	397	433
2nd story	Column	224	205	618	444
	Beam	178	155	488	321
3rd story	Column	190	170	523	347
	Beam	174	120	476	268
4th story	Column	189	127	511	295
	Beam	149	89	408	212
5th story	Column	165	96	449	254
	Beam	115	67	308	157
6th story	Column	127	81	340	189
	Beam	74	47	198	96
7th story	Column	82	46	219	118
	Beam	42	28	113	53

bases were evaluated in accordance with the provisions outlined in EC8. The output results clearly demonstrate the effectiveness of the isolator system in significantly and simultaneously reducing seismic responses, including floor accelerations, inter-story drifts, and base shear. In addition, it was observed that the isolation system with LRB bearings reduces internal forces caused by both gravity and seismic loads. As a result, it may be useful to consider the possibility of resizing the cross-sectional dimensions of structural elements, especially columns and beams, within the base-isolated building. This adjustment has the potential to enhance structural efficiency and yield cost savings.

References

AASHTO (2010). *Guide specifications for seismic isolation design*. 3rd edition. Washington, DC: AASHTO, 47 p.

Amanollah, F., Ostrovskaya, N., and Rutman, Y. (2023). Structural and parametric analysis of lead rubber bearings and effect of their characteristics on the response spectrum analysis. Architecture and Engineering, Vol. 8, No. 1, pp. 37–43. DOI: 10.23968/2500-0055-2023-8-1-37-43.

Asher, J. W., Hoskere, S. N., Ewing, R. D., Mayes, R. L., Button, M. R., and Van Volkinburg, D. R. (1997). Performance of seismically isolated structures in the 1994 Northridge and 1995 Kobe earthquakes. Building to Last, Leon Kempner, Jr. and Colin B. Brown, Editors, Proc. of Structures Congress XV, Published by ASCE, 1128-1132.

Attanasi, G., Auricchio, F., and Fenves, G. L. (2009). Feasibility assessment of an innovative isolation bearing system with shape memory alloys. *Journal of Earthquake Engineering*, Vol. 13, Issue S1, pp. 18–39. DOI: 10.1080/13632460902813216.

Cavdar, E. and Ozdemir G. (2022). Amplification in maximum isolator displacement of an LRB isolated building due to mass eccentricity. *Bulletin of Earthquake Engineering*, Vol. 20, pp. 607–631. DOI: 10.1007/s10518-021-01247-1.

Cheng, F. Y., Jiang, H., and Lou, K. (2008). *Smart structures. Innovative systems for seismic response control*. Boca Raton: CRC Press, 672 p.

SAP2000 Integrated software for structural analysis and design. (2000). Computers and Structures Inc. Computer software, Berkeley, California, USA.

Datta, T. K. (2010). *Seismic analysis of structures*. Singapore: John Wiley & Sons (Asia) Pte Ltd, 464 p.

Elghazouli, A. Y. (ed.). (2009). *Seismic design of buildings to Eurocode 8*. 2nd edition. Boca Raton: CRC Press, 363 p.

European Committee for Standardization (2004). *Eurocode 8: Design of structures for earthquake resistance. Part 1: General rules, seismic actions and rules for buildings*. Brussels: European Committee for Standardization, 230 p.

Gudainiyan, J. and Gupta, P. K. (2023). Effect of frequency content parameter of ground motion on the response of C-shaped base-isolated building. *Asian Journal of Civil Engineering*, Vol. 24, pp. 2973–2983. DOI: 10.1007/s42107-023-00688-0.

Hu, G.-J., Ye, K., and Tang, Z.-Y. (2023). Design and analysis of LRB base-isolated building structure for multilevel performance targets. *Structures*, Vol. 57, 105236. DOI: 10.1016/j.istruc.2023.105236.

Jain, S. K. (2004). Seismic isolation devices: a review. *Bridge and Structural Engineer (IABSE)*, Vol. 34, Issue 2, pp. 19–47.

Kelly, J. M. (1997). *Earthquake-resistant design with rubber*. 2nd edition. London: Springer, 243 p. DOI: 10.1007/978-1-4471-0971-6.

Koo, G.-H., Lee, J.-H., Lee, H.-Y., and Yoo, B. (1999). Stability of laminated rubber bearing and its application to seismic isolation. *KSME International Journal*, Vol. 13, Issue 8, pp. 595–604. DOI: 10.1007/BF03184553.

Mayes, R. L. and Naeim, F. (2001). Design of structures with seismic isolation. In: Naeim, F. (ed.). *The Seismic Design Handbook*. Boston: Springer, pp. 723–755. DOI: 10.1007/978-1-4615-1693-4_14.

Ministry of Housing and Urban-Rural Development of the People's Republic of China (2010). *GB50011-2010. Code for seismic design of buildings*. Beijing: Ministry of Housing and Urban-Rural Development of the People's Republic of China, 228 p.

Mori, A., Moss, P. J., Carr, A. J., and Cooke, N. (1998). Behaviour of lead-rubber bearings. Structural *Engineering and Mechanics*, Vol. 6, No. 1, pp. 1–15. DOI: 10.12989/sem.1998.6.1.001.

Naeim, F. and Kelly, J. M. (1999). *Design of seismic isolated structures: from theory to practice*. New York: John Wiley & Sons, Inc., 304 p.

Tamahloult, M. and Tiliouine, B. (2023). 3D nonlinear seismic analysis and design of base-isolated buildings under near field ground motions. *Građevinar*, Vol. 75, No. 5, pp. 483–493. DOI: 10.14256/JCE.3548.2022.

Wilson, E. L. (2002). *Three-dimensional static and dynamic analysis of structures*. 3rd edition. Berkeley: Computers and Structures Inc., 423 p.

ВЛИЯНИЕ СИСТЕМ СЕЙСМОИЗОЛЯЦИИ НА ОСНОВЕ СВИНЦОВО-РЕЗИНОВЫХ ОПОР НА СТРОИТЕЛЬНЫЕ КОНСТРУКЦИИ, СПРОЕКТИРОВАННЫЕ В СООТВЕТСТВИИ С ЕВРОКОДОМ 8

Мохаммед Тамалулт[1], Мулуд Уанани [2], Буалем Тилиуин[1]*

[1]Лаборатория сейсмостойкого строительства и динамики сооружений, факультет гражданского строительства
Национальная политехническая школа, Алжир

[2]Факультет гражданского строительства
Университет Джельфы, Алжир

*E-mail: boualem.tiliouine@g.enp.edu.dz

Аннотация
Введение: Сейсмоизоляция представляет собой систему защиты сооружений, минимизирующую воздействие сейсмических сил на сооружение во время землетрясения. Этого можно достичь с помощью различных устройств, таких как эластомерные опоры, скользящие опоры и гибридные системы. **Цель исследования**: оценить влияние свинцово-резиновых опор, используемых в строительных конструкциях в качестве системы сейсмоизоляции. **Методы:** для достижения указанной цели, с помощью алгоритма Fast Nonlinear Analysis (FNA) был проведен нелинейный динамический анализ семиэтажного здания с изолирующим устройством в основании и без него. Здание спроектировано в соответствии с критериями Еврокода 8 (EC8), а затем подвергнуто анализу с использованием данных о двух произошедших землетрясениях. **Результаты**: сделан вывод о том, что допущение о билинейном поведении, сделанное на этапе проектирования в соответствии с EC8, является обоснованным. Кроме того, применение системы сейсмоизоляции фундамента здания с использованием свинцово-резиновых опор может значительно улучшить эксплуатационные характеристики здания за счет уменьшения ускорений перекрытий, межэтажных перекосов и горизонтальной сейсмической реакции. Кроме того, показано, что сейсмоизоляция здания с помощью свинцово-резиновых опор эффективно уменьшает внутренние силы, возникающие как от гравитационных, так и от сейсмических нагрузок.

Ключевые слова: сейсмоизоляция; система свинцово-резиновых опор; трехмерный анализ нелинейной реакции на землетрясение; Еврокод 8; билинейный гистерезис.

DEFORMATION BEHAVIOR OF REINFORCED SHELLS UNDER THE ACTION OF WIND: AN EXPERIMENTAL STUDY

Vladimir Mushchanov, Maksim Tsepliaev*, Alexandr Mushchanov, Anatoly Orzhekhovsky

Donbas National Academy of Civil Engineering and Architecture, Makeyevka, Russia

*Corresponding author's e-mail: m.n.tsp@list.ru

Abstract

Introduction. The trends of increasing the cost-effectiveness and reliability of structures come into conflict and require the search for new approaches to design. Steel vertical cylindrical tanks, the use of which is constantly growing, are no exception. This study addresses the issue of buckling of a cylindrical tank wall due to the action of wind and vacuum loads. The **purpose of the study** was to conduct experimental verification of design solutions for improving the stability of the walls of vertical cylindrical tanks. **Methods**: Based on the previously performed numerical studies, a two-stage experimental procedure was developed to test the applicability of the reinforcement designs. Stage I includes the investigation of the shell behavior under the action of vacuum. Stage II considers different tank model designs under the action of actual wind load. The height of the stiffening rings and the angle of the stairs served as variable parameters. **Results**: An increase in the critical buckling load of up to 7 % in case of vacuum action and 27 % in case of wind action was established in the presence of stairs with the recommended parameters. The effect of an increase in stability due to the presence of stairs was noted only when they were oriented in the direction of maximum compressive wind action. In this case, stairs of sufficient stiffness reduce the risk of total structural failure from wind and vacuum, regardless of its location. Reinforcement with stiffening rings should be considered a more preferable method. The study results in the experimental confirmation of the effectiveness of the analyzed designs and the adequacy of the numerical models used.

Keywords: stability; tank; stress-strain state; finite element method; cylindrical shell; wind, stairs.

Introduction

Advances in technology, growth of liquid storage volumes, environmental and economic considerations drive the development of design methods for *vertical cylindrical tanks (VCTs).* The risk of man-made damage (Chang and Lin, 2006; Megdiche et al., 2022) requires the development of safer tank designs (Dong et al., 2021; Fedosov et al., 2019; Sengupta, 2019). At the same time, reliability and cost-effectiveness are in many respects mutually exclusive, which requires the development of new solutions (Fig. 1).

Wall strength and stability is the basis for the reliability of the entire tank. In real practice, buckling of a cylindrical tank wall is not uncommon (Azzuni and Guzey, 2022; Hornung and Saal, 2002; Jahangiri et al., 2012; Pasternak et al., 2022) — see Fig. 3b, c. Most damage is caused by wind and vacuum (Godoy, 2016). This is largely due to the use of approximate buckling analysis methods (Godoy and Flores, 2002; Hornung and Saal, 2002; Konopatskiy et al., 2023; Pasternak et al., 2022). Safe operation of tanks with such damage as well as their repair are impossible. Restoring the geometry of the metal makes it more brittle and prone to fatigue cracking (Zdravkov and Pantusheva, 2019). A more appropriate solution is to apply structural and technological (Zhao et al., 2020) methods to improve stability. Additional elements increasing tank wall stability can include *ring stiffeners (RS)* (Bu and Qian, 2015; Lemák and Studnička, 2005; Mushchanov and Tsepliaev, 2020; Sun et al., 2018; Uematsu et al, 2018; Zeybek et al., 2015), technological stairs (Hussien et al., 2020; Shokrzadeh et al., 2020; Tcepliaev et al., 2023), and alternative structures (Mushchanov et al., 2010).

Ring stiffeners represent a common design solution to increase wall stability under the action of wind and vacuum (Fig. 2a, b).

The perception of axial loads is only possible if the rings are regularly arranged throughout the height of the wall (Pasternak et al., 2022; Shiomitsu and Yanagihara, 2021). However, such solutions are rarely applied in practice. Among the studies addressing various peculiarities of using stiffening rings, studies by Bu and Qian (2015), Lemák and Studnička (2005), Sun et al. (2018), Uematsu et al. (2018) can be mentioned. These authors justified the overall effectiveness of RS use, without specifying the optimal arrangement or dimensions of the structures. Mushchanov and Tsepliaev (2020) filled in these gaps by offering recommendations on the optimal arrangement of stiffening rings in terms of ensuring maximum stability. The validity of the results in case of vacuum action is supported by experimental verification and comparison with similar studies (Fakhim et al., 2009; Rastgar and Showkati,
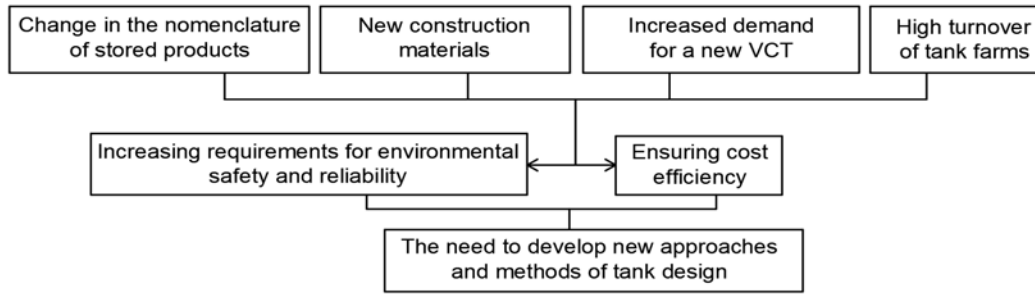
Fig. 1. Relevance of developing tank design methods

2017; Shokrzadeh and Sohrabi, 2016). The obtained method was not tested under the action of actual wind load.

With account for the trend of increasing the cost-effectiveness of structures, another solution considered is the reinforcement of tanks with technological stairs (Fig. 3a). Their interaction with the wall is not considered in engineering practice. At the same time, conducted studies (Davarzani et al., 2023; Fakhim et al., 2009; Hussien et al., 2020; Mushchanov et al., 2010; Rastgar and Showkati, 2017; Shiomitsu and Yanagihara, 2021; Shokrzadeh and Sohrabi, 2016; Shokrzadeh et al., 2020; Tcepliaev et al., 2023) show the positive effect of stairs on the overall stability of tanks.

Based on numerical studies and accident analysis (Fig. 3b, c), some papers (Hussien et al., 2020; Pasternak et al., 2022; Shokrzadeh et al., 2020) provide a rationale for specific types of stairs to improve stability. Based on numerical studies, Tcepliaev et al. (2023) determined recommended design parameters of stairs for tanks of different dimensions, making it possible to increase the critical buckling load by up to 28 %. The proposed solutions have not been verified experimentally under the action of actual wind. In this case, the justification for the use of such methods can be characterized as inadequate.

Therefore, the *purpose of the study* was to conduct experimental verification of design solutions for improving the stability of the walls of vertical cylindrical tanks.

The main objectives were as follows:
- experimental verification of a numerical model of a tank with stairs under the action of vacuum;
- analysis of the stress-strain state of a model of a tank with stairs;
- experimental verification of the effectiveness of the previously proposed methods for the arrangement of stiffening rings and technological stairs under the action of wind.

The problem statement makes the current study a logical continuation of comprehensive research (Mushchanov and Tsepliaev, 2020; Tcepliaev et al., 2023). The arrangement of stiffening rings and spiral stairs is determined based on the recommendations proposed in the above-mentioned works.

Materials and methods

The magnitude and direction of wind load corresponding to buckling of a tank wall can be ensured by continuous long-term observations. An alternative solution is to use scaled-down tank models that make it possible to reproduce the effect of buckling for the required number of times. Stress-strain state parameters, effects of buckling from uniform loads (Mushchanov and Tsepliaev, 2020; Pasternak et al., 2022; Shiomitsu and Yanagihara, 2021), and wind flow distribution (Davarzani et al., 2023; Mushchanov et al., 2013) are mainly studied on scaled-down tank models. Among the publications addressing experimental studies of buckling due to wind, a work of Uematsu and Uchiyama (1985) can be distinguished.

a) truss ring (https://www.flamax.ru)   b) solid section ring (https://tdrzmk.com)

Fig. 2. Use of stiffening rings for tanks

a) general view
(https://www.everypixel.com)

b) buckling due to wind (Pasternak et al., 2022)

c) buckling due to vacuum
(Shokrzadeh et al., 2020)

Fig. 3. Tanks with technological stairs

The results of the study by Uematsu et al. (2014) describe the specifics of the shape of polyester film shell deformations using wind-tunnel tests. The researchers recorded critical wind load and wall displacement values up to the moment of buckling. However, in terms of dimensions, the studied structures are similar to silos and the obtained results cannot be applied to compare the buckling parameters of the structures considered in this work. Uematsu et al. (2014) focused on studying the distribution of the wind flow over open-topped tank walls. In addition, using a laser detector, they recorded the deformations of the tank model in a wind tunnel. Due to the high elasticity of the shell material, the buckling effect was ambiguous. The shape of the shell was partially restored after the cessation of exposure to wind load. Both works did not consider the influence of structural reinforcement elements on the stability of the shell. Nevertheless, the results obtained by the researchers (Uematsu and Uchiyama, 1985; Uematsu et al., 2014) allow for a qualitative comparison of buckling shapes and provide a visual reference for the current tests. The applied principles of experimentation formed the basis for the method underlying the current tests, with account for the necessary modifications.

Buckling due to wind can only be captured for an ultra-thin shell model. In this case, the measurement of stresses is accompanied by excessive errors. A two-stage experimental procedure is a compromise solution.

Stage I consists in testing the reinforced steel tank model for buckling under the action of vacuum. The experimental testing method is based on the recommendations of researchers (Mushchanov and Tsepliaev, 2020; Tcepliaev and Mushchanov, 2018). This step makes it possible to verify the numerical model in terms of arising stresses and critical buckling force in case of buckling due to vacuum. Further, it will make it possible to determine the fundamental possibility of using the previously developed finite element model for the analysis of tanks with stairs (Tcepliaev et al., 2023).

Stage II consists in the experimental modeling of buckling effect from wind action using a wind tunnel, following the principles applied by researchers in their studies (Uematsu and Uchiyama, 1985; Uematsu et al., 2014). Structural solutions based on techniques of reinforcement with stiffening rings (Mushchanov and Tsepliaev, 2020) and spiral stairs (Tcepliaev et al., 2023) are considered. The implementation of this stage will allow for an experimental verification of the quality of the proposed techniques for reinforcement against the action of actual wind load.

Testing stage I method

The parameters of the experimental models were determined with account for the possibility of direct comparison with the results of previously performed experimental studies. The model is assembled from three separate elements made of 0.5 mm thick galvanized steel and corresponds to the parameters of a tank with a volume of 20,000 m^3 on a scale 1:100 (height — 200 mm, diameter — 400 mm). The wall is connected to the lid and bottom by a single lock joint, with the use of sealant. The shell end attachment assembly should be considered rigid. This is additionally ensured by the wooden frame inside the model body, which prevents the bottom and lid from tearing off. A 2NVR-5DM vacuum pump was used to create vacuum. The stairs were modeled by rigidly attaching a 0.5 mm thick and 10 mm wide steel strip to the cylindrical wall by soldering. The maximum increase in wall stability for the tank of the volume under consideration was observed at stairs angles (α) of 30…40° (Tcepliaev et al, 2023). The specified boundaries were adopted as options to consider. The length of the stairs in the models was 370 and 480 mm.

The stress values were determined by strain gauge method, using OWEN MV110-224.4TD modules for 24 sensors. Communication with the computer was established via an RS-485 switch and Owen OPC Server software. MasterScada software shell was used to output the final values. The moment of buckling was captured using high-speed video recording. Fig. 4 shows a diagram and photo of the test rig for Stage I of testing.

Testing stage II method

The MAT-1 wind tunnel of the Donbas National Academy of Civil Engineering and Architecture (Fig. 5) with the test section of the closed type has the following dimensions: height — 700 mm; turntable diameter — 900 mm; maximum air flow speed — 20 m/s; fan power — 8 kW. The moment of buckling is captured using high-speed video recording and compared to Owen device readings. Using an installed Pitot tube and low pressure sensors connected to the Owen system, the total wind flow pressure was recorded. The actual wind speed was determined by the following equation:

$$V = \sqrt{\frac{2P}{\rho}}, \qquad (1)$$

where P is the wind flow pressure, ρ is the air density.

The choice of model scale was justified by Tcepliaev and Mushchanov (2018), Tominaga et al. (2004). Fig. 6 shows schemes, photos and parameters of the options considered. The basis is the "mid-section" requirement, when the maximum area of the model projection on a plane perpendicular to the air flow should not exceed 10 % of the test section. The model is represented by a wooden frame (Fig. 6a), on which the wall is wound. As the shell material, 0.1 mm thick paper (Fig. 6b) with modulus of elasticity E = 0.04·10⁵ MPa and 0.02 mm thick aluminum foil (E = 0.7·10⁵ MPa) were considered. In addition to the shell without reinforcement (Fig. 6c, d), various arrangements of conditional rings and stairs were considered. Two options of stairs inclination (α) of 30° and 40° were taken as a variable parameter. The chord length (L) was 242 and 305 mm, respectively (Fig. 6e, f). The stiffening rings were at a height (h) of 100 and 147 mm from the base (Fig. 6g, h). The second option of RS arrangement was determined according to the recommendations of Mushchanov and Tsepliaev (2020). Tin wire with a diameter of 3 mm (E = 0.55·10⁵ MPa) served as the material for the stairs and rings. The stiffness ratio of the
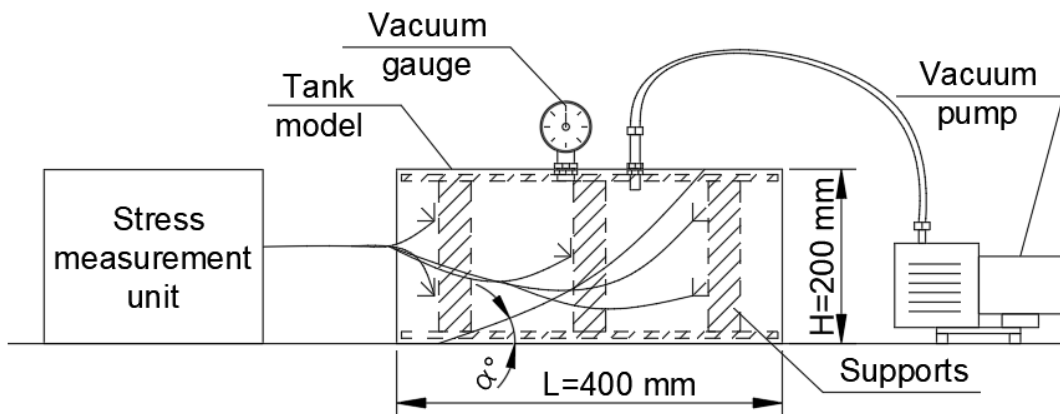
a) test rig diagram
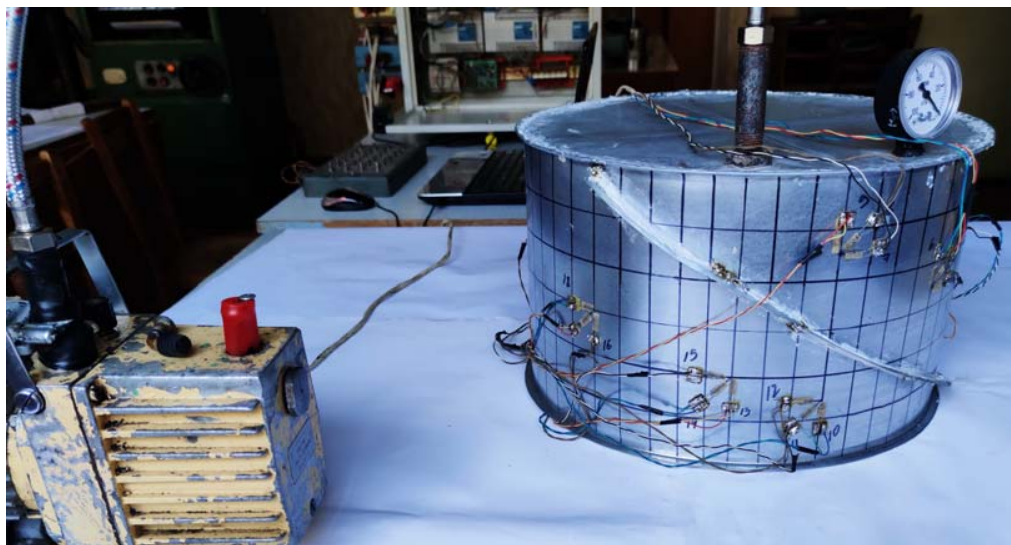
b) model photo No. 1

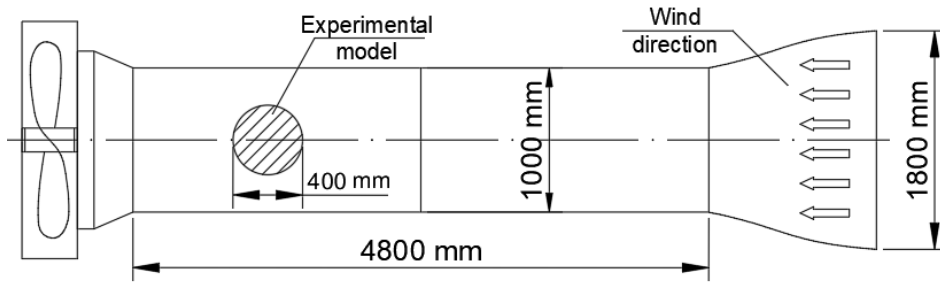Fig. 4. Test rig for Stage I of testing

Fig. 5. Wind tunnel (top view)

reinforcing elements in the experimental model corresponds to that in the existing tanks. The elements were connected by a special adhesive composition ensuring a rigid connection (Fig. 6f, h).

Parameters of the numerical models of tanks

The parameters of the finite element model are set to the experimental ones as close as possible to allow for direct comparison of the test results. The model designed in the LIRA-SAPR 2017 analysis software represents a shell, at the ends of which rods of 10x0.5 mm cross-section are added, modeling the joint with the lid and bottom. For four equidistant nodes at each end, linear displacements are forbidden. The wall shell is defined by finite element No. 44. The finite element mesh was selected based on the preliminary calculation of stress convergence. The difference in the results of finite element and analytical calculations was less than 3 %. The shell consists of 149 elements along the circumference and 12 rows along the height (Fig. 7a). Vacuum is modeled as uniform external pressure on the tank wall, wind is specified through a text file (Tcepliaev, 2016) — Fig. 7b, c. The values

of the indicated loads are equal to the values at which buckling of the corresponding experimental model occurred. For vacuum, it is the P_{cr} parameter (Table 2), for wind — the P_w parameter (Table 3). The shape of wind pressure distribution corresponds to the standard one for tanks of corresponding dimensions — see more details in (Tcepliaev, 2016). The stairs are oriented in the direction of the greatest wind pressure.

The arising stresses, the value of the critical force, and the model deformation shape are taken as the documented parameters of finite element analysis. Since the design combination does not include axial loads, the stability is directly related to the load in the circular direction. This allowed us to determine the critical pressures through the *stability factor (SF)* by the following equation:

$$SF = \frac{P_{cr}}{P}, \qquad (2)$$

where P_{cr} is the critical buckling pressure, P is the acting pressure.

The variable parameters of the tank models for the experimental studies are summarized in Table 1.

| a) model frame | c) without reinforcement (scheme) | e) model with stairs (scheme) | g) reinforcement with a stiffening ring (scheme) |

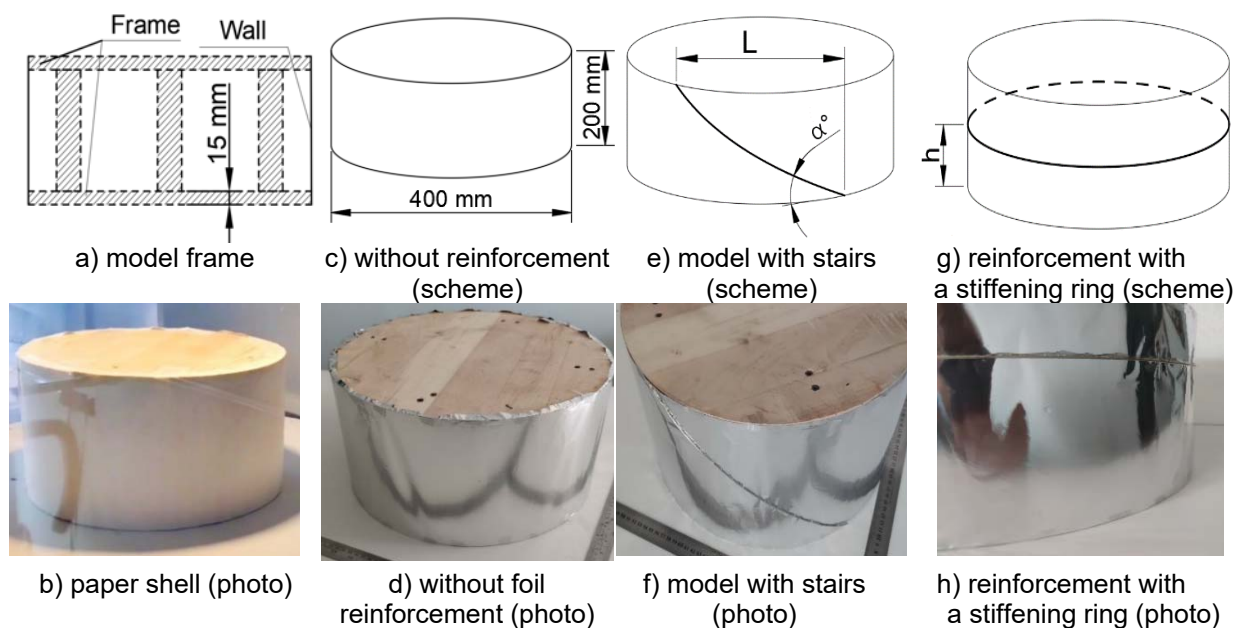| b) paper shell (photo) | d) without foil reinforcement (photo) | f) model with stairs (photo) | h) reinforcement with a stiffening ring (photo) |

Fig. 6. Scheme and general view of the models with reinforcement for Stage II of testing

With account for the studies conducted earlier, the value of critical force increase — increment S (%) (Eq. 3) — is adopted as an indicator of the effectiveness of reinforcement methods:

$$S = 100 \cdot \left(\frac{P_{cr,i}}{P_{cr,0}} - 1 \right), \qquad (3)$$

where $P_{cr,0}$ is the pressure at the moment of buckling for the shell without reinforcement, $P_{cr,i}$ is the pressure at the moment of buckling for the i-th design.

Based on the comparison of increments (S) obtained numerically and experimentally, a conclusion about adequacy and reliability of the results can be made. The calculated values and parameters S for vacuum and wind load are given in Tables 2 and 3, respectively.

Results and discussion

Results of testing stage I

According to Table 1, two steel models of tanks reinforced with stairs were tested under vacuum. The section without reinforcement was the first to buckle (Fig. 8a), which followed by the shell separation from the conditional stairs (Fig. 8c). The load value at the moment of buckling in the wall section without reinforcement varies from 29 to 31 kPa. The reinforced part lost stability in the range of 33…38 kPa. The pressure difference between the stages ranged from 6 to 27 % (2…8 kPa), depending on the design — see Table 2 for details. The shapes of buckling in experimental models 1 and 2 have no fundamental differences, the number of waves and their basic dimensions coincide. Fig. 8 shows a general view of the deformed shell shapes.

The deformed structures obtained by the finite element method (Fig. 8b) have some differences from the final experimental ones. For proper assessment, the comparison should be made with the original buckling shape (Fig. 8a). This is justified by the linear numerical calculation considering the first buckling shapes and not taking into account the post-buckling wall behavior. Similar buckling shapes

for a tank reinforced by stairs were obtained by Shokrzadeh et al. (2020).

The readings of 24 strain gauges for each model were grouped by the type of measured stresses, and average logarithmic dependencies up to the moment of buckling were determined with the use of mathematical algorithms (Fig. 9). In addition to the results of the current experiment, the results for the shell without reinforcement from the study by Mushchanov and Tsepliaev (2020) are given.

The strain gauges did not record significant differences in the stress state of the considered shells at the moment of buckling, except for the areas where the conditional stairs were located, where the following was noted:

- the circular stresses decreased by up to 20 % compared to the free part of the shell;
- the axial stresses in the analytical formulation should be close to 0, and in the experiment, their value reached 2.8 MPa;
- the reinforcing elements restrain the deformation of the wall, which is confirmed by buckling beyond the free part of the wall.

Another important recorded parameter is vacuum at the moment of buckling — the critical force. The comparison of the experimental ($P_{CR,i}$) and numerical values ($P_{CR,F}$) for the different model options was made with the use of the S_{EXP} and S_{FEM} parameters, respectively (Eq. 3). The results of the calculations are given in Table 2.

The experimental values of the axial stresses exceed those obtained by the finite element method. However, the mentioned parameter remains within the range of small values not exceeding 2.8 MPa and is caused by some pliability of the wooden frame. The differences between the experimental and numerical values of the circular stresses differ by no more than 3 %, which confirms the applicability of the design model. The reinforcing effect in case of uniform compression is observed only in the areas where the stairs are located and manifests itself after the beginning of buckling. Thus, the local perturbations of the axial and circular stresses in the stairs
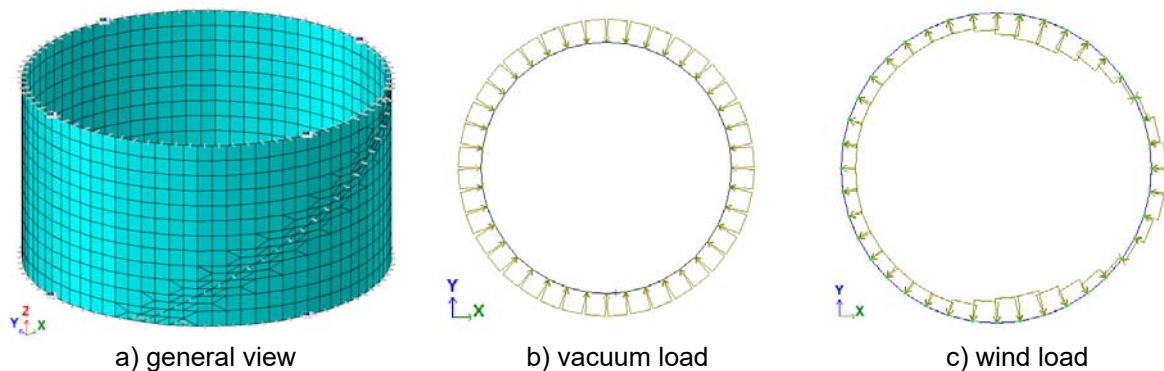

a) general view   b) vacuum load   c) wind load

Fig. 7. Finite element model of the tank

Table 1. **Options of experimental models**

Experimental stage	Model material	Type of reinforcement	Recorded parameters
Stage I (load: vacuum)	Galvanized steel $t = 0.5$ mm	1. Stairs with a 30° incline. 2. Stairs with a 40° incline. *Reinforcement material — steel: 10x0.5 mm strip*	- stresses; - vacuum at the moment of buckling; - buckling shape.
Stage II (load: wind)	Paper ($t = 0.1$ mm) or foil ($t = 0.02$ mm)	1. No reinforcement. 2. RS at a height of 100 mm. 3. RS at a height of 147 mm. 4. Stairs with a 30° incline. 5. Stairs with a 40° incline. *Reinforcement material — tin: round bar with a diameter of 3 mm*	- wind speed at the moment of buckling; - buckling shape.

attachment areas do not affect the overall stability of the shell.

An increase in critical force in the range of 2…7 % compared to the shell without stairs was observed. In this case, the actual critical load values increase by no more than 2 kPa. Reliability of bucking analysis is further supported by the similar buckling shape (Rastgar and Showkati, 2017; Shokrzadeh and Sohrabi, 2016) and critical load values (Fakhim et al., 2009).

The results of the first stage of the experiment make it possible to adopt the available numerical model with reinforcement in the form of stairs for subsequent studies in case of actual wind flow, as well as to experimentally verify the findings of Tcepliaev et al. (2023). It was also found that stairs cannot be considered an effective design solution to improve the overall stability under the action of vacuum.

Results of testing stage II

The second stage is the experimental verification of the effectiveness of the structural methods to increase the stability of the shells under the actual wind action. In terms of meeting the set research objectives, the experimental model with a wall made of foil of t = 0.02 mm is preferable. This is largely due to the high elasticity of the paper model and the different behavior of the shell depending on the orientation of the sheet (Fig. 10a). If a thinner material in the form of foil is used, the model collapses at the moment of buckling (Fig. 10b, c). In addition to recording the load, this makes it possible to assess the extent of damage to the models.

Buckling of the shells without reinforcement was observed only in the windward area, which is consistent with the findings of the experimental studies conducted by Uematsu and Uchiyama
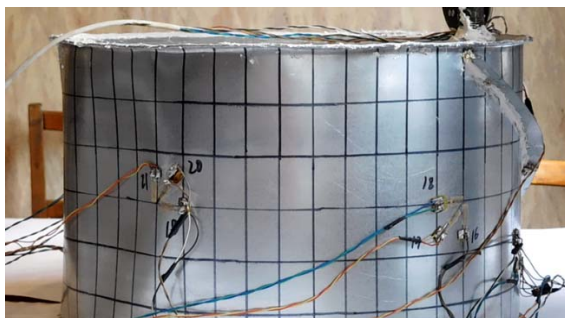
a) experimental model 1: buckling in the section without reinforcement
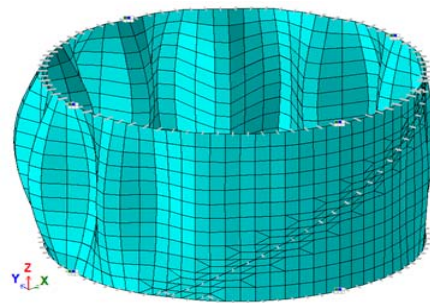
b) numerical model 1: buckling shape (with stairs α = 30˚)

c) experimental model 2: buckling in the entire shell

Fig. 8. Deformed tank model structure with deformations due to the action of vacuum

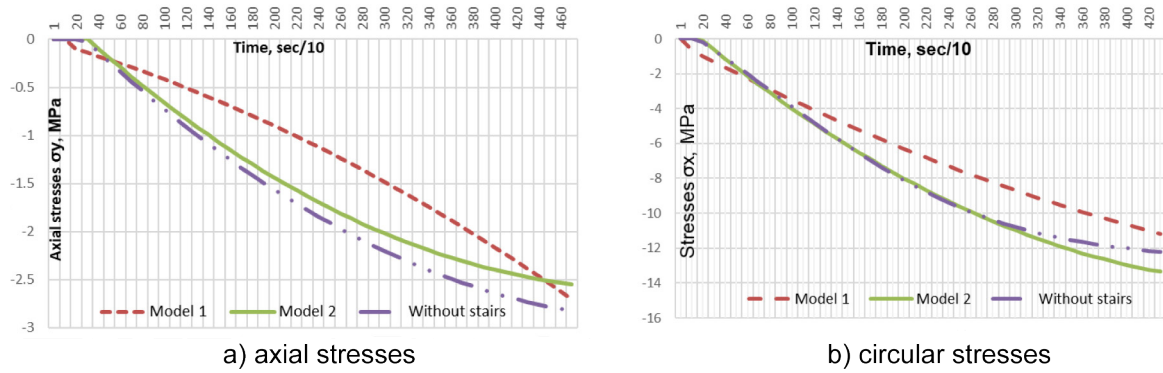a) axial stresses b) circular stresses

Fig. 9. Experimental values of stresses under the action of vacuum

(1985), Uematsu et al. (2014). The shapes of wall deformation up to the moment of buckling are also similar. Therefore, the adopted test models reflect the realistic behavior of the studied structures.

Fig. 1 shows the photos of the reinforced shells after exposure to wind load. The deformed scheme at the moment of buckling (Fig. 11a, c, e, g) and the resulting damage (Fig. 11b, d, f, h) are shown separately. To improve the validity of the results, each type of model was brought to failure at least twice. The availability of reinforcing elements prevented complete destruction of the models, which is confirmed by the consequences of real accidents (Fig. 3b, c).

The shape of buckling just before the wall failure is close to the numerical solution — refer to Fig. 8b and (Shokrzadeh et al., 2020). The extent of damage to the wall depending on the design is as follows:

1) model without reinforcement (most damaged);

2) wall with conditional stairs (30° incline); the wall is reinforced with a stiffening ring at a height of 100 mm;

3) wall with conditional stairs (40° incline);

4) the wall is reinforced with a stiffening ring at a height of 147 mm (least damaged).

Recording of the strain gauge readings in the Pitot tube, synchronized with video recording, was performed once per second. The obtained data array was transformed into load vs. time diagrams (Fig. 12).

The highlighted points show pressure at the moment of buckling in the corresponding model (see details of the models in Table 3). Using Eq. 3,

critical wind pressure increments (P_W) for the stability factor (SF) were calculated. Instead of the P_{cr} values, wind speed V and SF (for experimental and numerical models, respectively) were used. Table 3 presents the results of the numerical studies and their comparison with the experiment. The adequacy of the applied models is evaluated by comparing the S_{EXP} and S_{FEM} increments through the ΔS parameter.

Fig. 13 shows the first shapes of buckling of some numerical models. In a visual comparison with similar studies (Rastgar and Showkati, 2017; Shokrzadeh and Sohrabi, 2016; Shokrzadeh et al., 2020; Sun et al., 2018), a similar deformed scheme of numerical models can be noted. As in the case of the experiment, the deformations occur in the areas of negative wind load values. Depending on the design, the amplitude and frequency of the waves change.

The general trends related to the extent of damage to the experimental models were preserved in the numerical experiment. The greatest increase (approx. 50 %) in stability was observed when the stiffening ring was placed with account for the recommendations of Mushchanov and Tsepliaev (2020). The arrangement of longer stairs according to the method proposed by Tcepliaev et al. (2023) increases stability by almost 30 %. The maximum discrepancy for the S parameter between the experimental and numerical studies was 21.47 %. However, the general dynamics and character of deformations in the models allow us to conclude

Table 2. **Stress state of the models under the action of vacuum**

Model option	Critical buckling load of the wall, P$_{CR}$				Average stresses, MPa			
					circular σ$_x$		axial σ$_y$	
	Experimental (Exp.) P$_{CR, i}$, kPA	S$_{EXP}$, %	P$_{CR, F}$ kPA	S$_{FEM}$, %	Exp.	FEM	Exp.	FEM
No reinforcement	29	–	57.2	–	12.7	12.4	2.8	0.4
Model 1 (30°)	31; 33 (stairs area)	6.9	58.6	2.4	13	13.3	2.6	0.72
Model 2 (40°)	30 38 (stairs area)	3.4	60.1	5.1	13	12.9	2.5	0.68

a) deformation of paper model 1

b) foil model 1: moment of buckling
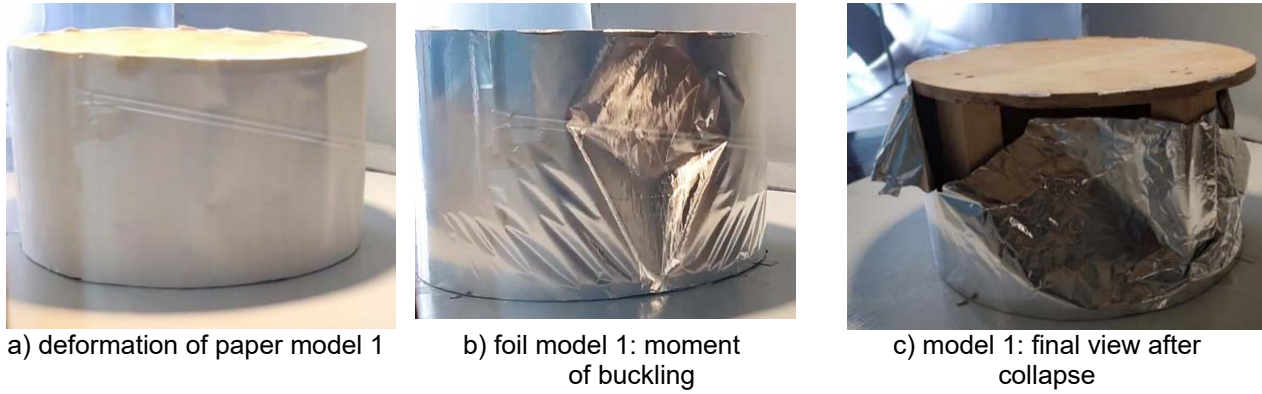
c) model 1: final view after collapse

Fig. 10. Damage to the shells without reinforcement under the action of wind

that the recommendations on reinforcement of walls with stiffening rings and spiral stairs under the wind action are applicable. The issue of accounting for the joint action of such elements and its reflection in analytical calculations remains open.

Conclusions

Options of reinforcing the walls of vertical cylindrical tanks with spiral process stairs and stiffening rings were considered. Wind and vacuum served as design loads. The main result of the conducted research is the experimental confirmation of the effectiveness of design solutions to increase the stability of the walls of vertical cylindrical tanks, with account for the advantages and disadvantages listed below.

1. Stairs have little effect on the overall stress-strain state of the shell under the wind action. Minimal
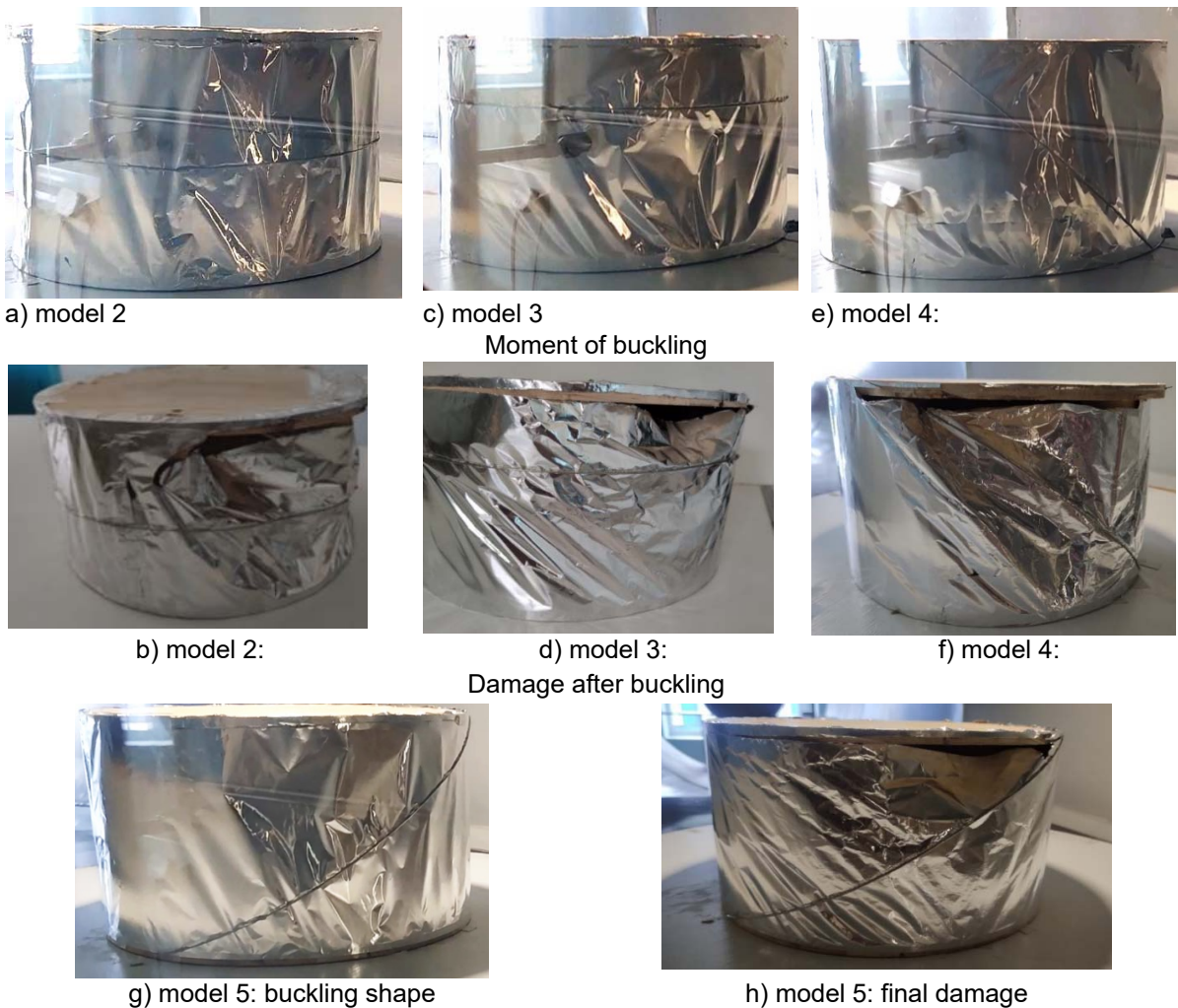

a) model 2

c) model 3

e) model 4:

Moment of buckling

b) model 2:

d) model 3:

f) model 4:

Damage after buckling

g) model 5: buckling shape

h) model 5: final damage

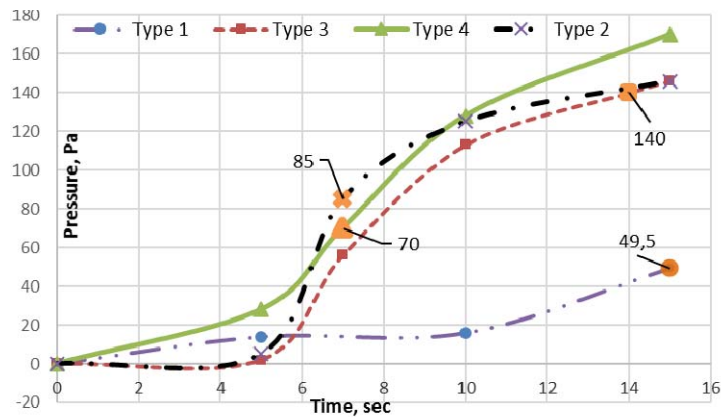Fig. 11. View of the models after buckling under the wind action

Fig. 12. Rate of wind flow pressure increase

Table 3. **Results of testing stage II**

Model type	Pitot values P_w, Pa	Flow speed V, m/s	S_{EXP}, %	SF	S_{FEM}, %	ΔS, %
1. No reinforcement.	49.5	9.18	–	0.56	–	–
2. RS (H = 100 mm)	85	12.03	31	0.732	30.7	1.1
3. RS (H = 147 mm)	140	15.44	68.2	0.86	53.6	21.47
4. Stairs (40°)	70	10.92	18.9	0.67	19.6	3.63
5. Stairs (30°)	80	11.67	27.1	0.715	27.7	2.04

perturbations of axial stresses and reduction in circular stresses (up to 20 %) in the stairs attachment area were recorded experimentally and numerically. Reduction in displacements of the wall with stairs due to an increase in total stiffness was observed. The deformed scheme and magnitude of stresses in the free part of the wall fully correlate with the shell without reinforcement.

2. The availability of stairs does not result in significant changes in the character of the shell buckling under the action of vacuum. The critical load values are minimally different from those obtained for the shell without reinforcement (within 2 kPa). The free section of the wall is the first to buckle, which is confirmed by numerical calculations. Complete buckling of the reinforced shell occurred at further increase of vacuum by the value from 6 to 27 % (2…8 kPa). In this way, the effect of "progressive collapse" is additionally counteracted.

3. The effect of an increase in the critical wind load with increasing stairs length was experimentally recorded. The arrangement of stairs as recommended by Tcepliaev et al. (2023) increases the critical wind load up to 27 % in comparison to the shell without reinforcement.

4. Experimental verification of the recommendations on the arrangement of stiffening rings (Mushchanov and Tsepliaev, 2020) confirmed their effectiveness in terms of improving stability under the action of wind load. A single ring increased the critical wind pressure by 50 % in comparison to the shell without reinforcement.

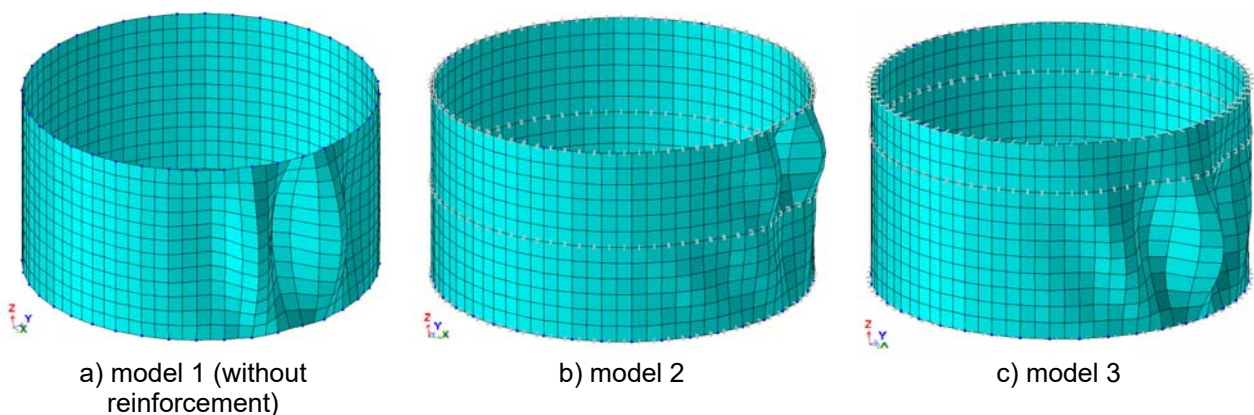a) model 1 (without reinforcement)　　　　b) model 2　　　　c) model 3

Fig. 13. First shape of buckling of the numerical models under the wind action

5. Stiffening rings increase the critical load under the action of vacuum and wind; the effect of stability improvement due to stairs is less pronounced under the action of vacuum and manifests itself when stairs are oriented in the direction of maximum compressive wind action. Accounting for stairs requires predictable wind direction, therefore, the use of stiffening rings is a more universal method.

References

Azzuni, E. and Guzey, S. (2022). Stability of aboveground storage tanks subjected to wind loading. *Analysis and Design of Plated Structures (Second Edition), Vol. 1: Stability*, pp. 479–495. DOI: 10.1016/B978-0-12-823570-6.00006-9.

Bu, F. and Qian, C. (2015). A rational design approach of intermediate wind girders on large storage tanks. *Thin-Walled Structures*, Vol. 92, pp. 76–81. DOI: 10.1016/j.tws.2015.02.024.

Chang, J. I. and Lin, C.-C. (2006). A study of storage tank accidents. *Journal of Loss Prevention in the Process Industries*, Vol. 19, Issue 1, pp. 51–59. DOI: 10.1016/j.jlp.2005.05.015.

Davarzani, H. R., Ganjali, A., Sadeghi, H., and Mohebbi, R. (2023). Numerical and experimental study of wind effect on the storage tanks based the tank adjacency. *Experimental Techniques*, Vol. 48, pp. 191–204. DOI: 10.1007/s40799-023-00653-1.

Dong, B., Zhang, D., Feng, G., and Lu, H. (2021). Design and development of tank farm operation safety training system. *Journal of Beijing University of Chemical Technology (Natural Science Edition)*, Vol. 48, Issue 3, pp. 88–98. DOI: 10.13543/j.bhxbzr.2021.03.011.

Fakhim, Y. G., Showkati, H., and Abedi, K. (2009). Experimental study on the buckling and post-buckling behavior of thin-walled cylindrical shells with varying thickness under hydrostatic pressure. In: Domingo, A. and Lazaro, C. (eds.). *Proceedings of the International Association for Shell and Spatial Structures (IASS) Symposium 2009*, 28 September – 2 October 2009, Valencia, Spain, pp. 2511–2522.

Fedosov, A. V., Abdrakhmanov, N. Kh., Vadulina, N. V., Khafizova, D. F., and Abdrakhmanova, K. N. (2019). Diagnosis of vertical steel tanks as a tool to improve safety operation of oil and gas facilities. Bulletin of the Tomsk Polytechnic University. *Geo Assets Engineering*, Vol. 330, No. 12, pp. 75–81. DOI: 10.18799/24131830/2019/12/2394.

Godoy, L. A. (2016). Buckling of vertical oil storage steel tanks: Review of static buckling studies. *Thin-Walled Structures*, Vol. 103, pp. 1–21. DOI: 10.1016/j.tws.2016.01.026.

Godoy, L. A. and Flores, F. G. (2002). Imperfection sensitivity to elastic buckling of wind loaded open cylindrical tanks. *Structural Engineering and Mechanics*, Vol. 13, No. 5, pp. 533–542. DOI: 10.12989/sem.2002.13.5.533.

Hornung, U. and Saal, H. (2002). Buckling loads of tank shells with imperfections. *International Journal of Non-Linear Mechanics*, Vol. 37, Issues 4–5, pp. 605–621. DOI: 10.1016/S0020-7462(01)00087-7.

Hussien, M. A., Hagag, S. Y. A., Maged, A., and Korashy, M. M. (2020). Stability of petroleum storage tanks considering the effect of helical stair beams. *International Journal of Research in Engineering and Management*, Vol. 4, No. 1, pp. 24–35.

Jahangiri, M., Fakhrabadi, M. H., and Jahangiri, M. (2012). Computational buckling analysis of wind loaded cylindrical storage tanks. *Majlesi Journal of Energy Management*, Vol. 1, No. 4, pp. 23–31.

Konopatskiy, E. V., Krysko, A. A., and Shevchuk, O. A. (2023). Use of interpolation methods for modeling the stress-strain state of operated oil storage tanks. *Structural Mechanics of Engineering Constructions and Buildings*, Vol. 19, No. 2, pp. 119–129. DOI: 10.22363/1815-5235-2023-19-2-119-129.

Lemák, D. and Studnička, J. (2005). Influence of ring stiffeners on a steel cylindrical shell. *Acta Polytechnica*, Vol. 45, No. 1, pp. 56–63. DOI: 10.14311/674.

Megdiche, I., Atherton, W., Allanson, D., and Harris, C. (2022). Effect of mitigation on the catastrophic failure of storage tanks. *Journal of Loss Prevention in the Process Industries*, Vol. 80, 104852. DOI: 10.1016/j.jlp.2022.104852.

Mushchanov, V., Bachurin, A., and Krysko, A. (2010). Latest approach of tank strengthening. *Proceedings of Donbas National Academy of Civil Engineering and Architecture*, No. 6 (86), pp. 145–151.

Mushchanov, V. and Tsepliaev, M. (2020). Rational design solutions of ensuring the walls of tanks stability to the action of transverse loads. *IOP Conference Series: Materials Science and Engineering*, Vol. 896, 012024. DOI: 10.1088/1757-899X/896/1/012024.

Mushchanov, V. F., Zubenko, A. V., and Moskalenko, I. V. (2013). Numerical simulation of wind pressure on a vertical cylindrical tank surface. *Metal Constructions*, Vol. 19, No. 3, pp. 173–181.

Pasternak, H., Li, Z., Juozapaitis, A., and Daniūnas, A. (2022). Ring stiffened cylindrical shell structures: state-of-the-art review. *Applied Sciences*, Vol. 12, Issue 22, 11665. DOI: 10.3390/app122211665.

Rastgar, M. and Showkati, H. (2017). Field study and evaluation of buckling behaviour of steel tanks under geometric imperfections. *Journal of Applied Mechanical Engineering*, Vol. 6, Issue 3, 1000268. DOI: 10.4172/2168-9873.1000268.

Sengupta, A. (2019). Optimal safe layout of fuel storage tanks exposed to pool fire: one dimensional deterministic modelling approach. *Fire Technology*, Vol. 55, pp. 1771–1799. DOI: 10.1007/s10694-019-00830-y.

Shiomitsu, D. and Yanagihara, D. (2021). Estimation of ultimate strength of ring-stiffened cylindrical shells under external pressure with local shell buckling or torsional buckling of stiffeners. *Thin-Walled Structures*, Vol. 161, 107416. DOI: 10.1016/j.tws.2020.107416.

Shokrzadeh, A. R., Mansuri, F., Asadi, M., and Sohrabi, M. R. (2020). Comparative analysis on buckling behavior of steel cylindrical tanks by consideration of more realistic numerical models. In: *5th World Congress on Civil, Structural, and Environmental Engineering*. Virtual Conference – October 2020. Paper No. ICSECT 159. DOI: 10.11159/icsect20.159.

Shokrzadeh, A. R. and Sohrabi, M. R. (2016). Buckling of ground based steel tanks subjected to wind and vacuum pressures considering uniform internal and external corrosion. *Thin-Walled Structures*, Vol. 108, pp. 333–350. DOI: 10.1016/j. tws.2016.09.007.

Sun, T., Azzuni, E., and Guzey, S. (2018). Stability of open-topped storage tanks with top stiffener and one intermediate stiffener subject to wind loading. *Journal of Pressure Vessel Technology*, Vol. 140, Issue 1, 011204. DOI: 10.1115/1.4038723.

Tcepliaev, M. N. (2016). Modeling of real loading diagrams of wind pressure on cylindrical tank using SCAD software. *Metal Constructions*, Vol. 22, No. 4, pp. 183–192.

Tcepliaev, M. N. and Mushchanov, V. F. (2018). Ensuring the stability of the walls of the tanks based on the rational arrangement of the stiffening rings. *Construction of Unique Buildings and Structures*, Issue 9 (72), pp. 58–73. DOI: 10.18720/ CUBS.72.4.

Tcepliaev, M. N., Mushchanov, V. F., Zubenko, A. V., Mushchanov, A. V., and Orzhehovsky, A. N. (2023). Tank shell stability: refined design schemes. *Magazine of Civil Engineering*, Issue 3 (119), 11906. DOI: 10.34910/MCE.119.6.

Tominaga, Y., Mochida, A., Harimoto, K., Kataoka, H., and Yoshie, R. (2004). Development of CFD method for predicting wind environment around a high-rise building. Part 3: The cross comparison of results for wind environment around building complex in actual urban area using different CFD codes. *AIJ Journal of Technology and Design*, No. 19, pp. 181–184. DOI: 10.3130/aijt.10.181.

Uematsu Y., Koo C., and Yasunaga J. (2014). Design wind force coefficients for open-topped oil storage tanks focusing on the wind-induced buckling. *Journal of Wind Engineering and Industrial Aerodynamics*, Vol. 130, pp. 16–29. DOI: 10.1016/j. jweia.2014.03.015.

Uematsu Y. and Uchiyama K. (1985). Deflection and buckling behavior of thin, circular cylindrical shells under wind loads. *Journal of Wind Engineering and Industrial Aerodynamics*, Vol. 18, Issue 3, pp. 245–261. DOI: 10.1016/0167-6105(85)90084-4.

Uematsu, Y., Yamaguchi, T., and Yasunaga, J. (2018). Effects of wind girders on the buckling of open-topped storage tanks under quasi-static wind loading. *Thin-Walled Structures*, Vol. 124, pp. 1–12. DOI: 10.1016/j.tws.2017.11.044.

Zdravkov, L. and Pantusheva, M. (2019). Typical damage in steel storage tanks in operation. *Procedia Structural Integrity*, Vol. 22, pp. 291–298. DOI: 10.1016/j.prostr.2020.01.037.

Zeybek, Ö., Topkaya, C., and Rotter, J. M. (2015). Strength and stiffness requirements for intermediate ring stiffeners on discretely supported cylindrical shells. *Thin-Walled Structures*, Vol. 96, pp. 64–74. DOI: 10.1016/j.tws.2015.08.004.

Zhao, Y., Liu, Q., Cai, S., and Dong, S. (2020). Internal wind pressures and buckling behavior of large cylindrical floating-roof tanks under various liquid levels. *Journal of Pressure Vessel Technology*, Vol. 142, Issue 5, 051401. DOI: 10.1115/1.4046982.

ДЕФОРМАЦИОННОЕ ПОВЕДЕНИЕ УСИЛЕННЫХ ОБОЛОЧЕК ПОД ВОЗДЕЙСТВИЕМ ВЕТРА: ЭКСПЕРИМЕНТАЛЬНОЕ ИССЛЕДОВАНИЕ

Мущанов Владимир Филиппович, Цепляев Максим Николаевич*, Мущанов Александр Владимирович, Оржеховский Анатолий Николаевич

ФГБОУ ВО «Донбасская национальная академия строительства и архитектуры», г. Макеевка, Россия

*E-mail: m.n.tsp@list.ru

Аннотация
Введение. Тенденции повышения экономичности и надёжности сооружений вступают в противоречие и требуют поиска новых подходов к проектированию. Не исключением являются стальные вертикальные цилиндрические резервуары, использование которых постоянно растёт. В данном исследовании рассматривается проблема потери устойчивости цилиндрической стенки резервуаров от действия ветровой и вакуумной нагрузок. **Цель исследования**: экспериментальная проверка конструктивных решений повышения устойчивости стенок вертикальных цилиндрических резервуаров. **Методы**: на основе ранее выполненных численных исследований, разработана методика двухэтапного эксперимента для проверки применимости конструктивных вариантов усиления. I этап относится к исследованию работы оболочки под действием вакуума. II этап рассматривает различные конструктивные варианты моделей резервуаров при действии реальной ветровой нагрузки. Вариативными параметрами являлись высота расположения колец жесткости и угол наклона лестницы. **Результаты**: установлено повышение критической нагрузки потери устойчивости от вакуума на величину до 7 % и на 27 % от ветра при наличии лестницы с рекомендуемыми параметрами. Эффект повышения устойчивости от лестниц отмечен только в случае их ориентации в направлении максимально сжимающего ветрового воздействия. При этом, наличие лестницы достаточной жёсткости снижает риск полного разрушения конструкции от ветра и вакуума вне зависимости от расположения. Усиление кольцами жёсткости следует считать более предпочтительным методом. Общим итогом работы является экспериментальное подтверждение эффективности исследуемых конструктивных решений и адекватности применяемых численных моделей.

Ключевые слова: устойчивость; резервуар; напряженно-деформированное состояние; метод конечных элементов; цилиндрическая оболочка; ветер; лестница.

RESULT VERIFICATION FOR NUMERICAL MODELING OF WIND EFFECTS ON UNIQUE BUILDINGS AND STRUCTURES

Olga Poddaeva

Research and Production Laboratory of Aerodynamic and Aeroacoustic Testing of Building Structures, Moscow State University of Civil Engineering, Moscow, Russia

E-mail: poddaevaoi@gmail.com

Abstract

Introduction: Despite the fact that wind tunnel testing is quite expensive and time-consuming, physical modeling in wind tunnels remains the primary method for determining wind effects on unique buildings and structures. Computational fluid dynamics (CFD) provides more variability, calculations are performed faster and at a lower cost. However, the issue of accuracy of integral characteristics obtained as a result of numerical modeling and, accordingly, verification procedure remains open. Currently, when using numerical modeling results in structural aerodynamics, it is mandatory to verify them with experimental data. In recent years, studies have explored the CFD potential for accurate wind load predictions, but there have not been studies presenting a comprehensive description and implementation of a verification and validation system to analyze wind effects on unique buildings and structures. The **purpose of the study** was to compare the CFD results with the wind tunnel test data for three different objects, analyze the results, and propose a method for verification and validation of CFD analysis of wind effects on unique buildings and structures. The following **methods** were used: physical testing of models of unique buildings and structures in a wind tunnel, including a detailed method of experimental studies to determine integral aerodynamic characteristics, as well as numerical modeling of wind effects using ANSYS. Numerical modeling was performed in two setups: with and without virtual wind tunnel modeling. As a **result**, it is shown that virtual wind tunnel modeling makes it possible to achieve better data consistency when verifying numerical modeling results with physical modeling data, and the proper use of numerical modeling technology can significantly reduce the time and cost of experimental studies in a wind tunnel and/or reduce the design time by decreasing the number of considered loading scenarios.

Keywords: verification; CFD; wind tunnel; integral aerodynamic characteristics.

Introduction

Experimental modeling in wind tunnels is the primary method of determining wind effects on unique buildings and structures, including facilities with a high criticality rating. This method is quite conservative and provided in the majority of regulatory documents pertaining to construction both in the Russian Federation and abroad. However, wind tunnel testing is expensive and time-consuming, which significantly complicates the design of unique buildings and structures (Kareem et al., 2013). Active development of software and computational capacities makes it possible to solve a number of problems using a more modern method — numerical modeling. Compared to wind tunnel testing, CFD ensures a higher variability of input data, calculations can be performed faster and at a lower cost (Galerkin et al., 2020). Compared to traditional tools, CFD has unique advantages, including: lower time- and cost-to-solution, greater flexibility in design parametrization, and access to flow conditions in the entire calculation domain (Blocken, 2014). At the same time, CFD is characterized by some difficulties mainly caused by the following factors: large Reynolds number, which requires fine grid resolution, complexity of flow field with impinging, sharp edges of a bluff body, flow obstacles at inflow and outflow (Murakami, 1998). At this stage of computational technology development, when using numerical modeling results in structural aerodynamics, it is mandatory to verify them with experimental data.

The integrated use of experimental and numerical modeling results makes it possible to obtain the most complete and reliable picture of wind effects on building structures.

The aerodynamic coefficients of external pressure on the surface of the facades and roofs of the facility under consideration represent a result of comprehensive computational and experimental studies of wind effects on building structures, in accordance with the requirements of regulatory documents. Studies are conducted for a representative set of wind flow directions. Usually, the model rotation step is 10–15°. Thus, as a result of the studies, it is possible to predict 24–36 different scenarios for loading the structure of the building under consideration with wind flow.

This information is redundant for a designer. In real design activity, it is sufficient to consider

3–4 most unfavorable cases. This brings up the following question: how to assess the need to take into account a particular loading scenario? The most obvious option is to estimate the total wind effect on the structure and the resultant aerodynamic force relative to the facility base.

The classical drainage aerodynamic experiment involves determining pressure at control points on the surface of the model. A system based on differential pressure sensors is used as a measuring system; special preparation of the model is required (pneumatic line routing in the intra-model space, sensor installation, etc.). To estimate the resultant aerodynamic force, it is necessary to sum up the values of wind pressure at control points, while taking into account the direction of the wind flow velocity vector and the orientation of the control point relative to that vector, which is a rather effort-demanding task that should be addressed for each model individually.

Therefore, in this case, it is recommended to perform additional tests using force-torque sensors, which make it possible to determine integral aerodynamic characteristics immediately and, based on them, easily calculate the resultant aerodynamic force. Such tests require fundamentally different model preparation. A single force-torque sensor is used, which is attached at the base of the model. It is necessary to prevent any model contact with the surrounding wind tunnel surface, etc. These factors do not allow for simultaneous measurement of pressure on the surface of the model and force-torque characteristics, and sometimes lead to the need to develop an additional model, which significantly increases the time and cost of experimental studies.

In this situation, mathematical (numerical) modeling can come to the aid. When performing CFD calculations in specialized software, an analyst can provide for any form of result output. Thus, in one calculation, it is possible to obtain both a pattern of pressure distribution over the surface of the model and integral characteristics of the wind effect for the relevant point.

The issue of accuracy of integral characteristics obtained as a result of numerical modeling and, accordingly, verification procedure remains open.

In recent years, some studies have explored the accuracy of predicting wind load on unique buildings and structures using CFD (Aboshosha et al., 2015; Ricci et al., 2018; Zhang et al., 2015). These studies show the CFD potential for accurate wind load predictions, but there have not been studies presenting a comprehensive description and implementation of a verification and validation system to analyze wind effects on unique buildings and structures.

Methods

This paper addresses verification of the results of experimental studies on integral wind loads using force-torque sensors with corresponding mathematical calculations in specialized ANSYS CFD software. Three structures of different types — a long low-rise building of an airport complex (Fig. 1), a high-rise residential complex (Fig. 2), and a chimney as part of a coke oven complex (Fig. 3) — were selected as objects of the study. All facilities selected for verification of numerical modeling are unique buildings and structures, which should have aerodynamic coefficients assigned according to the results of physical tests in wind tunnels.

The experimental studies were carried out with the use of a unique research setup — the Large Gradient Wind Tunnel, courtesy of the National Research University "Moscow State University of Civil Engineering". For the experimental studies, models of the structures were made at the following scales: 1:200 — the airport complex (Fig. 4), 1:150 — the residential complex (Fig. 5), 1:125 —

Fig. 1. Long airport complex building

the chimney as part of the coke oven complex (Fig. 6). The models were used for both drainage tests and force-torque tests (after a complete retrofit to match the specifics of the measurement equipment).

The methodology for the *experimental studies* was described in detail by Poddaeva (2022). When experimental tests are conducted to determine integral aerodynamic characteristics, the measurement system includes force-torque sensors. During this study, Schunk FTD sensors with the following characteristics were used:

Measuring range Fx, Fy: ± 660 N;
Measuring range Fz: ± 1980 N;
Measuring range Mx, My, Mz: ± 60 N*m;
Measuring accuracy Fx, Fy: ± 0.125 N;

Measuring accuracy Fz: ± 0.25 N;
Measuring accuracy Mx, My, Mz: ± 0.008 N*m.

Based on the test results, aerodynamic force and torque components along the X, Y and Z axes are determined. Based on the results of the tests to determine force-torque characteristics, aerodynamic coefficients are calculated according to the following equations:

$$C_x = \frac{F_x}{q_\infty S}; C_y = \frac{F_y}{q_\infty S}; C_z = \frac{F_z}{q_\infty S};$$

$$C_{Mx} = \frac{F_x}{q_\infty Sl}; C_{My} = \frac{F_y}{q_\infty Sl}; C_{Mz} = \frac{F_z}{q_\infty Sl}, \qquad (1)$$

where C_x — drag coefficient; C_y — transverse force coefficient; C_{Mz} — torque coefficient; q_∞ — dynamic pressure; S — reference frontal area of the model; l — arm in the given coordinate system.

Forces and torques are measured relative to the zero point of the force-torque sensor.

Fig. 2. High-rise residential complex

Fig. 3. Chimney as part of the coke oven complex

Fig. 4. Model of the airport complex, scale 1:200

Fig. 5. Model of the residential complex, scale 1:150

Fig. 6. Model of the chimney as part of the coke oven complex,
scale 1:125

The force-torque sensors used must be graduated prior to testing. Graduation is carried out by conducting control tests. Control tests should be performed not earlier than 2 days before aerodynamic tests.

Equipment included in the National Register of Measuring Equipment and having a valid certificate of measuring instrument verification issued by an organization having accreditation for the right to perform works and (or) render services on verification and calibration of measuring instruments shall be used as control equipment during graduation. It is recommended to use a set of weights, class E2, with a weight range from 10 g to 10 kg, as a control device for load application.

To conduct control tests, it is necessary to follow and fix the following external parameters during verification:

• ambient air temperature — not lower than 20º (fixation);

• atmospheric pressure (fixation);

• it is not allowed to have heat sources near the system being verified and the reference equipment.

During graduation, a load of a certain value (minimum measuring range) is applied to the force-torque sensor via a suspension system using weights.

Scales readings at a steady load applied to them are saved (in N) with the help of the control software. The value of the control load is recorded in the appropriate column of the graduation report.

Using the set of weights, the load on the scales is modified according to the graduation method (minimum measuring range) with a given step.

As part of preparations, a control model point is selected relative to which measurements will be made.

The force-torque sensor model is selected based on the weight of the model and preliminary calculation of the maximum possible load.

When placing the model in the operating area of the wind tunnel, it is necessary to provide a gap of 1–2 mm between the object under study and the components of the surrounding buildings not involved in the determination of the load, to prevent their contact.

After placing the model, a pressure-sensitive element tube is installed in the operating area to control flow velocity and perform aerodynamic coefficient calculations.

After preparations, the measuring system is energized and zero (in the absence of flow) readings of the force-torque sensor are taken, which is necessary to take into account initial displacement due to the sensor loading by the weight of the model structure.

In the tube, the flow rate corresponding to the experimental conditions is set and the data recording protocol is enabled. During the specified time, the force-torque sensor readings are being taken and two files are being recorded: load readings with a frequency of 1000 Hz and averaged load readings for the entire period of the recording program operation.

Rotation of the model in the tunnel is carried out with a step corresponding to the experimental conditions. The force-torque sensor readings are taken for each angle. Rotation of the model is carried out up to 360° to take control readings and then compare them to the zero readings.

Based on the results of the tests to determine force-torque characteristics, aerodynamic coefficients are calculated according to equations (1).

Mathematical modeling was performed in specialized ANSYS fluid dynamics software. The turbulent motion of the air medium near a body is described by a system of Reynolds equations closed using additional differential relations of a two-parameter dissipative turbulence model. The calculations were performed using the FLUENT computational technology (control volume method, interpolation of convective terms using the MARS scheme, implicit time step scheme, internal iterative PISO algorithm, k-w SST turbulence model).

An example of a three-dimensional computational domain with multi-scale unstructured grids with thickening in the vicinity of the building for the high-rise residential complex is shown in Fig. 7.

Discussion

Based on the data obtained from numerical and experimental modeling, verification of the studies was conducted for three objects of different types in two different numerical modeling setups: with and without virtual wind tunnel modeling. The verification results are shown in Figs. 8–10.

Based on the obtained data, it can be stated that the convergence of the results of experimental and mathematical modeling in determining the integral components of the average wind load is achieved
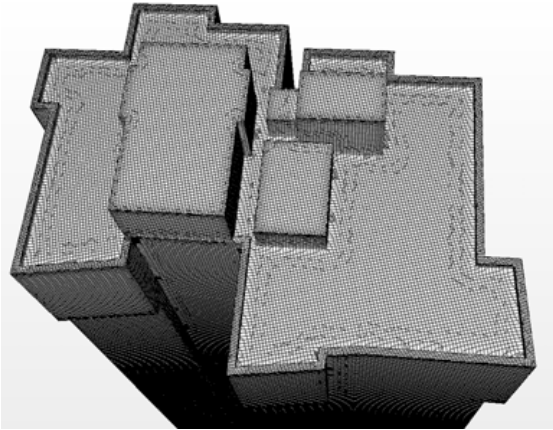
Fig. 7. Fragment of the computational grid in the vicinity of the residential complex building

with an error of no more than 20 % under the condition of virtual wind tunnel modeling. In a setup where the wind tunnel is not modeled, the error is up to 30 %. The obtained results suggest that it is possible to use numerical modeling when selecting critical wind flow directions, which should be taken into account in the analysis of load-bearing structures of construction facilities, and virtual wind tunnel modeling makes it possible to achieve better data consistency when verifying results with physical modeling data.

Thus, the proper use of numerical modeling technology can significantly reduce the time and cost of experimental studies in a wind tunnel and/or reduce the design time by decreasing the number of considered loading scenarios.

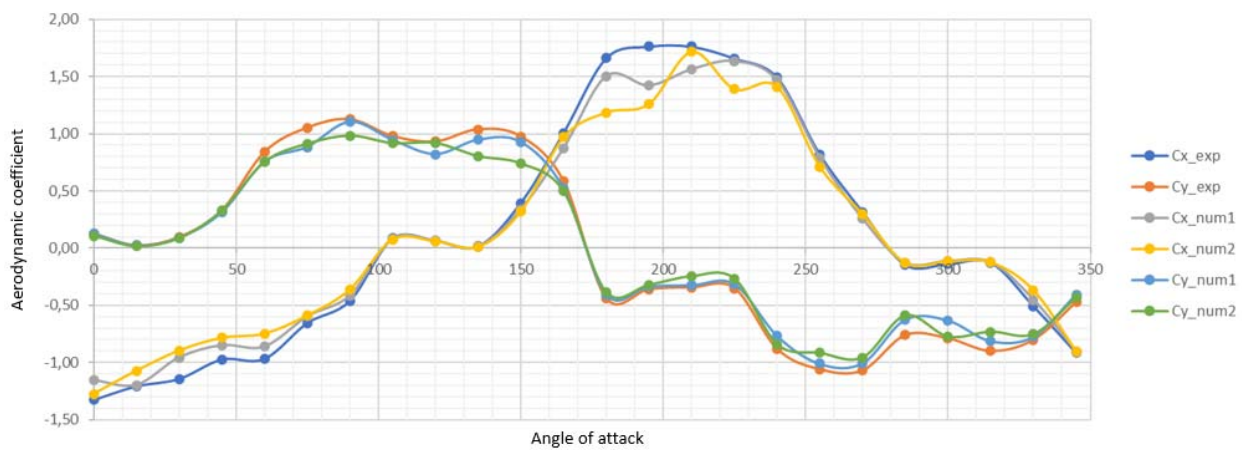Fig. 8. Results of the verification studies for the airport complex

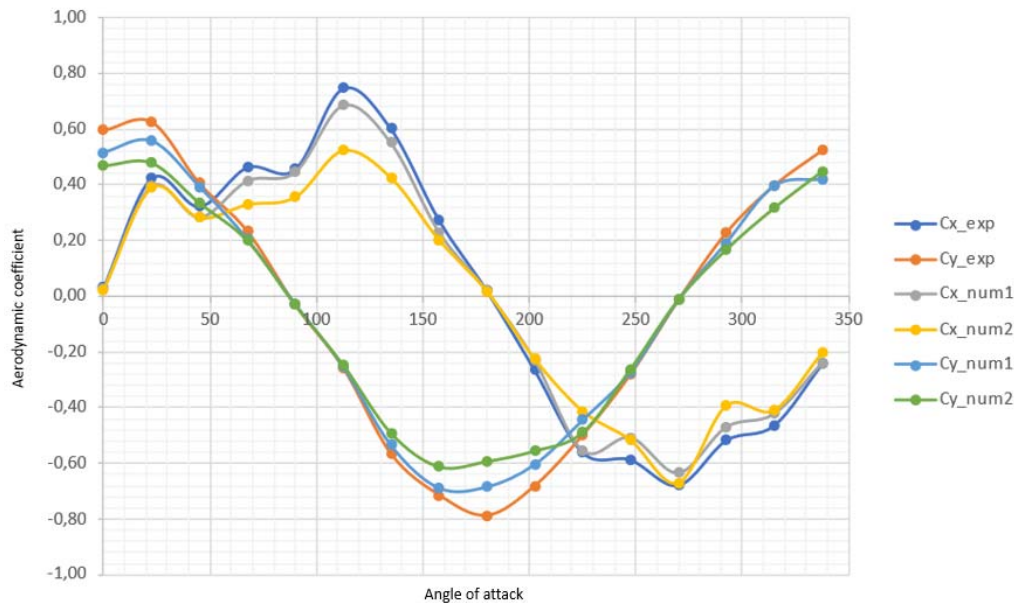Fig. 9. Results of the verification studies for the high-rise residential complex

83

Fig. 10. Results of the verification studies for the chimney as part of the coke oven complex

References

Aboshosha, H., Elshaer, A., Bitsuamlak, G. T., and El Damatty, A. (2015). Consistent inflow turbulence generator for LES evaluation of wind-induced responses for tall buildings. *Journal of Wind Engineering and Industrial Aerodynamics*, Vol. 142, pp. 198–216. DOI: 10.1016/j.jweia.2015.04.004.

Blocken, B. (2014). 50 years of computational wind engineering: past, present and future. *Journal of Wind Engineering and Industrial Aerodynamics*, Vol. 129, pp. 69–102. DOI: 10.1016/j.jweia.2014.03.008.

Galerkin, Y. B., Solovyeva, O. A., and Ucehovscy, A. A. (2020). Methodology of calculation and verification of vaneless diffusers test results in a virtual wind tunnel. *AIP Conference Proceedings*, Vol. 2285, Issue 1, 030059. DOI: 10.1063/5.0026537.

Kareem, A., Spence, S., Bernardini, E., Bobby, S., and Wei, D. (2013). Using computational fluid dynamics to optimize tall building design. *CTBUH Journal*, Issue III, pp. 38–43.

Murakami, S. (1998). Overview of turbulence models applied in CWE–1997. *Journal of Wind Engineering and Industrial Aerodynamics*, Vol. 74–76, pp. 1–24. DOI: 10.1016/s0167-6105(98)00004-x.

Poddaeva, O. (2022). *Fundamentals of ensuring technosphere safety of critical transportation infrastructure facilities within their life cycle*. DSc Thesis in Engineering. Russian University of Transport.

Ricci, M., Patruno, L., Kalkman, I., de Miranda, S., and Blocken, B. (2018). Towards LES as a design tool: wind loads assessment on a high-rise building. *Journal of Wind Engineering and Industrial Aerodynamics*, Vol. 180, pp. 1–18. DOI: 10.1016/j.jweia.2018.07.009.

Zhang, Y., Habashi, W. G., and Khurram, R. A. (2015). Predicting wind-induced vibrations of high-rise buildings using unsteady CFD and modal analysis. *Journal of Wind Engineering and Industrial Aerodynamics*, Vol. 136, pp. 165–179. DOI: 10.1016/j.jweia.2014.11.008.

ВЕРИФИКАЦИЯ РЕЗУЛЬТАТОВ ЧИСЛЕННОГО МОДЕЛИРОВАНИЯ ВЕТРОВЫХ ВОЗДЕЙСТВИЙ НА УНИКАЛЬНЫЕ ЗДАНИЯ И СООРУЖЕНИЯ

Поддаева Ольга Игоревна

УНПЛ АИИСК НИУ МГСУ, Москва, Россия

E-mail: poddaevaoi@gmail.ru

Аннотация

Введение: Основным методом определения ветрового воздействия на уникальные здания и сооружения остается физическое моделирование в аэродинамических трубах, однако испытания в аэродинамических трубах дорогостоящие и трудоемкие. CFD обеспечивает более высокую вариативность, расчеты выполняются быстрее и бюджетнее. Однако остается открытым вопрос корректности полученных в результате численного моделирования интегральных характеристики, соответственно, проведения процедуры верификации. На сегодняшний день в области строительной аэродинамики обязательным требованием к использованию результатов численного моделирования является их верификация с данными эксперимента. В исследованиях последних лет изучаются возможности CFD для точных прогнозов ветровой нагрузки, но не найдено ни одного исследования, которое представляло бы всестороннее описание и реализацию системы верификации и валидации для анализа ветровых воздействий на уникальные здания и сооружения. **Целью исследования** являлось сравнение результатов CFD с данными wind-tunnel test для трех различных объектов, анализ результатов и предложения по самой методики верификации и валидации CFD анализа ветровых воздействий на уникальные здания и сооружения. Были использованы следующие **методы**: физические испытания макетов уникальных зданий и сооружений в аэродинамической трубе, включая подробную методику экспериментальных исследований по определению интегральных аэродинамических характеристик, численное моделирование ветровых воздействий с использованием ПК ANSYS. Численное моделирование выполнялось в двух поставках: как с моделированием виртуальное аэродинамической трубы, так без моделирования. **В результате,** показано, что моделирование виртуальной аэродинамической трубы позволяет добиться лучшей согласованности данных при верификации результатов численного моделирования с данными физического моделирования, а корректное использование технологии численного моделирования может существенно сократить сроки и стоимость проведения экспериментальных исследований в аэродинамической трубе и/или сократить сроки проектирования уменьшив количество рассматриваемых сценариев нагружения.

Keywords: верификация; CFD; аэродинамическая труба; интегральные аэродинамические характеристики.

DEVELOPMENT OF FRAGILITY CURVES FOR REINFORCED CONCRETE BUILDINGS

Esma Souki[1,2]*, Kamel Abdou[1,2], Youcef Mehani[3]

[1]Department of Civil Engineering, Faculty of Sciences of Technology, Mentouri Brothers University (Constantine 1), Constantine, 25000, Algeria
[2]Laboratory of Materials and Construction Durability , Mentouri Brothers University (Constantine 1), Constantine, Algeria
[3]Department of Civil Engineering, National Earthquake Engineering Research Center CGS, Algiers, Algeria

*Corresponding author's e-mail: asma.souki@doc.umc.edu.dz

Abstract

Introduction: Algeria has experienced numerous destructive earthquakes, resulting in significant loss of human lives, buildings, and equipment. To mitigate this risk, **this study aims** to quantify the potential damage to existing strategic buildings in the city of Constantine, located in the northeast of Algeria. Many of these buildings are old, designed and constructed during the colonial era before the implementation of the Algerian seismic code. Thus, they are required to be strengthened and retrofitted. **Methods:** The LM2 method, defined in RISK-UE (WP4), based on nonlinear static analysis and spectral response, is used to develop fragility curves. In this context, a structural system mainly consists of moment-resisting reinforced concrete frames with partial infill walls. In this study, three types of strategic buildings are considered: low-rise (two stories), mid-rise (four stories), and high-rise (six stories). The current Algerian seismic code RPA99/ version 2003 (MHUV 2003) is used to assess the seismic demand. **As a result**, capacity curves are developed for two primary directions: local and global behavior, identified according to the limits specified in FEMA 356/273 and ATC 40. Based on these results, fragility curves are generated, defining four damage states: slight, moderate, extensive, and complete in terms of spectral displacement.

Keywords: fragility curves; damage states; LM2 method; nonlinear static analysis; RC building.

Introduction

Assessing the seismic vulnerability of existing buildings is a very important field. This issue affects almost all buildings in Algeria, mainly because they were constructed during a period when structures were designed without seismic standards, taking into account only the impact of vertical loads. Furthermore, changes in activity, unregulated transformations, lack of maintenance, and deterioration due to budget cuts predictably can lead to safety issues in future. Fragility curves are a very useful tool for mitigating seismic risk. As a result, defining the response of these structures to earthquakes is highly complex and depends on several parameters related to the building's characteristics and seismic excitation. In Algeria, the current level of knowledge regarding the seismic behavior of buildings is not highly advanced. In this context, our investigation will focus on developing a methodology to predict damage, as expressed by fragility curves, in order to quantify potential damage that is reached or exceeded. In the field of structural earthquake engineering, fragility functions can be used to estimate the probability of occurrence of various damage states in certain buildings at an observed value of a specified intensity measure (Folić and Čokić, 2021). Our case study is based on three models of the existing strategic constructions in the city of Constantine, which

is considered the third most important city in Algeria. The structural system most commonly used at that time mainly composed of moment-resisting reinforced concrete frames with partial infill walls. In this study, three types of strategic buildings are considered: low-rise (two stories), mid-rise (four stories), and high-rise (six stories).

Several previous studies conducted by various researchers considered the important role of fragility curves as a tool for assessing seismic vulnerability and expected damage to buildings after an earthquake. Below are citations from some of them:

In 2022, Fikri and Ingham investigated the behavior of non-ductile mid-rise masonry infill buildings in New Zealand. They used the Incremental Dynamic Analysis (IDA) method, along with the generation of fragility curves. The buildings were subjected to both mainshocks and aftershocks. Fragility curves for four damage states were determined in order to examine the failure of buildings constructed before the introduction of ductility criteria. Buildings were found to have suffered slight damage from the mainshocks and severe damage from the aftershocks (Fikri and Ingham, 2022).

In 2022, Zucconi et al. analyzed the seismic performance of a reinforced concrete building designed without any seismic criteria, characterized

by a seismically-stronger and a seismically-weaker direction, such as several existing reinforced concrete-framed structures designed for vertical load only. Bidirectional ground motions were applied to the structure. The OpenSees software was used to create a 3D model, taking into account the joint deformability of the panels, which enabled the derivation of fragility curves at various states of damage corresponding to the European earthquake standard (Zucconi et al., 2022).

In 2019, Al-Nimry conducted a study on the seismic fragility of low- and mid-rise RC infilled frame buildings of 2, 4, and 6 stories in Jordan. The buildings comprised of stone-concrete infill panels. Al-Nimry relied on expert reports and conducted pushover analyses to determine the capacity response of each modeled building. The study considered four damage states and defined corresponding thresholds (Al-Nimry, 2019).

In 2016, Vazurkar and Chaudhari developed fragility curves for three RC buildings with 3 and 4 stories. The method involved modeling the structures in SAP 2000 and using pushover analysis and then utilizing the results for plotting fragility curves, aiming to reduce seismic risk. The fragility curves were generated for four damage states considering spectral displacement (Vazurkar and Chaudhari, 2016).

In 2013, Mehani et al. aimed to develop fragility curves for existing low-rise and mid-rise RC buildings in Algeria. They used Japanese Seismic Index Methodology and characterized the observed damage states of existing buildings. The study was based on the designer's calculation method and the seismic code applied to four categories of buildings classified according to their construction period (pre-1955, during 1956–1980, during 1981–1999, and post-1999) (Mehani and al., 2013).

The main objective of these previous studies was to evaluate the effectiveness of the LM2 method to develop fragility curves, irrespective of research diversity. The parameters taken into account included various aspects, such as the typology of case studies, site characteristics, building construction systems, construction periods, software used for modeling, and compliance with seismic codes. Additionally, the methodology was applied. Despite the differences among the issues examined, this approach aims to estimate the probability of damage states and their corresponding thresholds, whether they are high or low. Finally, these results were used as preliminary data sources to assess the seismic vulnerability of buildings.

Basics of the LM2 method
Nonlinear static analysis

A building's capacity is represented by a force-displacement model (Fig. 1). It is obtained by applying the nonlinear static method, which defines
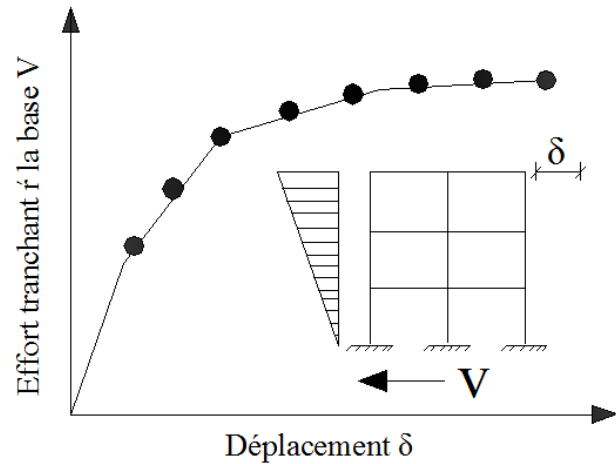

Fig. 1. The physical significance of the capacity curve defined by the base shear force as a function of displacement. (Roy and al., 2007)

the response of the structure when subjected to an increasing lateral load according to a predefined model assimilated to a system response. This response considers a single equivalent degree of freedom, driven by a single dominant vibration mode, until it reaches a target displacement (Souki and Djebbar, 2014). Additionally, it assesses the development of damage (Milutinovic and Trendafiloski, 2003). Bilinearization is used to build capacity curves, and the model is defined by control points — yield capacity and ultimate capacity in accordance with the FEMA 273 guidelines (FEMA 273, 1997).

Creating a capacity curve is the most important and challenging task, considering factors such as geometric configuration, material characteristics, type of construction system, technology used, and seismic code requirements (Milutinovic and Trendafiloski, 2003).

Development of fragility curves

Developing fragility curves for structures is based on analytical studies of structures. Fragility curves are derived from a resulting function identified in the damage probability matrix for buildings exceeding (Psk[Ds>ds|Y=yk]) or being (Psk[Ds=ds|Y=yk]) within a particular damage state threshold (Milutinovic and Trendafiloski, 2003). This is a function of nonlinear response, determined by spectral demand or seismic intensity (Nollet and al., 2009). Damage states can be classified into four categories: slight, moderate, extensive, and complete. It is standard practice to exclude the "D" or "No Damage" state from fragility curves (Baylon and al., 2023). A fragility curve from a model is characterized by the median value and the log-normal standard deviation (β) of seismic hazard parameter, i.e., the spectral displacement Sd (Milutinovic and Trendafiloski, 2003):

$$P\left[d_s / S_d\right] = \varphi\left[\frac{1}{ds}\ln\left(\frac{S_d}{\bar{S}_{d,ds}}\right)\right], \qquad (1)$$

87

S_d: is the spectral displacement (seismic hazard parameter).

$S_{d,ds}$: is the median value of spectral displacement at which the building reaches a certain threshold of the damage state d_s (Milutinovic and Trendafiloski, 2003).

β_{ds}: is the standard deviation of the natural logarithm of spectral displacement of the damage state d_s.

Φ: is the standard normal cumulative distribution function.

Damage states

The damage probability matrix (DPM) for systematic damage situations, derived from the harm caused by a previous earthquake or an appropriate parametric structural response, is used to study the expected likelihood of damage occurring in existing buildings. However, simplified methods were used to study the damage state thresholds (d_s), which are determined by the capacity curves calculated from the studied structures. Based on the fragility curves, specific damage states (ds) are defined in terms of four categories: slight, moderate, extensive, and complete. The threshold value ($\overline{S}_d$) and the standard deviation (β_{ds}) for each damage state can be determined using the bi-linear spectrum curve (Barbat and al., 2010; Lantada and al., 2010) (Fig. 2, Table 1), based on the threshold value of the
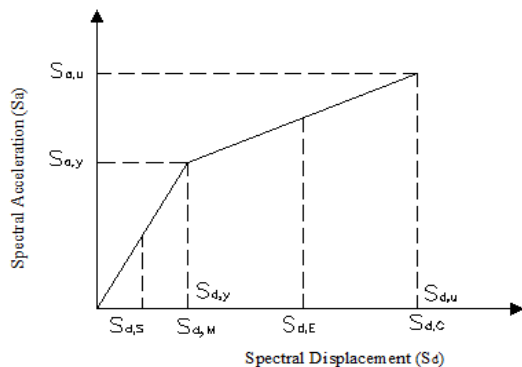
damage state according to the LM2 method of RISK-UE (Milutinovic and Trendafiloski, 2003).

Methodology guideline

Estimating the probability of damage involves a series of steps summarized in this guideline:

1. Selecting and identifying buildings, taking into account their span and number of stories.

2. Defining the behavioral laws of materials according to the Algerian concrete standard (DTR, B., 1993), modeled as confined and unconfined concrete (Mander and al, 1988), with longitudinal and transverse steel.

3. Modeling the structure in 3D using appropriate software, considering static loading conditions including dead and live loads.

4. Defining the seismic demand according to the Algerian seismic code RPA99/version 2003 (MHUV 2003). It can be expressed by Eq. (2) below:

$$\frac{S_a}{g} = \begin{cases} 1.25A\left(1+\dfrac{T}{T_1}\left(2.5\eta\dfrac{Q}{R}-1\right)\right) & 0 \leq T \leq T_1; \\[3mm] 2.5\eta(1.25A)\left(\dfrac{Q}{R}\right) & T_1 \leq T \leq T_2; \\[3mm] 2.5\eta(1.25A)\left(\dfrac{Q}{R}\right)\left(\dfrac{T_2}{T}\right)^{2/3} & T_2 \leq T \leq 3.0s; \\[3mm] 2.5\eta(1.25A)\left(\dfrac{T_2}{3}\right)^{2/3}\left(\dfrac{3}{T}\right)^{5/3}\left(\dfrac{Q}{R}\right) & T > 3.0s, \end{cases} \tag{2}$$

where:

A: the ground acceleration of 0.25 g. The soil is classified as a firm site (S2) according to the Algerian seismic code RPA99/version 2003 (MHUV 2003). The vibration periods corresponding to the horizontal axis as a function of spectral acceleration are T1 = 0.15 s and T2 = 0.40 s, with R representing the global behavior factor.

5. The identification of plastic hinges, as described by an idealized behavioral law and performance limits outlined in FEMA 356 (FEMA, 2000), applies to composite bending columns and simple bending beams.

Fig. 2. Threshold values of the damage state as a function of the bilinear capacity spectrum (Nagashree and al., 2016)

Table 1. **Relationship between the threshold ($\overline{S}_d$) and standard deviation (β_{ds}) for each damage state**

Damage states	Median value	Standard deviation
Slight	$\overline{S}_{d_1} = 0.7D_y$	$S_{d1} = 0.25 + 0.07\ln(\mu_u)$
Moderate	$\overline{S}_{d_2} = D_y$	$S_{d2} = 0.2 + 0.18\ln(\mu_u)$
Extensive	$\overline{S}_{d_3} = D_y + 0.25(D_u - D_y)$	$S_{d1} = 0.1 + 0.4\ln(\mu_u)$
Complete	$\overline{S}_{d_4} = D_u$	$S_{d1} = 0.15 + 0.5\ln(\mu_u)$

Where:

$\overline{S}_d$: is the median value of spectral displacement, and subscripts 1, 2, 3, and 4 indicate the damage state: slight, moderate, extensive, and complete, respectively.

D_y : is the yield spectral displacement.

D_u : is the ultimate spectral displacement.

6. The evolution of the capacity curves in the case studies (force-displacement) progresses differently along the two primary directions, XX and YY.

7. Converting the demand and capacity curves into the Acceleration Displacement Response Spectrum (ADRS) form (Hemsas and Elachachi, 2007), according to the ATC 40 guidelines (Applied Technology Council, 1996).

8. The bilinear idealization (Fig. 3) of ADRS curves is characterized by two limit states: Yield and ultimate (Milutinovic and Trendafiloski, 2003), according to the FEMA 273 guidelines (FEMA 273, 1997).

9. Overlaying two curves of capacity and demand to determine the performance point at their intersection (Fig. 4).

10. The evolution of the fragility curve is based on the shape of the log-normal probability of predicted damage in terms of spectral displacement. Damage states are categorized as slight, moderate, extensive, and complete.

11. Estimating the probabilities of damage for each potential damage state described for a given performance point according to the appropriate fragility model (Fig. 5).
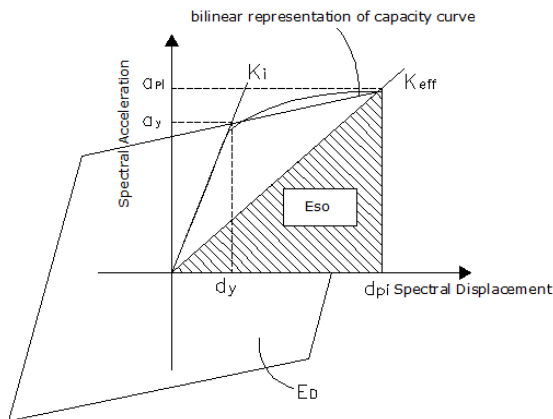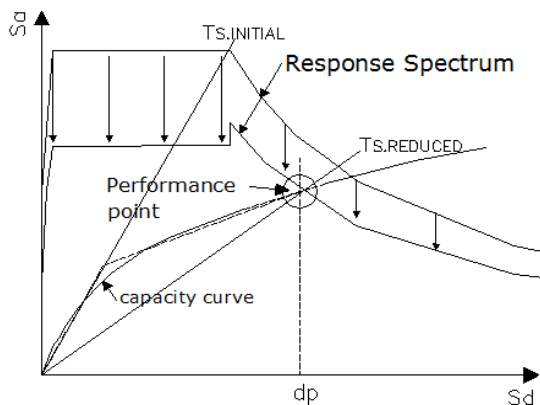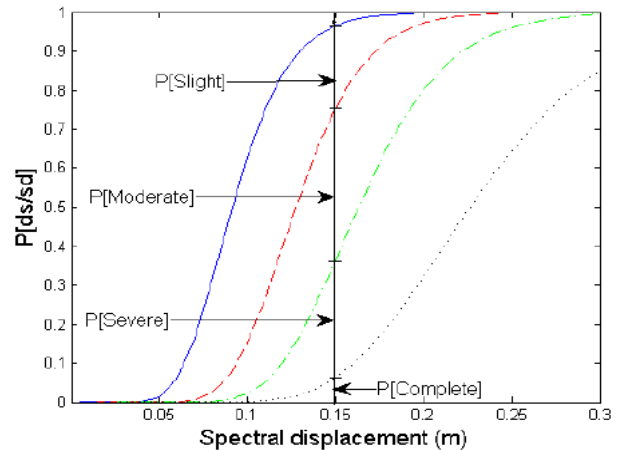

Fig. 5. Probability for each damage state as a function of spectral displacement (Barbat et al, 2012)

Analytical modeling

This paper presents the development of fragility curves using the LM2 method described in RISK-UE (Milutinovic and Trendafiloski, 2003), using two sets of functions: capacity and building demand. The structural system of the models consists of frame-type structures with partial infill walls, applied to three types of existing strategic reinforced concrete buildings. The buildings were constructed between 1980 and 2008 in accordance with Algerian regulations and are therefore classified as having low code compliance. The models are low-, medium-, and high-rise, with 2, 4, and 6 stories, respectively. Each model is characterized by a different number of stories. The design of these buildings considering the response spectrum was numerically modeled in three dimensions using ETABS version 9.7.2 and SAP 2000 version 2014 to calculate plastic hinges. The structures were designed to withstand dead and live loads, as well as seismic forces, based on the response spectrum of zone IIa, group 1A, and design acceleration of 0.25 g in accordance with RPA99/version 2003 (MHUV 2003). The modeling of buildings depends on various parameters related to the structural design and seismic excitation, considering geometric sizes, material properties, and reinforcement of structural elements according to load guidelines (DTR, B. C. 2.2, 1988). It is worth noting that the lateral resistance systems of the three models differ: model 1 features external walls and internal partitions made of brick, model 2 incorporates filled hollow bricks in masonry, while model 3 uses external walls made of concrete blocks. The modeled structures are shown in Fig. 6.

The following Tables 2 and 3 summarize all the parameters mentioned above.

The simultaneous effects of gravity and lateral loads are typically included in the nonlinear analysis of structures (Al-Nimry, 2019). Therefore, a triangular loading model is employed to account for lateral
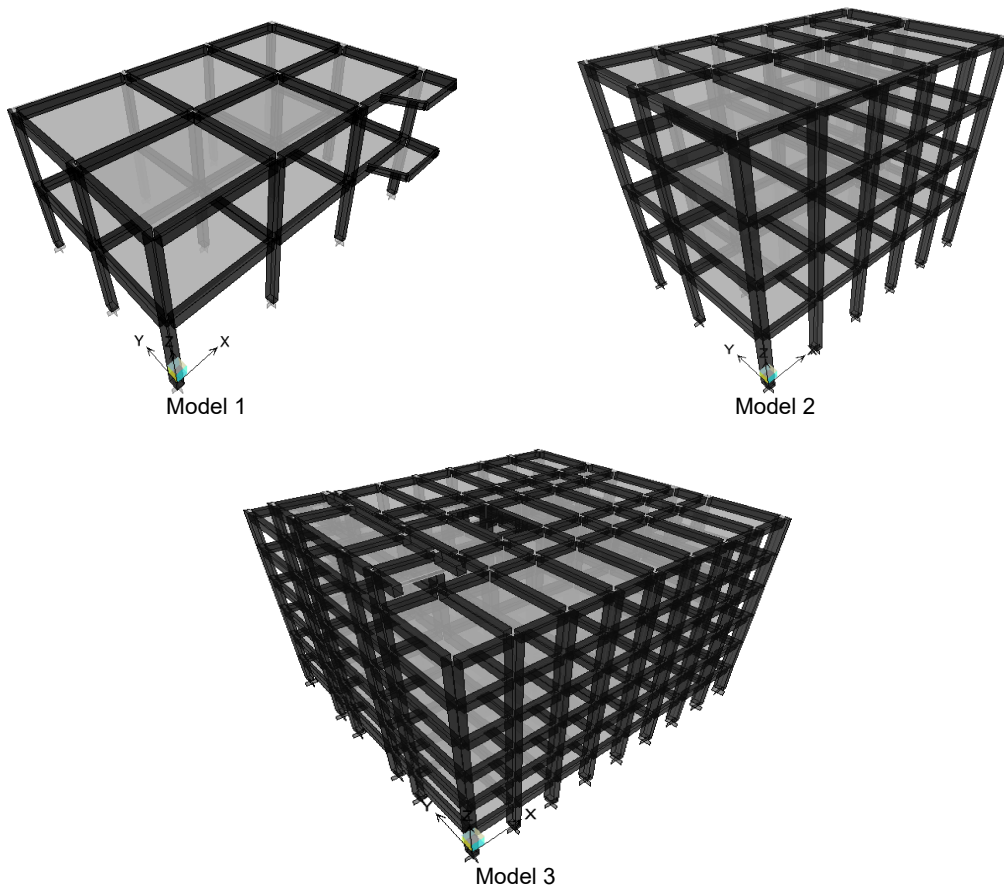

Fig. 3. Capacity curve in ADRS format (Mouroux and al., 2021)

Fig. 4. Determination of the performance point (Mouroux and al, 2021)

Fig. 6. Representative building structure models

Table 2. **Geometric and structural characteristics of different buildings**

Model 3	Model 2	Model 1	Model characteristics
6	4	2	No. of stories
Story '1' H = 3.45 m Stories ,2, 3, 4, 5, 6' H = 3.55 m	Story '1' H = 4.36 m Stories ,2, 3, 4' H = 3.6 m	Stories '1, 2' H = 3.5 m	Height of stories
Built in the 1980s	817.0675 m² Built in 2008	456.705 m² Built in 2000	Floor area (m²) Period of construction
Hospital administrative and medical unit El Khroub	Administrative unit of the government building, Daksi	Surgical clinic of the children's hospital, El Mansourah	Location
Hollow concrete block, thickness: 20 + 5 cm	Hollow concrete block, thickness: 16 + 4 cm	Full slab, thickness: 20 cm	Floor type
Corner (50x90) cm² 8ϕ16 + 10ϕ16 Edge (35x55) cm² 8ϕ16 + 4ϕ14	Corner (35x55) cm² 8ϕ16 + 4ϕ14 Edge (35x55) cm² 8ϕ16 + 4ϕ14 Center (35x55) cm² 8ϕ16 + 4ϕ14	Corner (30x45) cm² 6ϕ14 + 2ϕ12 Edge (30x45) cm² 6ϕ14 + 2ϕ12 Center (30x45) cm² 6ϕ14 + 2ϕ12	Columns (dimensions, reinforcement)
Principal (50x75) cm² 8ϕ14 + 6ϕ12 Chainage (50x75) cm² 8ϕ14 + 6ϕ12	Principal (35x55) cm² 6ϕ14 + 2ϕ10 Chainage type 1 (35x40) cm² 6ϕ12 + 2ϕ10 Chainage type 2 (35x75) cm² 6ϕ14 + 4ϕ12	Corner (30x45) cm² 6ϕ10 + 2ϕ12 Center (30x45) cm² 6ϕ10 + 2ϕ12	Beams (dimensions, reinforcement)

Table 3. **Characteristics of concrete and steel materials**

Steel	Concrete	Characteristics of materials
–	20 MPa	Compressive strength
2.1E+5 (MPa)	29,858.594 (MPa)	Modulus of elasticity
0.002	0.002	Elastic strain
0.01	0.0035	Ultimate strain
–	15 cm	Spacing of confinement
78 (kN/m³)	25 (kN/m³)	Unit weight
400 MPa (HD)	–	Yield strength
400 MPa	–	Ultimate strength

forces, considering (G + bQ), and an additional vertical force due to the structure's weight defined by the combination (G + Q). The behavioral law of a plastic hinge for composite bending columns and simple bending beams is described using the Section Designer calculation of SAP 2000 software version 2014 and is idealized in two parts. The first part is limited by the initial yield, which involves the appearance of cracking in the concrete and the initial softening of the steel. The second part is limited by the point of maximum strength and deformation (Souki and djebbar, 2014). Additionally, the shear capacity of columns and beams is considered, including axial force from the vertical load, shear strength, and flexural strength, which are indicated in Eq. (3) (Waenpracha et al., 2023).

$$L_P = 0.08L_V + 0.022f_y d_{bl}, \qquad (3)$$

L_V : shear length.
L_P: plastic hinge length.
d_{bl}: diameter of the longitudinal rebar.
f_y: yield strength of the longitudinal rebar.
This is recorded as the extent of the plastic hinge (Park et al., 1982). It was developed based on experimental findings from specimens of reinforced

concrete with well-detailed plastic hinge regions consisting of deformed reinforcing bars (Souki and Djebbar, 2014). The details of the previously established plastic hinge law are shown in Fig. 7.

Results and discussion

The analysis of different structures using the nonlinear static procedure, more commonly known as pushover analysis, provided us with capacity curves. These curves were obtained for the two considered directions (XX) and (YY) for each model (Fig. 8).

Following the analysis of the capacity curves beyond the elastic range and considering the development of plastic hinges from their appearance in any structural element up to a certain level of damage, their characteristics include resistance to bending and deformation capacity. They are influenced by several factors such as the intensity of the normal force, the volumetric ratio of transverse reinforcement, the longitudinal reinforcement ratio, and the material behavior laws applied. In general, their properties are determined by the nature, typology, and geometry of the structures.

The base shear capacity obtained in model 3 is twice as high as that obtained in models 1 and 2 in both directions XX and YY. However, the displacements recorded in model 1 are higher than those obtained in models 2 and 3, with variations ranging from 18 to 31 % in the YY direction and 30 % in the XX direction.

This implies that building model 3 demonstrates the greatest capacity to resist lateral loads in both directions compared to building models 1 and 2. Conversely, model 1 exhibits the lowest capacity to resist lateral loads in both directions. Additionally, it undergoes greater displacement and experiences higher energy dissipation compared to models 2 and 3. This suggests that model 3 is more rigid and resistant, whereas model 1 offers significant ductility and flexibility, enabling it to endure greater deformations before failure. Physically, these differences could be attributed to various factors
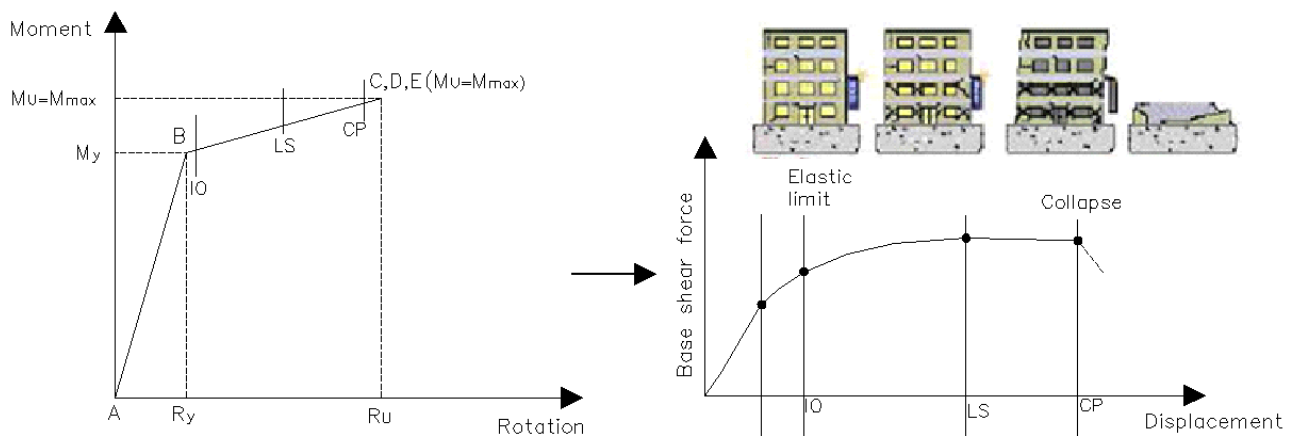

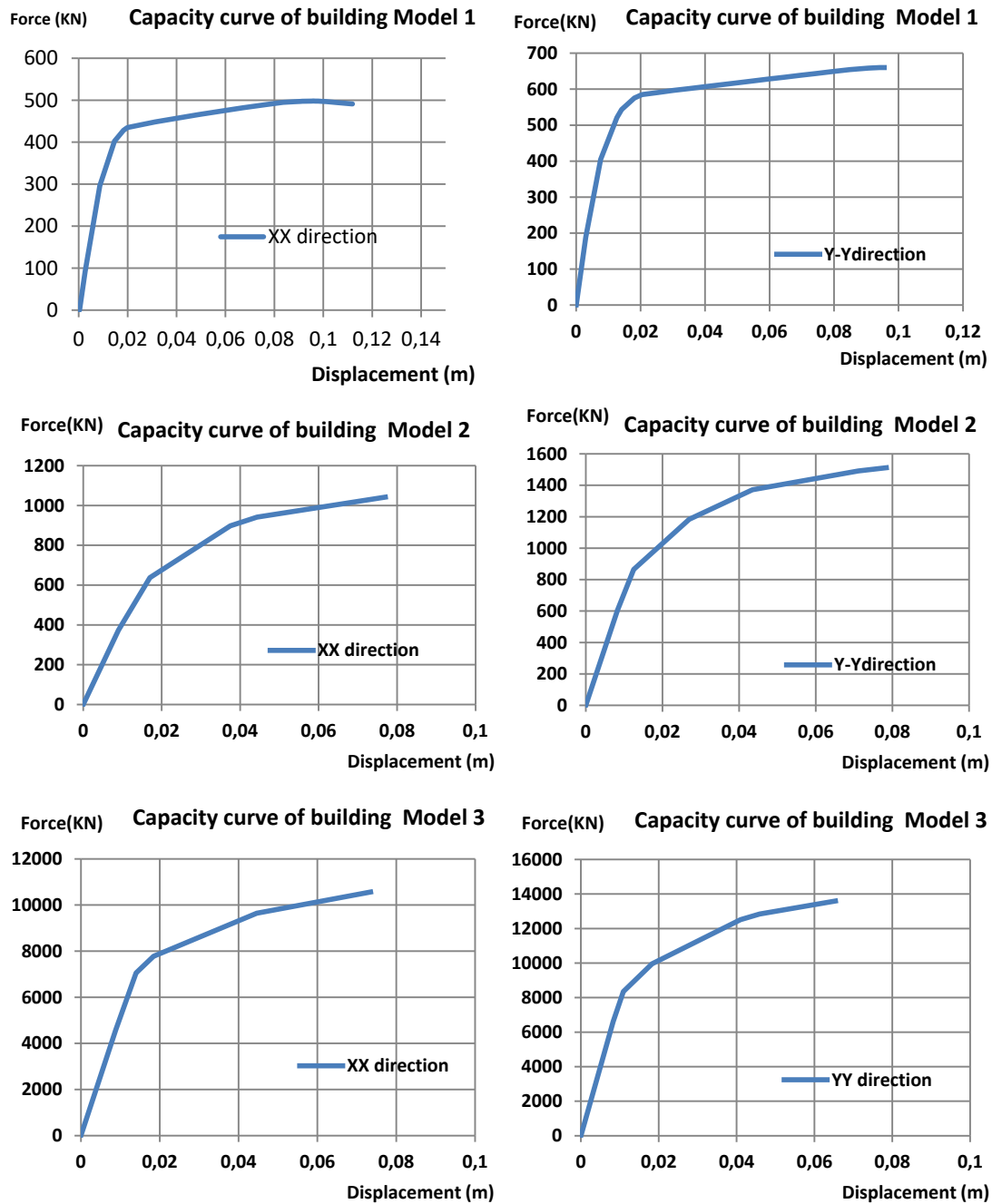Fig. 7. Simplified plastic hinge law and capacity curve

Fig. 8. Capacity curves of low-, mid- and high-rise buildings in the XX and YY directions

such as building geometry, mass distribution, and the stiffness of structural elements. Model 3 has more favorable geometry, optimized mass distribution, and stiffer structural elements, contributing to its higher capacity and lower displacement under lateral loads. Conversely, model 1 has smaller geometry, mass, and structural elements, which result in lower capacity and greater displacement under lateral loads.

The real behavior laws were converted into curves in the form of ADRS (acceleration displacement response spectrum) in accordance with the ATC-40 guide (Applied Technology Council, 1996). The curves are idealized in a bilinear form, taking into

account the limits established by the FEMA 356 guide (FEMA, 2000). Finally, the results of the two boundary states, elastic and ultimate, of spectral acceleration and displacement, as well as the mean value and standard deviation S_A and S_d of each damage state, are summarized in Table 4.

The fragility curves were determined by the log-normal standard deviation (β) and the median value $(\overline{S}_d)$, which are influenced by spectral displacement S_d (Fig. 9).

The results indicate that incorporating three-dimensional structural modeling and considering bi-directional ground motion are fundamental aspects

Table 4. **Damage states with considered yield and ultimate points**

| Building models	Yield point		Ultimate point		Damage state thresholds (spectral displacement in cm)							
	SAy (%g)	SDy (cm)	SAu (%g)	SDu (cm)	$\overline{S}_{d_1}$	β1	$\overline{S}_{d_2}$	β2	$\overline{S}_{d_3}$	β3	$\overline{S}_{d_4}$	β4
Model '1' xx	0.12	1.37	0.13	4.25	0.95	0.32	1.37	0.40	2.09	0.55	4.25	0.71
Model '2' xx	0.12	2.00	0.14	11.4	1.40	0.37	2.00	0.51	4.35	0.79	11.4	1.02
Model '3' xx	0.13	1.16	0.16	7.89	0.81	0.38	1.16	0.54	2.84	0.86	7.89	1.10
Model '1' yy	0.18	1.10	0.19	8.28	0.75	0.39	1.08	0.56	2.88	0.91	8.28	1.16
Model '2' yy	0.15	4.29	0.16	9.20	3.00	0.36	4.29	0.48	5.51	0.73	9.20	0.94
Model '3' yy	0.18	1.80	0.21	6.60	1.26	0.34	1.80	0.43	3.00	0.61	6.60	0.79
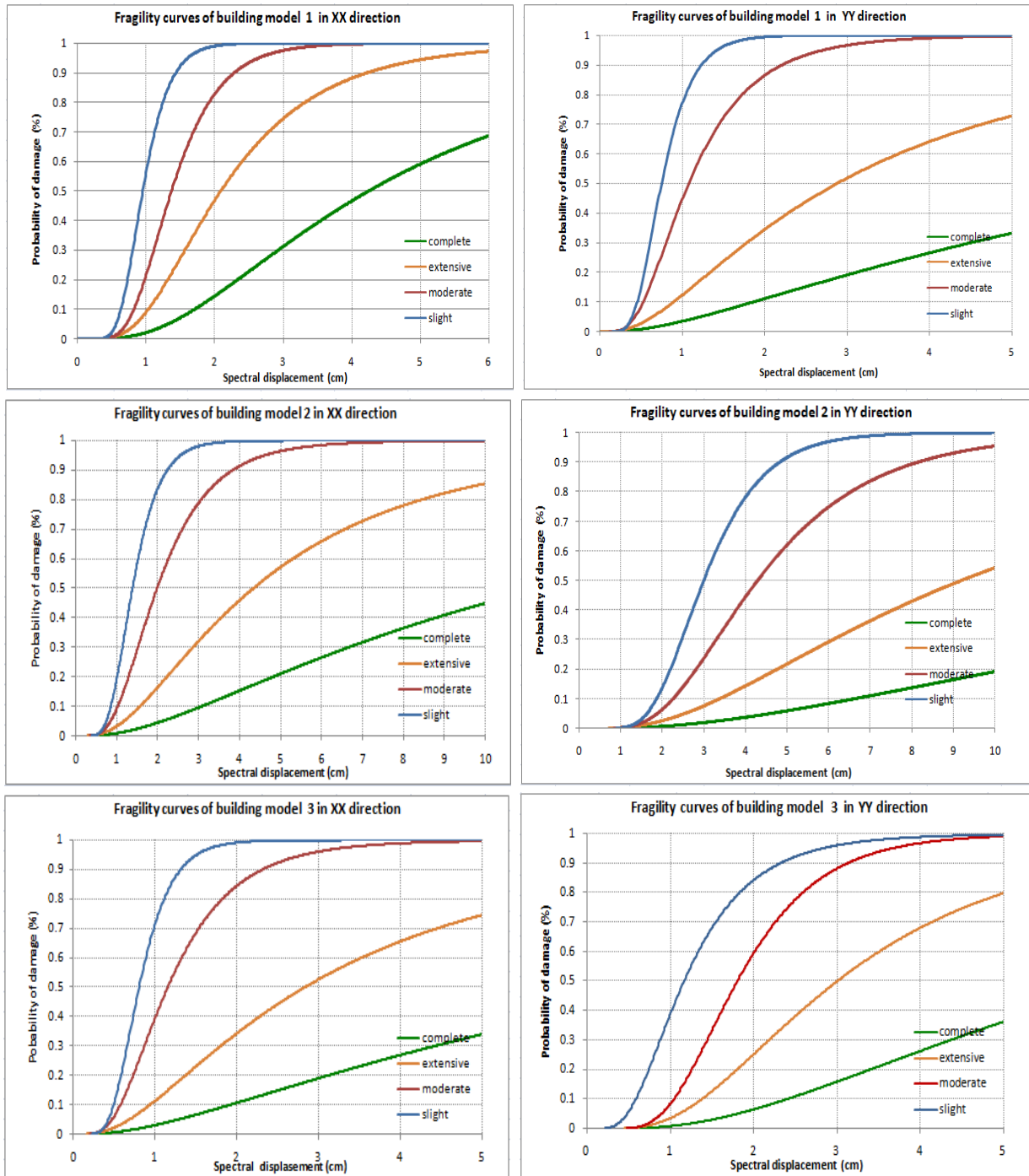
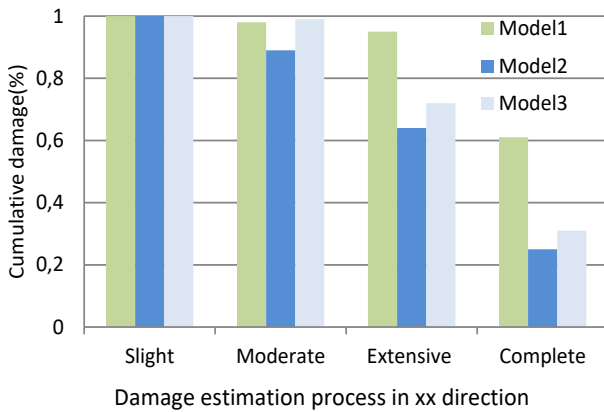Fig. 9. Fragility curves for RC building models in the XX and YY directions

Fig. 10. Damage probability evaluation for RC building models in the XX direction
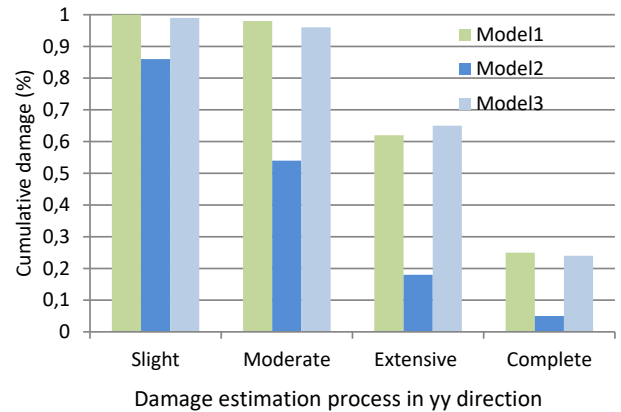

Fig. 11. Damage probability evaluation for RC building models in the YY direction

in analyzing fragility curves. Specifically, the findings highlight that fragility curves show a steeper incline for the "slight" and "moderate" damage thresholds in both the XX and YY directions across all three examined models. This suggests that models 1, 2, and 3 are more susceptible to fragility and vulnerability in both orientations. Furthermore, this structural behavior is confirmed in Table 4, which reveals that the median values of the fragility curves are consistently lower in both directions and for both damage thresholds, "slight" and "moderate", regardless of the model under consideration. Conversely, the fragility curves for the "extensive" and "complete" damage states illustrate reduced vulnerability of the structures. This is supported by the slight upward trend observed in the fragility curves, aligning with higher median values across all three models and in both directions analyzed.

The results of the damage probability evaluation for each damage state in the XX and YY directions for the studied buildings are shown in Figs. 10 and 11, respectively.

The main objective of this study was to assess the seismic vulnerability of structures by calibrating the fragility curves using the LM2 method, as outlined in RISK-UE. Significant emphasis was placed on the structural modeling of the analyzed models, as well as on characterizing seismic inputs and identifying damage state thresholds. Ultimately, the results of the probability of damage states estimated from the analysis of the fragility curves of the examined buildings indicate higher vulnerability, primarily observed in most models for slight and moderate damage states

in both the XX and YY directions. Conversely, for extensive and complete damage states, vulnerability is comparatively lower and more restrictive, which is particularly evident in model 2 in the YY direction.

Conclusion

This paper discusses the application of the concepts of the LM2 method, as described in RISK-UE, for the development of fragility curves for existing strategic reinforced concrete buildings, using the nonlinear static analysis approach, which is a function of spectral displacement or seismic earthquake parameters. The pushover analysis demonstrates the true behavior of the structure and enables the estimation of various resistance and displacement characteristics. It also facilitates specifying the level of damage assessment and deducing the degree of ductility. This study contributes to assessing the seismic vulnerability of strategic buildings in major Algerian cities, focusing on Constantine, the eastern capital, with the aim of mitigating seismic risks. Furthermore, it aims to review and improve various earthquake regulations and seismic rules. The findings from the fragility curve analysis provide a broader vision and perspective for a more precise understanding of Algeria's seismic risk. The fragility curve is considered an excellent source for preliminary seismic analysis to assess the level of seismic vulnerability, as well as for upgrading and retrofitting existing buildings in Algeria. In future research, our goal will be to study other constructions involving shear walls and dual systems.

References

Al-Nimry, H. (2019). Development of seismic fragility curves of RC infilled frame buildings in Jordan. MATEC Web of Conferences, Vol. 281, 01012. DOI: 10.1051/matecconf/201928101012.

Applied Technology Council (1996). ATC-40. Seismic evaluation and retrofit of concrete buildings. Redwood City: Applied Technology Council, 346 p, California, USA.

Barbat, A. H., Carreño, M. L., Pujades, L. G., Lantada, N., Cardona, O. D., Mabel, C., and Marulanda, M. C. (2010). Seismic vulnerability and risk evaluation methods for urban areas. A review with application to a pilot area. *Structure and Infrastructure Engineering*, Vol. 6, Issue 1–2, pp. 17–38. DOI: 10.1080/15732470802663763.

Barbat, A. H., Vargas, Y. F., Pujades, L. G., and Hurtado, J. E. (2012). Probabilistic assessment of the seismic damage in reinforced concrete buildings. In: *Computational Civil Engineering – CCE2012. 43 International Symposium*, May 25, 2012, Iasi, Romania, pp. 43–61.

Baylon, M. B., Sevilla, M. E. P., Cutora, M. D. L., Villa, R. M. S., Reynes, P. M. P., and Montemayor, J. M. V. (2023). Development of fragility curves for seismic vulnerability assessment: the case of Philippine General Hospital spine building. *International Research Journal of Science, Technology, Education, and Management*, Vol. 2, No. 4, pp. 1–11. DOI: 10.5281/zenodo.7559408.

Ministry of Housing and Urbanism, M.H.U.V., and National Center of Applied Research in Earthquake Engineering, C.G.S. (2003). Algerian Seismic Regulation, RPA 99 version 2003, D.T.R - B. C. 2.48 Algeria.

FEMA (1997). NEHRP guidelines for the seismic rehabilitation of buildings. FEMA 273. Washington, DC: FEMA, 435 p.

FEMA (2000). *Prestandard and commentary for the seismic rehabilitation of buildings*. FEMA 356. Washington, DC: FEMA, 518 p.

Fikri, R. and Ingham, J. (2022). Seismic response and aftershock fragility curves for non-ductile mid-rise buildings comprised of reinforced concrete frame with masonry infill. *Structures*, Vol. 45, pp. 1688–1700. DOI: 10.1016/j.istruc.2022.09.108.

Folić, R. and Čokić, M. (2021). Fragility and vulnerability analysis of an RC building with the application of nonlinear analysis. *Buildings*, Vol. 11, Issue 9, 390. DOI: 10.3390/buildings11090390.

DTR, B. C. 2.2 (1988). Dead loads and live loads. Edition of the National Center for Applied Research in Earthquake Engineering,C.G.S.

Hemsas, M. and Elachachi, S. M. (2007). Performance evaluation and analysis of the nonlinear behavior of reinforced concrete shear walls subjected to seismic action. 25th AUGC Meeting, p. 23-25.

Lantada, N., Irizarry, J., Barbat, A. H., Goula, X., Roca, A., Susagna, T., and Pujades, L. G. (2010). Seismic hazard and risk scenarios for Barcelona, Spain, using the Risk-UE vulnerability index method. Bulletin of Earthquake Engineering, Vol. 8, pp. 201–229. DOI: 10.1007/s10518-009-9148-z.

Mander, J. B., Priestley, M. J. N., and Park, R. (1988). Theoretical stress-strain model for confined concrete. Journal of Structural Engineering, Vol. 114, Issue 8, pp. 1804–1826. DOI: 10.1061/(ASCE)0733-9445(1988)114:8(1804).

Mehani, Y., Bechtoula, H., Kibboua, A., and Naili, M. (2013). Assessment of seismic fragility curves for existing RC buildings in Algiers after the 2003 Boumerdes earthquake. Structural Engineering and Mechanics, Vol. 46, No. 6, pp. 791–808. DOI: 10.12989/sem.2013.46.6.791.

Milutinovic, Z. V. and Trendafiloski, G. S. (2003).RISK-UE. An advanced approach to earthquake risk scenarios with applications to different European towns. Contract: EVK4-CT-2000-00014, WP4: Vulnerability of current buildings, p. 1-111. [online]   Available:at:http://www.civil.ist.utl.pt/~mlopes/conteudos/DamageStates/Risk%20UE%20WP04_Vulnerability.pdf [Date accessed: May 15, 2022].

Mouroux, P., Negulescu, C., and Belvaux, M. (2021). Practical comparison between displacement methods, leading to performance point and ductility demand, from ATC 40 (in damping) and Eurocode 8 (in ductility). Conference paper: January 2021, pp. 2-3.

Nagashree, B. K., Ravi Kumar, C. M., and Reddy, V. (2016). A parametric study on seismic fragility analysis of RC buildings. *Earthquakes and Structures*, Vol. 10, No. 3, pp. 629–643. DOI: 10.12989/eas.2016.10.3.629.

Nollet, M.-J., Karbassi, A., Lefebvre, K., and Chaallal, O. (2009). Development of fragility curves for existing buildings using the applied element method. 9th National Symposium on Structural Calculation. Giens, France, paper A3H91805.

Park, R., Priestley, M. J. N., and Gill, W. D. (1982). Ductility of square-confined concrete columns. Journal of the Structural Division, Vol. 108, Issue 4, pp. 929–950. DOI: 10.1061/JSDEAG.0005933.

DTR, B. (1993). BC 2-41: Design and calculation rule for Reinforced Concrete Structures „CBA 93". Edition of the National Center for Applied Research in Earthquake Engineering, C.G.S. Approved by ministerial decree of, 165-167.

Roy, N., Paultre, P., and Proulx, J. (2007). Seismic evaluation and rehabilitation of reinforced concrete viaduct columns. Seismic Engineering and Structural Dynamics Research Center (CRGP). Sherbrooke University, Montreal.

Souki, A., Djebbar, N. (2014). Influence of confinement reinforcement on the seismic performance of reinforced concrete columns. University of Constantine 1, Algeria.

Vazurkar, U. Y. and Chaudhari, D. J. (2016). Development of fragility curves for RC buildings. *International Journal of Engineering Research*, Vol. 5, Issue Special 3, pp. 591–594. DOI: 10.17950/ijer/v5i3/016.

Waenpracha, S., Foytong, P., Suppasri, A., Tirapat, S., Thanasisathit, N., Maneekul, P., and Ornthammarath, T. (2023). Development of fragility curves for reinforced-concrete building with masonry infilled wall under tsunami. *Advances in Civil Engineering*, Vol. 2023, 8021378. DOI: 10.1155/2023/8021378.

Zucconi, M., Bovo, M., and Ferracuti, B. (2022). Fragility curves of existing RC buildings accounting for bidirectional ground motion. *Buildings*, Vol. 12, Issue 7, 872. DOI: 10.3390/buildings 12070872.

ПОСТРОЕНИЕ КРИВЫХ ХРУПКОСТИ ДЛЯ ЖЕЛЕЗОБЕТОННЫХ ЗДАНИЙ

Эсма Суки[1,2], Камель Абду[1,2], Юсеф Механи[3]

[1]Кафедра гражданского строительства, факультет технологических наук, Университет братьев Ментури (Константина 1), Константина, 25000, Алжир
[2]Лаборатория материалов и долговечности конструкций, Университет братьев Ментури (Константина 1), Константина, 25000, Алжир
[3]Отдел гражданского строительства, Национальный исследовательский центр сейсмостойкого строительства CGS, Алжир, Алжир

*E-mail: asma.souki@doc.umc.edu.dz

Аннотация
Введение: Алжир пережил множество разрушительных землетрясений, приведших к значительным человеческим жертвам, разрушениям зданий и оборудования. **Цель данного исследования** — количественная оценка потенциального ущерба существующих стратегических зданий в городе Константина, расположенном на северо-востоке Алжира, с тем чтобы минимизировать сейсмический риск. Многие из этих зданий — старые, спроектированы и построены в колониальную эпоху, до введения в действие алжирских сейсмических норм. Поэтому их необходимо укрепить и модернизировать.
Методы: Для построения кривых хрупкости используется метод LM2, определенный в RISK-UE (WP4), который основан на нелинейном статическом анализе и спектральном отклике. В этом контексте конструктивная система состоит в основном из жестких железобетонных каркасов с неполным стеновым заполнением. В данном исследовании рассматриваются три типа стратегических зданий: малоэтажные (два этажа), среднеэтажные (четыре этажа) и высотные (шесть этажей). Для оценки сейсмических требований используются действующие алжирские сейсмические нормы (RPA99 версии 2003 года). **В результате** построены кривые прочности для двух основных направлений, локального и глобального поведения, которые определяются в соответствии с ограничениями, указанными в FEMA 356/273 и ATC 40. На основе этих результатов построены кривые хрупкости, определяющие четыре состояния разрушения: незначительное, умеренное, обширное и полное с точки зрения спектрального перемещения.

Ключевые слова: кривые хрупкости; состояние разрушения; метод LM2; нелинейный статический анализ; железобетонное здание.

Guide for Authors
for submitting a manuscript for publication in the «Architecture and Engineering»

The journal is an electronic media and accepts the manuscripts via the online submission. Please register on the website of the journal http://aej.spbgasu.ru/, log in and press "Submit article" button or send it via email aejeditorialoffice@gmail.com.

Please ensure that the submitted work has neither been previously published nor has been currently submitted for publication in another journal.

Main topics of the journal:

1. Architecture
2. Civil Engineering
3. Geotechnical Engineering and Engineering Geology
4. Urban Planning
5. Technique and Technology of Land Transport in Construction

Title page

The title page should include:

The title of the article in bold (max. 90 characters with spaces, only conventional abbreviations should be used); The name(s) of the author(s); Author's(s') affiliation(s); The name of the corresponding author.

Abstract and keywords

Please provide an abstract of 100 to 250 words. The abstract should not contain any undefined abbreviations or unspecified references. Use the IMRAD structure in the abstract (introduction, methods, results, discussion).

Please provide 4 to 6 keywords which can be used for indexing purposes. The keywords should be mentioned in order of relevance.

Main text

It should have the following structure:
1) Introduction,
2) Scope, Objectives and Methodology (with subparagraphs),
3) Results and Discussion (may also include subparagraphs, but should not repeat the previous section or numerical data already presented),
4) Conclusions,
5) Acknowledgements (the section is not obligatory, but should be included in case of participation of people, grants, funds, etc. in preparation of the article. The names of funding organizations should be written in full).

General comments on formatting:

- Subtitles should be printed in Bold,
- Use MathType for equations,
- Tables should be inserted in separate paragraphs. The consecutive number and title of the table should be placed before it in separate paragraphs. The references to the tables should be placed in parentheses (Table 1),
- Use "Top and Bottom" wrapping for figures. Figure captions should be placed in the main text after the image. Figures should be referred to as (Fig. 1) in the text.

References

The journal uses Harvard (author, date) style for references:
- The recent research (Kent and Park, 1990)...
- V. Zhukov (1999) stated that…

Reference list

The list of references should only include works that are cited in the text and that have been published or accepted for publication. Personal communications and unpublished works should only be mentioned in the text. Do not use footnotes or endnotes as a substitute for a proper reference list. All references must be listed in full at the end of the paper in alphabetical order, irrespective of where they are cited in the text. Reference made to sources published in languages other than English or Russian should contain English translation of the original title together with a note of the used language.

Peer Review Process

Articles submitted to the journal undergo a double blind peer-review procedure, which means that the reviewer is not informed about the identity of the author of the article, and the author is not given information about the reviewer.
On average, the review process takes from one to five months.